

A Comparison and Validation of Traditional and Three-Dimensional Anthropometric Methods
for Measuring the Hand through Reliability, Precision, and Visual Analysis

A Thesis

SUBMITTED TO THE FACULTY OF THE

UNIVERSITY OF MINNESOTA

BY

Emily Ann Seifert

IN PARTIAL FULFILLMENT OF THE REQUIREMENTS

FOR THE DEGREE OF MASTER OF SCIENCE

Linsey Griffin, Ph.D.

December 2020

Emily Seifert

2020 ©

Acknowledgement

I would like to acknowledge my advisor, Dr. Linsey Griffin. I am very thankful for all the time and energy that she spent guiding me through this process, the words of encouragement that she gave me, and the knowledge that she was able to instill through her research experience. Without her, this paper would not exist.

I would like to acknowledge my other committee members - Dr. Brad Holschuh and Dr. Tom Albin. Dr. Brad Holschuh provided positive suggestions and helped me to better understand precision-based analysis. Dr. Tom Albin provided words of encouragement and offered valuable knowledge on statistical analysis.

I would like to acknowledge the College of Design, who provided funding for this project through the Design Graduate Program Research and Creative Scholarship Grant.

I would like to acknowledge the Human Dimensioning Lab at the University of Minnesota, who provided me with the original scans used as participants within this study.

I would like to acknowledge the staff at the Earl E. Bakken Medical Device Center, who printed the three-dimensionally printing twelve (12) hands at the very beginning of COVID-19 pandemic and hand-delivered them to my house.

I would like to acknowledge Elisheva Savvateev, who provided an overview of coding in R which assisted greatly.

I would like to acknowledge the staff at the College of Design, Sue Finnegan, Elizabeth Goebel, and Julie Hillman, who each has provided me with warm smiles and lively conversations.

Lastly, I would like to acknowledge my family and friends, who have provided me with the support and love needed to complete this task. I could have never been able to accomplish this without their assistance whether through childcare, meals, ‘sanity breaks’, willingness to listen to me talk about research, helpful distractions, numerous text messages, or postcards, I am forever grateful.

Dedication

To the two great loves of my life my husband, Leigh Seifert, and our daughter, Evelyn Seifert.

You both motivate and inspire me to do better things.

Abstract

This study examines the reliability and precision of three (3) different tools for collecting anthropometric data of the hand, traditional anthropometric tools (caliper and tape measure) and two (2) full-color hand-held three-dimensional scanners (Occipital Structure Sensor and Artec Leo). A visual analysis of the three-dimensional models provided from the two (2) full-color hand-held three-dimensional scanners (Occipital Structure Sensor and Artec Leo) took place during the post-processing stage to determine the three-dimensional visual reliability and precision. Twelve (12) three-dimensional hand scans, from a more extensive database taken by the Human Dimensioning Lab at the University of Minnesota, were three-dimensionally printed. Eight (8) defined measurements were analyzed for Anthropometric Tool Reliability Analysis and Anthropometric Tool Precision Analysis. This study found that the Artec Leo scanner was more reliable than traditional methods (caliper and tape measure) and the Occipital Structure Sensor. The Occipital Structure Sensor was more reliable than traditional methods (caliper and tape measure) and less reliable than the Occipital Structure Sensor. Within the Anthropometric Tool Precision Analysis, the Artec Leo captured comparable measurements to those collected using traditional methods (caliper and tape measure). The Occipital Structure Sensor captured comparable measurements, except for Index Finger Length and Index Finger Circumference at the Distal Interphalangeal Joint measurements compared to traditional methods (caliper and tape measure) and the Artec Leo. The Anthropometric Tool Precision Analysis included independent identification of landmarks at Fingertips of Digit 2 and 3 for six (6) out of twelve (12) Occipital Structure scans, which impacted two (2) measurements, Hand Length and Index Finger Length. Due to this, a Secondary Anthropometric Tool Precision Analysis took place for the six (6) participants with complete landmarks. During the Secondary Anthropometric Tool Precision Analysis, no statistical significance was found when comparing scans that did not require independent landmark identification. The scans provided by the two (2) three-dimensional scanners (the Occipital Structure Sensor and Artec Leo) were analyzed during the post-processing stage for the Three-Dimensional Visual Reliability Analysis and Three-Dimensional Visual Precision Analysis using a Post-Processing Visual Analysis Likert Scale (Juhnke, Pokorny, and Griffin, 2021). Three-Dimensional Visual Reliability and the Three-Dimensional Visual Precision Analysis found that the Occipital Structure Sensor and Artec Leo are comparable for all locations, except for the Visibility of Landmark location. This study validates the Artec Leo for use in further anthropometric data collection for the hand. The results provided by the Occipital Structure Sensor were promising compared to those collected using traditional methods (caliper and tape measure) when visible landmarking is used. The use of visual analysis as a form of

evaluation for the validation of three-dimensional scanners was crucial to understanding where the scan's quality might affect the data collection outcomes and should be considered within future studies.

Table of Contents

Acknowledgement	i
Dedication	ii
Abstract	iii
Table of Contents	v
List of Tables	viii
List of Figures	x
Chapter One: Introduction	1
The Problem.....	3
Purpose.....	3
Significance and Rationale	4
Definitions	4
Chapter Two: Literature Review	5
Overview of the Anatomy of the Hand.....	5
Hand Anthropometric Data.....	6
Tools used to Gather Anthropometric Data for the Hand	9
Traditional Methods (Caliper and Tape Measure).....	9
Two-Dimensional Capture Tools (Flatbed Scanning and Photography)	12
Three-dimensional Scanning	15
Previous comparison studies of three-dimensional scanners for hand anthropometry	17
Standards for Measurement Comparison between Three-Dimensional Scanning and Traditional Methods (caliper and tape measure).....	22
Research Questions.....	22
Summary.....	23
Chapter Three: Methods	24
Setting	24
Participants.....	24
Tools	27
Traditional Methods (caliper and tape measure).....	27
Three-Dimensional Scanners	28
Landmarking.....	29
Measurements	32
Researcher Experience.....	34
Pilot.....	34
Data Collection	36

Traditional Anthropometric Measurement Process	36
Three-Dimensional Scanning Process	39
Three-Dimensional Scan Processing and Editing	41
Three-Dimensional Anthropometric Measurement Process	45
Data Analysis	48
Evaluation and Statistical Analysis.....	49
Anthropometric Tool Reliability Analysis.....	50
Anthropometric Tool Precision Analysis.....	51
Three-Dimensional Visual Analysis	52
Three-Dimensional Visual Reliability Analysis	55
Three-Dimensional Visual Precision Analysis	55
Hypotheses and Null Hypotheses	56
Summary.....	57
Chapter 4. Results for Anthropometric Tool Reliability Analysis and Anthropometric Tool Precision Analysis.....	58
Anthropometric Tool Reliability Analysis.....	58
Descriptive Statistics for the Anthropometric Tool Reliability Analysis	59
Comparison of the Mean of the Absolute Difference Values to ISO 20685:2018 for the Anthropometric Tool Reliability Analysis.....	60
One-Way ANOVA and Post-Hoc Analysis for the Anthropometric Tool Reliability Analysis	62
Results from for the Anthropometric Tool Reliability Analysis.....	64
Anthropometric Tool Precision.....	66
Descriptive Statistics for the Anthropometric Tool Precision Analysis	66
Comparison of the Mean of the Absolute Difference Values to ISO 20685:2018 for the Anthropometric Tool Precision Analysis.....	68
One-Way ANOVA and Post-Hoc Analysis for the Anthropometric Tool Precision Analysis	70
Results for the Anthropometric Tool Precision Analysis	71
Secondary Anthropometric Tool Precision Analysis.....	73
Descriptive Statistics for Secondary Anthropometric Tool Precision Analysis	73
One-way ANOVA for the Secondary Anthropometric Tool Precision Analysis	74
Results for the Secondary Anthropometric Tool Precision Analysis.....	75
Summary.....	76
Chapter 5. Three-Dimensional Visual Reliability and Three-Dimensional Visual Precision.....	77
Three-Dimensional Visual Reliability Analysis	84

Descriptive Statistics for Three-Dimensional Visual Reliability Analysis.....	85
One-Way ANOVA and Post Hoc Analysis for Three-Dimensional Visual Reliability Analysis	86
Results for the Three-Dimensional Visual Reliability Analysis	88
Three-Dimensional Visual Precision Analysis	89
Descriptive Statistics for the Three-Dimensional Visual Precision Analysis	90
One-Way ANOVA and Post-Hoc Analysis for the Three-Dimensional Visual Precision Analysis	91
Results for the Three-Dimensional Visual Precision Analysis	93
Connection between Three-Dimensional Visual Precision Analysis and Anthropometric Tool Precision Analysis.....	94
Summary	95
Chapter 6. Discussion and Conclusion	96
Discussion.....	96
Limitations	98
Recommendation for Future Research.....	99
Conclusions.....	100
Chapter 7. Bibliography.....	101

List of Tables

Table 1. Past Anthropometric Studies as Measurement Resources.	7
Table 2. Three-dimensional scanners previously used in hand anthropometric studies.	15
Table 3. Three-dimensional scanner comparing other methods in studies for hand anthropometry.	18
Table 4. Hand Breadth summary statistics provided by Gordon, Blackwell, et al. (2012).....	26
Table 5. Demographics of study participants based on the Hand Breadth range defined by Gordon, Blackwell, et al. (2012).....	26
Table 6. Tools for the traditional method (calipers and tape measure).....	28
Table 7. Comparison of specification for the full-color hand-held three-dimensional scanners organized following the 3D Hand Scanning Attributes Framework (3DHSAF) by Sokolowski, Griffin, & Chandrasekhar (2018).....	29
Table 8. Landmark Locations and Definitions.....	30
Table 9. Defined Measurements.	32
Table 10. Defined Measurements Definitions for Manual Measuring.	37
Table 11. Defined Measurements Definitions for Digital Measuring in Anthroscan.	46
Table 12. Post-Processing Visual Analysis Likert Scale (modified via Juhnke, Pokorny, and Griffin (2021).....	53
Table 13. Descriptive Statistics for Anthropometric Tool Reliability Analysis (mm).	59
Table 14. Mean of the Absolute Difference Values of the Differences for the Anthropometric Tool Reliability Analysis (mm).	60
Table 15. One-sample t-tests to assess significant difference from one (1) for the Mean of the Absolute Difference Values for the Anthropometric Tool Reliability Analysis.....	61
Table 16. Anthropometric Tool Reliability Analysis One-Way ANOVA.....	62
Table 17. Anthropometric Tool Reliability Analysis Post-Hoc Pairwise Analysis using Tukey Honestly Significant Difference (HSD) Method.	63
Table 18. Anthropometric Tool Reliability Analysis Results Summary.	65
Table 19. Anthropometric Tool Precision Analysis Descriptive Statistics (mm).	67
Table 20. Mean of the Absolute Difference Values of the Differences for the Anthropometric Tool Precision Analysis (mm).	68
Table 21. One-sample t-tests to assess significant difference from one (1) for the Mean of the Absolute Difference Values for the Anthropometric Tool Precision Analysis.....	69
Table 22. Anthropometric Tool Precision Analysis One-Way ANOVA.....	70

Table 23. Anthropometric Tool Precision Analysis Post-Hoc Pairwise Analysis using Tukey Honestly Significant Difference (HSD) Method.	71
Table 24. Anthropometric Tool Precision Analysis Results Summary.	72
Table 25. Secondary Anthropometric Tool Analysis Descriptive Statistics.	74
Table 26. Secondary Anthropometric Tool Precision Analysis One-Way ANOVA.	74
Table 27. Comparison of Results from the Anthropometric Tool Precision and Secondary Anthropometric Tool Precision Analysis One-Way ANOVA.	75
Table 28. Secondary Anthropometric Tool Precision Analysis Results Summary.	75
Table 29. Example of areas viewed for each location of the Post-Processing Visual Analysis Likert Scale (modified via Juhnke, Pokorny, & Griffin (2021)).	80
Table 30. Three-dimensional Visual Reliability Analysis Descriptive Statistics.	86
Table 31. Three-Dimensional Visual Reliability Analysis One-Way ANOVA.	87
Table 32. Three-dimensional Visual Reliability Analysis Post-Hoc Pairwise Analysis using Tukey Honestly Significant Difference (HSD) Method.	87
Table 33. Three-Dimensional Visual Reliability Results Summary.	88
Table 34. Three-Dimensional Visual Precision Analysis Descriptive Statistics.	90
Table 35. Three-Dimensional Visual Precision Analysis One-Way ANOVA.	92
Table 36. Three-Dimensional Visual Precision Analysis Post-Hoc Pairwise Analysis using Tukey Honestly Significant Difference (HSD) Method.	92
Table 37. Three-Dimensional Visual Precision Analysis Results Summary.	93

List of Figures

Figure 1. Bones of the Hand (Image from Lumley, Craven, & Tunstall, 2019).....	5
Figure 2. Types of calipers (from left to right: large sliding caliper, sliding caliper, and spreading caliper) (Image from Kouchi, 2020).	10
Figure 3. A caliper capturing the Hand Length measurement (Image from Gordon, Blackwell, Bradtmiller, et al., 2012).	10
Figure 4. How to measure with a tape measure (Image from Kouchi, 2020).	11
Figure 5. Hand positions used during traditional method (caliper and tape measure) (from right to left: flat hand and splayed hand positions) (Images from International Organization for Standardization, 2017).	11
Figure 6. Flatbed scanning (Image from Yu, Yick, Ng, & Yip, 2013).	12
Figure 7. Hand dimension measurement extraction on a 2D image using CorelDRAW software (Images from Yu, Yick, Ng, & Yip, 2013).	13
Figure 8. Relaxed hand position (Image from Vergara, Agost, & Bayarri, 2019).....	14
Figure 9. Completed three-dimensional printed hand before cleaning on the Creality CR-10 three-dimensional printer (image provided by the Earl E. Bakken Medical Devices Center at the University of Minnesota).	24
Figure 10. Hand Breadth measurement taken during the 2019 Minnesota State Fair through the Driven to Discover (D2D) research program.....	25
Figure 11. Poech Sliding Caliper (image from Gordon, Blackwell, et al., 2012).....	28
Figure 12. Fully landmarked hand (Palmar and Dorsal side).	30
Figure 13. Comparison of visual quality of new Occipital Structure Sensor (Mark II) on the Palmar (A) and Dorsal (B) to the original Structure Sensor Palmar (C) and Dorsal (D).....	35
Figure 14. Data Collection Summary.	36
Figure 15. Scanning area diagram.	39
Figure 16. Slow paneling scanning method.	40
Figure 17. Smooth motion scanning method.	41
Figure 18. Original, unedited Occipital Structure scan in Meshmixer.	42
Figure 19. Edited Occipital Structure scan in Meshmixer.	42
Figure 20. Occipital Structure scan in Meshmixer with visible cracks.....	43
Figure 21. Edited hand with cracks filled.	43
Figure 22. Editing of the Artec Leo scan in Artec Studio 14 Professional Software.....	44

Figure 23. Adding texture/color to the Artec Leo scan in Artec Studio 14 Professional Software.	44
Figure 24. Digital Landmarking in Anthroscan.	45
Figure 25. Interaction between Data Collection and Data Analysis.	48
Figure 26. Statistical Analysis.	50
Figure 27. Overview of Anthropometric Tool Reliability Analysis and Anthropometric Tool Precision Analysis.....	58
Figure 28. Overview of Visual Analysis.....	77
Figure 29. The three (3) scans taken with the Occipital Structure Sensor for each participant.	84
Figure 30. The three (3) scans taken with the Artec Leo for each participant.	85
Figure 31. Final scans from original three-dimensional scan used to create the three-dimensional printed model.	89
Figure 32. Final scans taken with the Occipital Structure Sensor.....	89
Figure 33. Final scans taken with the Artec Leo.....	90
Figure 34. The Three-Dimensional Visual Analysis of the Fingertips of Digits 2 and 3 (visible landmarks at this location occurred at P1, P2, P7, P10, P11, and P12).	95
Figure 35. Opportunities from the validation of full-color, hand-held three-dimensional scanners.	97
Figure 36. Visual Analysis from Occipital Structure Sensor (Top Row) and Artec Leo (Bottom Row).....	98

Chapter One: Introduction

Anthropometry is the study and analysis of the human bodies' shape and size. Anthropometric data helps researchers and designers see how significantly the dimensions, proportions, and shape of human bodies vary (Gupta, 2014).

Hand anthropometric data is used to develop and size a wide variety of products and helps designers and manufacturers create products that interact with the hand to improve work efficiency, comfort, and safety (Vergara, Agost, & Gracia-Ibáñez, 2018).

Researchers rely on tools to assist in capturing hand anthropometric data. Many different tools are available for gathering anthropometric data from the hand, including traditional methods (caliper and tape measure), two-dimensional capture (flatbed scanning and photography), and three-dimensional scanning tools.

Traditional methods, which includes the use of caliper and tape measure, have been used in a wide variety of studies to collect anthropometric measurements from the hand (White, 1980, Gordon, Churchill, Clauser, et al., 1989, Gordon, Bradtmiller, et al., 2012, and Robinette, Blackwell, Daanen, et al., 2002). The caliper is used to take linear measurements, such as length and depth, while the tape measure is used to record the human body's lengths at surface measurements, such as circumferences (Gupta, 2014). Traditional methods (caliper and tape measure) have been used to collect measurements from the hand in either a flat or splayed hand position (International Organization for Standardization, 2017).

Flatbed scanners (Yu, Yick, Ng, & Yip, 2013, and Hsiao, Whitestone, Kau, & Hildreth, 2015) and photography (Habibi, Soury, & Zadeh, 2013, Vergara, Agost, & Gracia-Ibáñez, 2018, and Vergara, Agost, & Bayarri, 2019) have assisted in gathering anthropometric data of the hand from two-dimensional captures. Flatbed scanners capture two-dimensional images of the hand by placing the participant's hand directly on the scanning screen with the palm facing down.

Photography includes placing the participant's hand on a sheet of gridded paper or with a ruler in the background for scale. Photographs can then be taken of the hand with the palmar or dorsal side facing the camera. Images of the thumb have also been taken from different angles using photographs to test the ability to take more measurements from the digits (Vergara, Agost, & Gracia-Ibáñez, 2018). With flatbed scanning and photography, two-dimensional images can be imported into a computer software program to measure the hand dimensions. The use of two-dimensional capture tools only provides linear measurements. Traditional methods (caliper and tape measure) (Hsiao, Whitestone, Kau, & Hildreth, 2015) or estimation and calculation (Yu,

Yick, Ng, & Yip, 2013) are used instead to gather circumferences, depth, and surface measurements, which are not possible using two-dimensional capture tools.

The use of three-dimensional scanning has become an increasingly viable method for capturing anthropometric data of the hand. A wide variety of three-dimensional scanners have been validated for or have previously been used to collect anthropometric data from the hand (Li, Chang, Dempsey, Ouyang, & Duan, 2008, Klepser, Babin, Loercher, et al., 2012, Yu, Yick, Ng, & Yip, 2013, Nasir, Troynikov, & Watson, 2015, Hoevenaren, Maal, Krikken, et al., 2018, Griffin, Sokolowski, Lee, et al., 2018, Seifert, Curry, & Griffin, 2019, Pokorny, Seifert, Griffin, et al., 2019, and Dunbar & Chapates, 2019). Many studies that have previously used three-dimensional hand scanning collect scans of the hand in the splayed hand position. However, three-dimensional scanning also allows for the ability to gather anthropometric hand data from functional hand positions. Functional hand positions consist of the hand in task-orientated or dynamic positioning. Three-dimensional scanning also allows for the collection of surface measurements.

Many companies use anthropometric measurements obtained from a defined average to create a base size for their products. For products like gloves, where sizes increase or decrease, alternative sizing is graded proportionally to the base size. Hands can be very different and rarely fit the defined proportion. Hands can differ in size depending on various factors, such as gender, race, age, and occupational group (Hsiao, Whitestone, Kau, & Hildreth, 2015). Verga, Agost, & Bayarri (2019) found nine (9) independent combinations of palm and hand shapes, of which five (5) appeared more frequently. Even though the size and proportions of hands vary, many products created for the hand do not have alternative sizing, which leads the users to experience poor fit with the product.

When gloves fit incorrectly, it can interfere with productivity and lead to a hand injury. When gloves are too small, they can cause hand fatigue. When gloves are too big, they can get caught in machinery, causing serious injury (Padron, 2018). A tight-fitting glove can constrict finger circulation and may increase the risk of injuries. On the other hand, gloves that fit too loosely hinder the accomplishment of tasks that require fine dexterity and gripping (Hsiao, Whitestone, Kau, & Hildreth, 2015).

The Bureau of Labor Statistics reported that in 2018, 43 percent of upper extremity injuries in the United States occurred on the hand (Bureau of Labor Statistics). According to a report from the Occupational Safety & Health Administration (OSHA), 70.9 percent of hand and arm injuries

could have been prevented if the individual would have used protective gloves (Baugh, 2020). However, workers will either not use or frequently remove gloves if they are uncomfortable (Padron, 2018).

To improve glove fit and sizing, broader and more diverse databases of hand anthropometric data are essential. Hand-held three-dimensional scanners allow for research to occur outside of a lab setting. The use of hand-held three-dimensional scanners also allows for collecting hand anthropometric data from varying hand positions. Gaining more information on critical measurements and measurement changes found in varying hand positions could significantly impact the future design of products that interact with the hand.

The Problem

Full-color, hand-held three-dimensional scanners may provide further opportunities for collecting hand anthropometric data. No other full-color, hand-held three-dimensional scanner has been validated to collect hand anthropometric data as of this writing. Validation studies have previously taken place using three-dimensional scanners to collect anthropometric data from the hand; however, they have lacked color-capture capabilities (Li, Chang, Dempsey, Ouyang, & Duan, 2008 and Yu, Yick, Ng, & Yip, 2013), are not hand-held (Yu, Yick, Ng, & Yip, 2013 and Dunbar & Chapates, 2019), or needed further analysis to confirm viability (Pokorny, Seifert, Griffin, et al., 2019). The validation of tools is vital to ensure the integrity of the data that they produce. However, there is a need to test a method for validating the reliability and precision between traditional methods (caliper and tape measure) and three-dimensional scanning for hand anthropometry. Three-dimensional scanning includes visual analysis of the scans produced, which has mostly been referenced in passing within past research studies and has yet to be analyzed in comparison studies.

Purpose

The purpose of this study was to examine the reliability and precision of three (3) different tools for collecting anthropometric data of the hand. The tools compared in this study include traditional anthropometric tools (caliper and tape measure) and two (2) full-color hand-held three-dimensional scanners (Occipital Structure Sensor and Artec Leo). Additionally, a visual analysis of the three-dimensional models provided from the two (2) full-color hand-held three-dimensional scanners occurred in the post-processing stage to determine the three-dimensional visual reliability and three-dimensional visual precision.

The remainder of this chapter will explain this research's significance and rationale and end with a list of key terms. Chapter two discusses and critiques the previous literature. Chapter three shares the methodology behind the research. Chapter four presents the results of the reliability and precision of the three (3) different tools for collecting anthropometric data of the hand. Chapter five presents the visual analysis results that address both the three-dimensional visual reliability and three-dimensional visual precision. Chapter six concludes with a discussion of the results, as well as future research recommendations.

Significance and Rationale

The information provided in this study will benefit the collection of anthropometric data for the hand. This study will validate two (2) different full-color hand-held three-dimensional scanning tools. It will also provide a method for visual analysis of the three-dimensional models provided by three-dimensional scanners to determine the three-dimensional visual reliability and three-dimensional visual precision. Ultimately, these processes will lead to more opportunities to collect data for the hand, which will help design products that interact with the hand.

Definitions

Anthropometric Tool Reliability- the ability for each anthropometric tool to measure and collect data consistently.

Measurement Error- variability between measurement values.

Intra-observer reliability- the ability of the same observer to obtain consistent measurements.

Anthropometric Tool Precision- the exactness and accuracy of the measurement technique.

Three-Dimensional Visual Reliability- the ability for each scanner to capture the scan consistently.

Three-Dimensional Visual Precision- the exactness and accuracy of the final scans used for digital measuring.

Functional hand position- the hand is in task-orientated or dynamic positioning.

Flat hand position- the hand is flat, fingers are held together, and thumb stays in a natural position.

Splayed hand position- the hand is stretched out flat with fingers spread.

Chapter Two: Literature Review

There is a long history and evolution to the processes and techniques used to collect anthropometric data. For a long time, this data was used to understand human populations. Now, anthropometric data can be used to influence design, sizing, and manufacturing. Over time, many different tools have been used to capture anthropometric data and data collection has become more focused on specific areas, such as the hand. The act of measuring the hand itself is complex. As hand anthropometric data has expanded and technology improved, we are now at a point where we need to expand how we use this data, which requires different evaluation techniques.

This chapter examines the anatomy of the hand, hand anthropometric data, tools used to collect hand anthropometric data, and previous studies that have compared three-dimensional scanners to other anthropometric measurement capture tools.

Overview of the Anatomy of the Hand

There are 27 bones in the human hand, include eight (8) carpus bones, five (5) metacarpal bones, and fourteen (14) phalanges bones (see Figure 1). The eight (8) carpus bones form two (2) rows with four (4) bones in each row. The carpus bones' proximal row consists of the scaphoid, lunate, triquetrum, and pisiform. The carpus bones' distal row includes the trapezium, trapezoid, capitate, and hamate. There are five (5) metacarpal bones, which form the palm. The metacarpal heads produce the knuckles, and the base articulates with the bones in the carpus's distal row. There are fourteen (14) phalanges bones. There are three (3) bones in each of the fingers (from tip to base: distal, middle, and proximal), except the thumb, which has two (2) bones (from tip to base: distal and proximal) (Standring, 2016 and Lumley, Craven, & Tunstall, 2019).



Figure 1. Bones of the Hand (Image from Lumley, Craven, & Tunstall, 2019).

The hand's functions rely on complex interactions between the bones, ligaments, and muscles to carry out a wide variety of complicated tasks every day (Panchal-Kildare & Malone, 2013). The hand can reach, grasp, and manipulate objects. It is a sensory and tactile organ that can identify an objects' properties (such as texture or thermal). Additionally, the hand offers an alternative source of non-verbal communication through gestures, writing, or touch (Jones & Lederman, 2006 and Hirt, Seyhan, Wagner, & Zumhasch, 2017).

Hand Anthropometric Data

The following section examines the application and collection of hand anthropometric data. It also reviews common anthropometric hand measurements seen in previous studies.

Hand anthropometric data can be applied to improve the fit and sizing of various products, including gloves. Gloves are worn in a variety of settings. They have many uses ranging from protecting the hand against possible hazards (weather, chemicals, abrasion, cuts, scrapes, and blood/bodily fluids) to protecting delicate objects from the hand's oils, such as artifacts and computer chips. Occupational fields, such as construction and healthcare, rely on tools that are fit for the hand to conduct their work safely and effectively.

Anthropometric data is collected from the hand by using tools to collect selected measurements. The tools available to collect anthropometric data from the hand include traditional methods (caliper and tape measure), two-dimensional capture (flatbed scanning and photography), and three-dimensional scanning. Landmarks can be placed on anatomical locations to assist in capturing a particular measurement. The definitions of landmark locations are imperative to measuring, as errors in landmark locations could lead to issues in the design, sizing, and fitting of products (Gupta, 2020). Anthropometric data provides designers and researchers with statistical information from specific defined measurements for a population.

Most large anthropometric studies of the body include simple hand measurements, such as Hand Breadth, Hand Length, and Hand Circumference. These measurements directly correlate with the measurements frequently seen in sizing charts for gloves and other products that interact with the hand (Kwon, Jung, You, & Kim, 2009).

An overview of the types of measurements (lengths, breadths, and circumferences), locations of the measurements, and which past anthropometric studies reference the measurement's location are shown in Table 1.

Table 1. Past Anthropometric Studies as Measurement Resources.

Type of Measure	Location of Measurements	Past Anthropometric Studies that Reference the Location of Measurement
Length (Perpendicular)	Hand	White, 1980, Gordon, Churchill, Clauser, et al., 1989, Gordon, Blackwell, Bradtmiller, et al., 2012, Robinette, Blackwell, Daanen, et al., 2002, International Organization for Standardization, 2017, Greiner, 1991, Yu, Yick, Ng, & Yip, 2013, Hsiao, Whitestone, Kau, & Hildreth, 2015, Habibi, Soury, & Zadeh, 2013, Vergara, Agost, & Gracia-Ibáñez, 2018, Vergara, Agost, & Bayarri, 2019, Li, Chang, Dempsey, Ouyang, & Duan, 2008, and Dunbar & Chapates, 2019.
	Palm	White, 1980, Gordon, Blackwell, Bradtmiller, et al., 2012, International Organization for Standardization, 2017, Greiner, 1991, Yu, Yick, Ng, & Yip, 2013, Hsiao, Whitestone, Kau, & Hildreth, 2015, Habibi, Soury, & Zadeh, 2013, and Vergara, Agost, & Bayarri, 2019.
	Digit	International Organization for Standardization, 2017, Greiner, 1991, Yu, Yick, Ng, & Yip, 2013, Hsiao, Whitestone, Kau, & Hildreth, 2015, Habibi, Soury, & Zadeh, 2013, Vergara, Agost, & Gracia-Ibáñez, 2018, Li, Chang, Dempsey, Ouyang, & Duan, 2008, and Klepser, Babin, Loercher, et al., 2012.
	Digit link length	Greiner, 1991, Li, Chang, Dempsey, Ouyang, & Duan, 2008, Klepser, Babin, Loercher, et al., 2012, and Nasir, Troynikov, & Watson, 2015.
	Wrist to fingertips	Greiner, 1991, Yu, Yick, Ng, & Yip, 2013, and Vergara, Agost, & Bayarri, 2019.
	Root of finger to root of finger	Yu, Yick, Ng, & Yip, 2013.
Length (Surface)	Hand	Griffin, Sokolowski, Lee, et al., 2018 and Seifert, Curry, & Griffin, 2019.
	Webspace/Fingertip to finger crotch	Seifert, Curry, & Griffin, 2019 and Dunbar & Chapates, 2019.

	Root of the finger to knuckle	Nasir, Troynikov, & Watson, 2015.
	Knuckle to wrist on the dorsal side	Nasir, Troynikov, & Watson, 2015.
	Metacarpal-Phalangeal Joint Spread	Griffin, Sokolowski, Lee, et al., 2018 and Seifert, Curry, & Griffin, 2019.
	Phalangeal Spread	Griffin, Sokolowski, Lee, et al., 2018.
Breath	Hand	White, 1980, Gordon, Churchill, Clauser, et al., 1989, Gordon, Blackwell, Bradtmiller, et al., 2012, International Organization for Standardization, 2017, Greiner, 1991, Yu, Yick, Ng, & Yip, 2013, Hsiao, Whitestone, Kau, & Hildreth, 2015, and Dunbar & Chapates, 2019.
	Wrist	Greiner, 1991, Yu, Yick, Ng, & Yip, 2013, Habibi, Soury, & Zadeh, 2013, Vergara, Agost, & Gracia-Ibáñez, 2018, and Li, Chang, Dempsey, Ouyang, & Duan, 2008.
	Palm	Hsiao, Whitestone, Kau, & Hildreth, 2015 and Habibi, Soury, & Zadeh, 2013.
	Joints on digits	Gordon, Churchill, Clauser, et al., 1989, International Organization for Standardization, 2017, Greiner, 1991, Hsiao, Whitestone, Kau, & Hildreth, 2015, Habibi, Soury, & Zadeh, 2013, Vergara, Agost, & Gracia-Ibáñez, 2018, and Li, Chang, Dempsey, Ouyang, & Duan, 2008.
Circumferences	Hand	White, 1980, Gordon, Churchill, Clauser, et al., 1989, Gordon, Blackwell, Bradtmiller, et al., 2012, Robinette, Blackwell, Daanen, et al., 2002, Greiner, 1991, Yu, Yick, Ng, & Yip, 2013, Griffin, Sokolowski, Lee, et al., 2018, Seifert, Curry, & Griffin, 2019, and Dunbar & Chapates, 2019.
	Wrist	White, 1980, Gordon, Churchill, Clauser, et al., 1989, Gordon, Blackwell, Bradtmiller, et al., 2012, Greiner, 1991, Yu, Yick, Ng, & Yip, 2013, Li, Chang,

		Dempsey, Ouyang, & Duan, 2008, and Klepser, Babin, Loercher, et al., 2012.
	Joints on digits	Gordon, Churchill, Clauser, et al., 1989, International Organization for Standardization, 2017, Greiner, 1991, Yu, Yick, Ng, & Yip, 2013, Li, Chang, Dempsey, Ouyang, & Duan, 2008, Klepser, Babin, Loercher, et al., 2012, Seifert, Curry, & Griffin, 2019, and Dunbar & Chapates, 2019.
Depths	Digits	Vergara, Agost, & Gracia-Ibáñez, 2018 and Li, Chang, Dempsey, Ouyang, & Duan, 2008.
	Palm	Vergara, Agost, & Gracia-Ibáñez, 2018.
	Wrist	Vergara, Agost, & Gracia-Ibáñez, 2018.

Product considerations can help determine which measurements to use to collect the appropriate dimensions needed to assist with design, sizing, and fit. Inadequate and poor fitting products that interact with the hand reveal a need for new, more robust anthropometric measurements. The inclusion of surface measurements allowed by three-dimensional scanning, such as the fingers' webspace, provides more information on areas that have previously been unavailable for capture. Surface measurements could have implications on the design of products that interact with the hand.

Tools used to Gather Anthropometric Data for the Hand

There are various tools available to collect anthropometric data from the hand, such as traditional methods (caliper and tape measure), two-dimensional capture (flatbed scanning and photography), and three-dimensional scanning. The following section introduces the measurement tool, describes the hand positions that have been used for the tool, and gives an overview of each tool's limitations.

Traditional Methods (Caliper and Tape Measure)

Traditional methods rely on tools, such as calipers and tape measure, to collect anthropometric data from the hand. Traditional methods (caliper and tape measure) have been used in a wide variety of hand anthropometric studies (White, 1980, Gordon, Churchill, Clauser, et al., 1989, Gordon, Blackwell, Bradtmiller, et al., 2012, and Robinette, Blackwell, Daanen, et al., 2002) and continues to be used today.

Tools used in traditional methods (caliper and tape measure)

Calipers can collect linear measurements between two (2) landmarks (such as length, breadth, and depth). Three (3) types of calipers have been used in hand anthropometric studies, the large sliding caliper, sliding caliper, and spreading caliper (see Figure 2). A large sliding caliper can capture longer measurements from the body, while a sliding caliper can capture shorter ones. Spreading calipers can capture depth measurements (Kouchi, 2020). The overall design of calipers has not changed since its development in 1890 (Gupta, 2020).

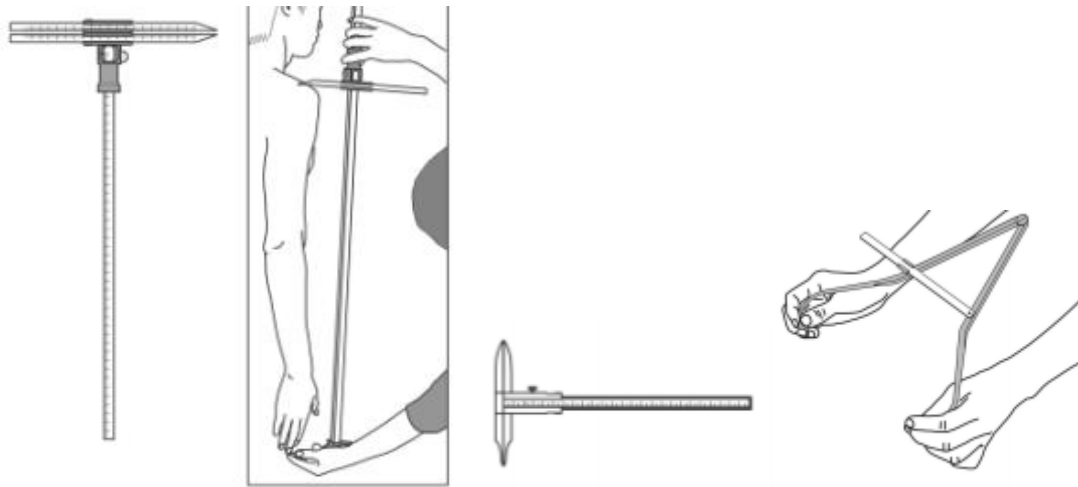


Figure 2. Types of calipers (from left to right: large sliding caliper, sliding caliper, and spreading caliper) (Image from Kouchi, 2020).

When taking a linear measurement on the hand, the caliper ends are lined up with the center of two (2) defined landmarks (see Figure 3).



Figure 3. A caliper capturing the Hand Length measurement (Image from Gordon, Blackwell, Bradtmiller, et al., 2012).

The tape measure was developed around 1820 and is used to collect surface and circumference measurements (Gupta, 2014). Tape measures can be made of steel or plastic, although most anthropometric studies use a steel tape measure (Gordon, Churchill, Clauser, et al., 1989 and Gordon, Blackwell, Bradtmiller, et al., 2012).

When using a tape measure to collect surface measurements, the tape passes over a series of defined landmarks. The tape measure's zero point should overlap the tape measure scale during use, as seen in Figure 4 (Kouchi, 2020).



Figure 4. How to measure with a tape measure (Image from Kouchi, 2020).

Hand positions used in traditional methods (caliper and tape measure)

The flat hand and splayed hand positions are the most common hand positions used in traditional methods (International Organization for Standardization, 2017). In the flat hand position, the hand is flat, the fingers are held together, and the thumb stays in a natural position. In the splayed hand position, the hand is flat and the fingers are spread apart (see Figure 5).

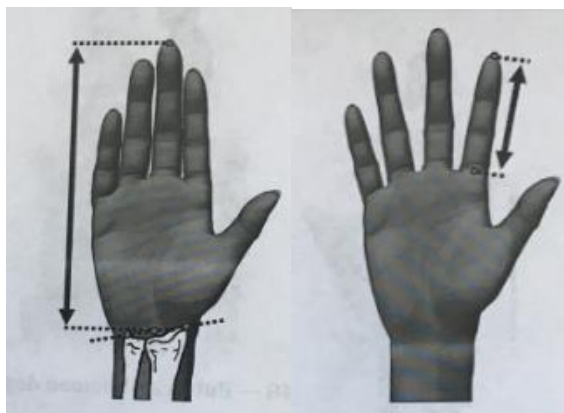


Figure 5. Hand positions used during traditional method (caliper and tape measure) (from right to left: flat hand and splayed hand positions) (Images from International Organization for Standardization, 2017).

Calipers and tape measure allow measurements to take place on the palmar and dorsal side of the hand. However, most hand anthropometric studies are performed on the hand's palmar side (Vergara, Agost, & Gracia-Ibáñez, 2018).

Limitations of traditional methods (caliper and tape measure)

The use of traditional methods (caliper and tape measure) requires time to complete the measurement for each person at the time of collection and it is prone to error (Kouchi, 2020). Errors can occur in traditional methods (caliper and tape measure) because it relies on the accuracy of the tool being used to collect the measurement and the capability of the individual taking the measure (Kouchi, Mochimaru, Bradtmiller, et al., 2012). Traditional methods can have low accuracy for hand studies due to the hand's complex anatomy and the influence of compression on the hand's tissues. During measurement, the hand's position can also influence the hand dimension results (Yu, Yick, Ng, & Yip, 2013).

Two-Dimensional Capture Tools (Flatbed Scanning and Photography)

One of the first studies to use two-dimensional capture (Greiner, 1991) occurred in correlation with the ANSUR I survey (Gordon, Churchill, Clauser, et al., 1989). Greiner (1991) collected two-dimensional images of hands using a photo box and digitized the hand to analyze the images. The use of two-dimensional images in this study allowed for a total of 72 measurements to occur on the hand, which was much more extensive than measurements previously gathered by traditional methods. More recently, flatbed scanners (Yu, Yick, Ng, & Yip, 2013 and Hsiao, Whitestone, Kau, & Hildreth, 2015) and photography (Greiner, 1991, Habibi, Soury, & Zadeh, 2013, Vergara, Agost, & Gracia-Ibáñez, 2018, and Vergara, Agost, & Bayarri, 2019) have been used for two-dimensional capture to gather anthropometric measurements of the hand.

Tools used in flatbed scanning

The flatbed scanners used for two-dimensional capture methods are scanner/copy machines (Yu, Yick, Ng, & Yip, 2013 and Hsiao, Whitestone, Kau, & Hildreth, 2015). A flatbed scanner can be used to capture a scanned image of the hand. That image can then be imported into computer software to measure the defined hand dimensions (see Figure 6).

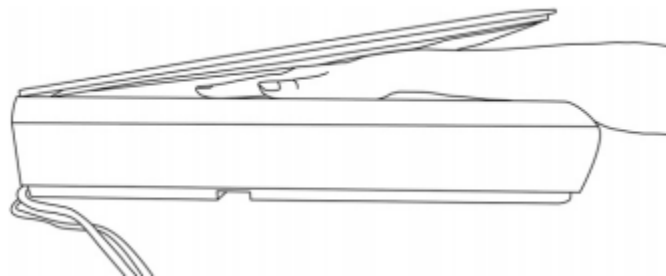


Figure 6. Flatbed scanning (Image from Yu, Yick, Ng, & Yip, 2013).

Hand positions used in flatbed scanning

In current studies that have used flatbed scanning, the hand was placed with the palm facing down in a splayed hand position (Yu, Yick, Ng, & Yip, 2013 and Hsiao, Whitestone, Kau, & Hildreth, 2015) (see Figure 7).



Figure 7. Hand dimension measurement extraction on a 2D image using CorelDRAW software (Images from Yu, Yick, Ng, & Yip, 2013).

Flatbed scanning allows only for linear measurements to take place. This method only captures the palmar side of the hand and does not capture the dorsal side. This method does not allow for complete data collection, as circumferences, surface, and depth measurements are not possible to take on a two-dimensional image. Due to the lack of data at these measurement locations, traditional methods (caliper) (Hsiao, Whitestone, Kau, & Hildreth, 2015) or estimation/calculation (Yu, Yick, Ng, & Yip, 2013) are used to gain complete data collection.

Limitations of flatbed scanning

As mentioned previously, the hand's positioning during flatbed scanning was with the hand flat on the scanning screen with the palm facing down, which only captures the palmar side of the hand. This method does not allow for measurements to be taken on the dorsal side of the hand. This method also only allows for linear measurement. Circumferences, surface, and depth measurements are not possible to take on a two-dimensional image.

Due to poor contact with the scanning screen, three-dimensional hand models have been found to provide inconsistent results, leading to accurate measurement capture (Yu, Yick, Ng, & Yip, 2013).

Tools used in photography

Photography can be used to create a two-dimensional image of the hand, and that image can then be imported into computer software to measure the defined hand dimensions.

Hand positions used in photography

Within current studies, the hand was placed in a relaxed position (Habibi, Soury, & Zadeh, 2013, Vergara, Agost, & Gracia-Ibáñez, 2018 and Vergara, Agost, & Bayarri, 2019) (see Figure 8).



Figure 8. Relaxed hand position (Image from Vergara, Agost, & Bayarri, 2019).

Although photography allows for two-dimensional images of the hand to be taken from the dorsal and palmar side, it still does not capture circumferences, surface, or depth measurements.

Traditional methods (caliper and tape measure) (Habibi, Soury, & Zadeh, 2013, Vergara, Agost, & Gracia-Ibáñez, 2018 and Vergara, Agost, & Bayarri, 2019) have been used to capture any incomplete data collection.

Limitations of photography

Photography allows for linear measurement to be taken on the hand. Circumferences, surface, and depth measurements are not possible to take on a two-dimensional image.

Studies using photography rely on ensuring the photograph's scale was correct by using a ruler or gridded sheet of paper (Habibi, Soury, & Zadeh, 2013, Vergara, Agost, & Gracia-Ibáñez, 2018 and Vergara, Agost, & Bayarri, 2019), however, distortion can still occur. Distortion can be minimized using the highest camera zoom and adjusting the camera's distance to frame the hand (Vergara, Agost, & Gracia-Ibáñez, 2018).

Three-dimensional Scanning

Previous studies have used three-dimensional scanning for the collection of anthropometric data from the full-body (Robinette, Blackwell, Daanen, et al., 2002, Ashdown, Loker, Schoenfelder, & Lyman-Clarke, 2004, Hsiao, Whitestone, & Kau, 2007, Apeageyi, 2010, Gordon, Blackwell, Bradtmiller, et al., 2012, and Hsiao & Cooke, 2013), the head (Skals, Ellena, Subic, Mustafa, & Pang, 2016, Zhuang, Slice, Benson, Lynch, & Viscusi, 2010, and Hsiao & Cooke, 2013), and the feet (Park, 2013, Chen, Chang, Wang, & Tsao, 2018, and Irzmańska & Okrasa, 2018).

An assortment of three-dimensional scanners have been compared against other tools to validate them or have previously been used to collect anthropometric data from the hand (Li, Chang, Dempsey, Ouyang, & Duan, 2008, Klepser, Babin, Loercher, et al., 2012, Yu, Yick, Ng, & Yip, 2013, Nasir, Troynikov, & Watson, 2015, Hoevenaren, Maal, Krikken, et al., 2018, Griffin, Sokolowski, Lee, et al., 2018, Seifert, Curry, & Griffin, 2019, Pokorny, Seifert, Griffin, et al., 2019, and Dunbar & Chapates, 2019).

The use of three-dimensional scanning for hand anthropometry allows for the capture of functional positioning. It allows for further measurement extraction that may assist with further design implications, such as the webspace or the fingertip to finger crotch area.

Tools used in three-dimensional scanning

As technology increases, a wide variety of three-dimensional scanners have either been compared against other methods or have previously been used to collect anthropometric data from the hand (see Table 2).

Table 2. Three-dimensional scanners previously used in hand anthropometric studies.

Scanner Name	Laser vs Light	Color-Capture ability	Hand-held capability	Study
FastSCAN Cobra	Laser	No color capture	Held-held, not wireless	Li, Chang, Dempsey, Ouyang, & Duan, 2008
Creaform Ergo Handyscan	Laser	No color capture	Hand-held, not wireless	Klepser, Babin, Loercher, et al., 2012
NextEngine Inc.	Laser	No color capture	Stationary	Yu, Yick, Ng, & Yip, 2013

3D INFOOT Scanner	Laser	No color-capture	Stationary	Nasir, Troynikov, & Watson, 2015
3dMD Full Motion Capture Photogrammetric System with the 3dMDface set-up	Light	Color capture	Stationary	Hoevenaren, Maal, Krikken, et al., 2015
Occipital Structure Sensor	Light	Color capture	Hand-held, wireless	Griffin, Sokolowski, Lee, et al., 2018 and Seifert, Curry, & Griffin, 2019
Artec Eva	Light	Color Capture	Hand-held, not wireless	Pokorny, Seifert, Griffin, et al., 2019
3dMD Full Motion Capture Photogrammetric System with the 3dMDhand set-up	Light	Color capture	Stationary	Dunbar & Chapates, 2019

Choosing a three-dimensional scanner that will facilitate all of the needs for scanning the hand is essential to a hand anthropometric study's success. Sokolowski, Griffin, & Chandrasekar (2018) created the minimum three-dimensional scanner guidelines for hand anthropometric studies for choosing a three-dimensional scanner. A three-dimensional hand scanner must have the ability to capture any participant's hand and wrist, including the hand being in various functional positions. Three-dimensional hand scanners must have the ability to capture any skin color to obtain a database that reflects a diverse array of participants. A three-dimensional hand scanner should also achieve visual clarity of the landmarks used for anthropometric measurement gathering. Ideally, the resolution on the three-dimensional hand scanner should produce scans with clear visibility of the skin folds and wrinkles of the hand. The three-dimensional hand scanner's output should also be usable in different software packages to measure or assist with design purposes. Finally, a three-dimensional hand scanner should be portable to travel (Sokolowski, Griffin, & Chandrasekar, 2018).

Hand positions used in three-dimensional scanning

Most of the studies that have previously used three-dimensional hand scanning to collect anthropometric data from the hand have collected scans of the hand in the splayed hand position (Li, Chang, Dempsey, Ouyang, & Duan, 2008, Klepser, Babin, Loercher, et al., 2012, Yu, Yick, Ng, & Yip, 2013, Hoevenaren, Maal, Krikken, et al., 2018, Griffin, Sokolowski, Lee, et al., 2018,

Seifert, Curry, & Griffin, 2019, Pokorny, Seifert, Griffin, et al., 2019, and Dunbar & Chapates, 2019).

Functional hand positions have also been collected using three-dimensional hand scans. The results from each of these studies have shown statistically significant areas of change occurring within certain areas or in specific measurements that could affect the design of products that interact with the hand (Nasir, Troynikov, & Watson, 2015, Griffin, Kim, Carufel, Sokolowski, Lee, & Seifert, 2019, and Seifert, Curry, & Griffin, 2019).

Limitations to three-dimensional scanning

Some limitations of three-dimensional scanning include the cost of purchase and the possibility of incomplete data (Istook & Hwang, 2001). Successful three-dimensional scanning relies on the technology of the scanner, any software used within post-processing and analysis, the skill in applying digital landmarks and taking digital measurements and limiting the amount of sway from the participant during scanning (Kouchi, Mochimaru, Bradtmiller, et al., 2012).

Although collecting three-dimensional scans is less time-consuming than traditional methods, it still relies on a certain amount of time for the participant to hold a position. The more time needed to scan, the more the possibility of involuntary hand movements and posture changes at any of the more than 20 segments/joints of the hand (Li, Chang, Dempsey, Ouyang, & Duan, 2008). Any involuntary movements or posture changes can lead to possible distortion in the three-dimensional scans gathered. There are two (2) options to assist with involuntary movements for the hand, through support systems/stability frames or by creating three-dimensional hand models. Support systems/stability frames can be built to assist with keeping the arm and hand in place. However, many of the support systems and stability frames rely on the participant placing their hands on a piece of plexiglass which could distort the hand (Li, Chang, Dempsey, Ouyang, & Duan, 2008, Klepser, Babin, Loercher, et al., 2012, and Griffin, Sokolowski, Lee, et al., 2018). Plexiglass can also cause issues with some three-dimensional scanners due to light-refraction. Three-dimensional hand models have been used to assist with minimizing involuntary movements, using various techniques including resin (Li, Chang, Dempsey, Ouyang, & Duan, 2008), plaster (Yu, Yick, Ng, & Yip, 2013), and three-dimensionally printed materials (Dunbar & Chapates, 2019).

Previous comparison studies of three-dimensional scanners for hand anthropometry

Three-dimensional scanners have been compared against other tools for collecting hand anthropometric data in several studies (Li, Chang, Dempsey, Ouyang, & Duan, 2008, Yu, Yick,

Ng, & Yip, 2013, Pokorny, Seifert, Griffin, et al., 2019, and Dunbar & Chapates, 2019). Table 3 describes the methods used, what comparison was made, the statistical analysis used, and the results of four (4) different comparison studies.

Table 3. Three-dimensional scanner comparing other methods in studies for hand anthropometry.

Study	Methods	Comparison	Statistical Analysis	Results
Li, Chang, Dempsey, Ouyang, & Duan (2008)	<p><u>Tools:</u> Traditional methods (caliper and tape measure) and FastSCAN Cobra™.</p> <p><u>Participants:</u> <u>Level One:</u> Resin hand model</p> <p><u>Level Two:</u> Resin hand model and live participants.</p> <p><u>Level Three:</u> Forty (40) participants, females.</p> <p><u>Notes:</u> Landmarks were placed on after scanning with a stylus due to a lack of color capture.</p>	<p><u>Level One:</u> Reliability through the repeatability of a three-dimensional scanning to digitally measure.</p> <p>Ten (10) scans were taken to create ten (10) samples.</p> <p><u>Level Two:</u> Compared traditional method (caliper and tape measure) to three-dimensional method for repeatability.</p> <p>Ten (10) measurements were taken using traditional methods on a live participant.</p> <p>Ten (10) scans were taken with the resin hand from that participant.</p> <p><u>Level Three:</u></p>	<p><u>Level One:</u> Descriptive Statistics (Min, Max, Mean, SD, CV).</p> <p><u>Level Two:</u> Descriptive Statistics (Mean and SD), Mean Difference, and Paired T-test.</p> <p><u>Level Three:</u> Descriptive Statistics (Mean, CV, SD), Mean Difference, and Paired T-test.</p>	<p><u>Level One:</u> Repeatability was found to be acceptable for the three-dimensional method, as all the standard deviations except hand length and wrist breadth were smaller than 1 mm.</p> <p><u>Level Two:</u> Repeatability was found to be acceptable for the three-dimensional method, as all the standard deviations except hand length, wrist breadth, and wrist circumference were smaller than 1 mm.</p> <p><u>Level Three:</u> Statistically significant difference occurred at nine (9) dimensions.</p> <p>39 of the 64 dimensions extracted by the three-dimensional scanner were compatible with traditional methods under the ISO</p>

		The compatibility of the 3-D method with the traditional method (caliper and tape measure) for 64 measurements with results to be validated according to ISO 20685: 2005 standard.		20685:2005 error specification (under 1 mm difference).
Yu, Yick, Ng, & Yip (2013)	<p><u>Tools:</u> Traditional methods (caliper and tape measure), two-dimensional capture using flatbed scanning (Method IM-I), and two (2) methods of three-dimensional scanning (Method IM-II and IM-III) (both used the NextEngine, Inc. scanner).</p> <p>Method IM-II combined ten (10) captures from a plaster hand on a rotatable disk.</p> <p>Method IM-III combined three (3) captures from a plaster hand laid flat on a surface.</p> <p><u>Participants:</u> Plaster hands from ten (10) participants (five (5) males and five (5) females).</p>	Compare two-dimensional scanning and two (2) methods for three-dimensional scanning against traditional methods (caliper and tape measure).	<p><u>Level One:</u> ANOVA and Sidak pairwise comparison tests for post-hoc analysis.</p> <p><u>Level Two:</u> Pearson correlation analysis.</p> <p><u>Level Three:</u> The root mean square error.</p>	<p><u>Level One:</u> Significant differences were found at 26 out of the 33 hand dimensions between the four (4) methods.</p> <p><u>Level Two:</u> Each method was highly correlated with one another.</p> <p><u>Level Three:</u> Three-dimensional scanning methods obtained results close to direct measurements.</p>
Pokorny, Seifert,	<u>Tools:</u>	Compared traditional	Descriptive Statistics	Statistically significant

<p>Griffin, et al., 2019</p>	<p>Traditional method (caliper and tape measure) and Artec Eva.</p> <p><u>Participants:</u> Ten (10) participants (five (5) men and five (5) women).</p>	<p>methods (caliper and tape measure) against the Artec Eva.</p>	<p>(Min, Max, Mean, SD, CI), Paired T-tests.</p>	<p>differences found in Hand Length and Hand Thickness.</p> <p>Results indicated that further analysis was needed to validate methods.</p>
<p>Dunbar & Chapates (2019)</p>	<p><u>Tools:</u> Traditional methods (caliper and tape measure) and 3dMD Full Motion capture photogrammetric system with 3dMDhand.t system (3dMD).</p> <p><u>Participants:</u> Three-dimensional printed hands from 5 participants (two (2) females and three (3) males).</p>	<p><u>Level One:</u> The repeatability of measuring one (1) participant's hand with traditional methods. Five (5) times.</p> <p><u>Level Two:</u> Comparison of traditional methods (caliper and tape measure) and 3dMD.</p> <p><u>Level Three:</u> Comparison of Traditional methods (caliper and tape measure), 3dMD, and three-dimensional printed hand.</p>	<p><u>Level One:</u> Measurement Values and SD.</p> <p><u>Level Two:</u> Measurement Values and Paired T-test.</p> <p><u>Level Three:</u> Measurement Values and Paired T-test.</p>	<p><u>Level One:</u> Used to analyze the skill levels of the researchers to determine who would measure (using traditional methods) in level two (2) and three (3).</p> <p><u>Level Two:</u> No statistical differences found between traditional methods (caliper and tape measure) and the 3dMD. Large p-values used to determine statistical significance, instead of a p-value of less than 0.05.</p> <p><u>Level Three:</u> No statistical differences found between traditional methods (caliper and tape measure), the 3dMD, and the three-dimensional printed hand. Large p-values used to determine statistical significance, instead of a p-value of less than 0.05.</p>

Previous studies that have compared tools for collecting hand anthropometric data tend to focus on the precision or accuracy of the anthropometric measurement tools (see Table 3). Many of the studies reported statistically significant differences to compare the precision of the tools used. Li, Chang, Dempsey, Ouyang, & Duan (2008) also validated the precision of the tools according to ISO 20685:2005 standard, which defines the maximum allowable error for hands at 1 mm when comparing measurements obtained using traditional methods (caliper and tape measure) and three-dimensional scanners (International Organization for Standardization, 2005). A review of the updated ISO 20685:2018 standard continues to suggest 1 mm as the maximum allowable error for the hand (International Organization for Standardization, 2018).

The reliability of different measurement tools for collecting anthropometric data of the hand was examined in two (2) of the four (4) comparison studies reviewed (Li, Chang, Dempsey, Ouyang, & Duan, 2008 and Dunbar & Chapates, 2019). Li, Chang, Dempsey, Ouyang, & Duan (2008) explored the reliability through repeatability of three-dimensional scanning to digitally measure a resin hand model. They also compared the reliability between traditional methods (caliper and tape measure) and three-dimensional scanning using the FastSCAN Cobra™. Within this analysis, they digitally measured hand scans from the resin hand model and traditionally measuring the real hand used to create the resin hand model. Statistically significant differences were attributed to the contact of the tool with the skin and landmark capture.

Dunbar & Chapates (2019) both digitally and traditionally measured three-dimensional printed hands. They tested reliability by assessing the operator's ability to capture traditional methods (caliper and tape). They used the information provided by this assessment to decide which researcher would take the measurements for the primary portion of the study to reduce intra-observer reliability. Intra-observer reliability is the ability of the same observer to obtain consistent measurements. They did not test the reliability of digitally measuring the scans provided by the three-dimensional scanner (the 3dMD Full Motion Capture Photogrammetric System with 3dMDhand set-up).

Visual analysis within three-dimensional scanning has mostly been referenced in passing within past research studies. Pokorny, Seifert, Griffin, et al., 2019 mentioned that the scans produced by the Artec Eva were of high quality, which included good landmark capture and detail visibility. Yu, Yick, Ng, & Yip (2013) compared two (2) different methods for capturing three-dimensional scans and briefly described three-dimensional scanning's visual aspect within their results. Descriptive words comparing scan quality between methods and images were used to illustrate the differences between capturing a full model (Yu, Yick, Ng, & Yip, 2013).

The most detailed description of visual analysis for three-dimensional scanning occurred in Dunbar & Chapates (2019). Since the 3dMD Full Motion Capture Photogrammetric System with 3dMDhand set-up captures multiple frames, each frame was reviewed. The best surface mesh was visually selected out of these frames to measure. The best surface mesh was defined as free of stray points, uniform mesh size, free of any artificial "webbing" in between the fingers, and free of errors in mapping the 2D color texture on the surface (Dunbar & Chapates, 2019).

Standards for Measurement Comparison between Three-Dimensional Scanning and Traditional Methods (caliper and tape measure)

The ISO 20685:2018 standard has been used to compare three-dimensional scanning and traditional methods (caliper and tape measure) (Li, Chang, Dempsey, Ouyang, & Duan, 2008).

The ISO 20685:2018 standard sets a maximum difference between measurements observed using traditional methods (caliper and tape measure), and the three-dimensional scanner for hand measurements was 1 mm. The recommended sample size to detect a statistically significant difference per ISO 20685:2018 standards is 40 test subjects (International Organization for Standardization, 2018).

Research Questions

Four research questions were developed to understand the reliability, precision, and repeatability between traditional methods (caliper and tape measure) and three-dimensional scanning.

Research Question One (RQ1): How reliable are traditional methods (caliper and tape measure), the Occipital Structure Sensor, and the Artec Leo are for gathering hand anthropometric data?

Research Question Two, part a (RQ2a): How precise are the three (3) tools (traditional methods (caliper and tape measure), the Occipital Structure Sensor, and the Artec Leo) are for collecting hand anthropometric measurements?

Research Question Two, part b (RQ2b): How does the inclusion of complete landmarking, that does not rely on independent identification of landmarks, impact the precision of the three-dimensional scans?

Research Question Three (RQ3): How reliable is the quality of the scans from the three-dimensional scanners (the Occipital Structure Sensor and the Artec Leo) for use in collecting hand anthropometric data?

Research Question Four (RQ4): How precise is the quality of the scans from the three-dimensional scanners (the Occipital Structure Sensor and Artec Leo), compared to each other and the original three-dimensional scan, for use in collecting hand anthropometric data?

Summary

Anthropometric data from the hand has been used to improve the fit and sizing of various products. Many different types of anthropometric measurements have been collected previously, including lengths, breadths, and circumferences. These measurements have been collected by various tools (traditional methods (caliper and tape measure), two-dimensional capture (flatbed scanning and photography), and three-dimensional scanning). Each anthropometric measurement tool has limitations to its uses for collecting anthropometric measurements. Some of the limitations seen within anthropometric measurement tools could create errors within the data they produce, which justifies their validation. Even though previous comparison studies have taken place using three-dimensional scanning, there is still a need to test a method for validating the reliability, precision, and repeatability between traditional methods and three-dimensional scanning for hand anthropometry.

Chapter Three: Methods

This chapter discusses the research methods, including the research purpose, setting, participants, tools, procedures, data analysis, and evaluation and statistical analysis.

The methods for this study were developed to evaluate the goals of this research purpose. This research aimed to assess all three (3) tools based on the data collection considerations of reliability and precision. Additionally, visual analysis of the three-dimensional models provided from the two (2) full-color hand-held three-dimensional scanners occurred in the post-processing stage to determine the three-dimensional visual reliability and three-dimensional visual precision.

Setting

Due to the COVID-19 pandemic, this study occurred in the researcher's place of residence located in Saint Paul, Minnesota.

Participants

For this study, twelve (12) three-dimensional hand scans were printed with a Creality CR-10 three-dimensional printer using white PLA materials by the Earl E. Bakken Medical Device Center (see Figure 9).

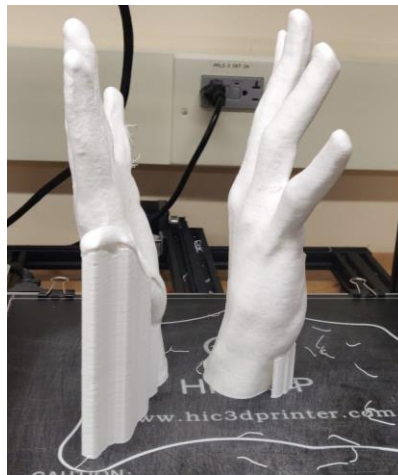


Figure 9. Completed three-dimensional printed hand before cleaning on the Creality CR-10 three-dimensional printer (image provided by the Earl E. Bakken Medical Devices Center at the University of Minnesota).

Three-dimensional printed hands were used to minimize possible inconsistencies and have been previously used in studies that have validated three-dimensional scanners (Li, Chang, Dempsey, Ouyang, & Duan, 2008, Yu, Yick, Ng, & Yip, 2013, and Dunbar & Chapates, 2019).

The twelve (12) three-dimensional hand scans chosen for this study were part of a more extensive database taken by the Human Dimensioning Lab at the University of Minnesota. Participants for this database were recruited at the 2019 Minnesota State Fair through the Driven to Discover (D2D) research program. The database included basic demographic information and manual hand breadth data for each participant (see Figure 10). The study's inclusion was based on a stratified sample of participants representing a distribution of 95% to 5% measurements of Hand Breadth. Stratified samples are essential in anthropometric studies because it provides better coverage of the population.



Figure 10. Hand Breadth measurement taken during the 2019 Minnesota State Fair through the Driven to Discover (D2D) research program.

Hand Breadth is one of the commonly used measurements (Hand Breadth, Hand Length, and Hand Circumference) seen in most large anthropometric studies and is frequently used in sizing charts for gloves and other products that interact with the hand (Kwon, Jung, You, & Kim, 2009).

The database taken by the Human Dimensioning Lab at the University of Minnesota was selected for use, as it is the first large-scale database of hand scans from civilians. Although this database used the Occipital Structure Sensor and the Artec Leo to capture hand scans, only scans taken with the Artec Leo were used for this study. The original three-dimensional hand scans used for this study were taken in the splayed hand position, as recommended by the International Organization for Standardization (2017).

For this study, Hand Breadth was determined based on the summary statistics provided by the ANSUR II database (Gordon, Blackwell, et al., 2012) (see Table 4). The participant's final demographics represent a range of Hand Breadth chosen to cover over 95% to under 5%. This study included six (6) male and six (6) female participants between 16 and 64 of Caucasian and Asian descent.

Table 4. Hand Breadth summary statistics provided by Gordon, Blackwell, et al. (2012).

Percentile	Female	Male
Over 95%	8.5 cm and over	9.6 cm and over
95% to 75% Male	8.5 cm to 8 cm	9.6 cm to 9.1 cm
75% to 50%	8 cm to 7.8 cm	9.1 cm to 8.8 cm
50% to 25%	7.8 cm to 7.5 cm	8.8 cm to 8.5 cm
25% to 5%	7.5 cm to 7.2 cm	8.5 cm to 8.1 cm
Under 5%	7.2 cm and under	8.1 cm and under

A visual assessment in Artec Studio 14 Professional took place to ensure the three-dimensional scans' quality for three-dimensional printing. The visual assessment of the three-dimensional scans consisted of reviewing three-dimensional scanned hands from the University of Minnesota database, which fit into the range of Hand Breadth. Deformities on the hand scans occurred due to involuntary hand movements and posture changes from the participants scanned. Minor deformities still occurred on the hand models used in this study. However, hand scans with significant deformities were disqualified.

The final demographics for the participants chosen for this study are seen in Table 5.

Table 5. Demographics of study participants based on the Hand Breadth range defined by Gordon, Blackwell, et al. (2012).

#	Hand Breadth range defined by Gordon, Blackwell, et al. (2012).	Hand Breadth	Gender Identification	Age	Race/Ethnicity
1	Over 95% Male (9.6 cm and over)	10.1 cm	Male	61	White
2	Over 95% Female (8.5 cm and over)	9.2 cm	Female	29	White
3	95% to 75% Male (9.6 cm to 9.1 cm)	9.3	Male	63	White
4	95% to 75% Female (8.5 cm to 8 cm)	8.1 cm	Female	44	White
5	75% to 50% Male (9.1 cm to 8.8 cm)	9.1	Male	56	White

6	75% to 50% Female (8 cm to 7.8 cm)	7.8	Female	64	White
7	50% to 25% Male (8.8 cm to 8.5 cm)	8.7	Male	23	White
8	50% to 25% Female (7.8 cm to 7.5 cm)	7.6	Female	36	White
9	25% to 5% Male (8.5 cm to 8.1 cm)	8.3	Male	51	White
10	25% to 5% Female (7.5 cm to 7.2 cm)	7.4	Female	58	White
11	Under 5% Male (8.1 cm and under)	7.4 cm	Male	16	Asian
12	Under 5% Female (7.2 cm and under)	7 cm	Female	38	White

Tools

This study examined three (3) different tools for collecting anthropometric data: traditional methods (caliper and tape measure), the Occipital Structure Sensor, and the Artec Leo. Two-dimensional image capture was not assessed in this comparison, as it does not capture circumferences, surface, or depth measurements.

Traditional Methods (caliper and tape measure)

The Lufkin Executive Diameter metric tape measure (W606PM) was used for the Wrist Circumference, Hand Circumference, and Index Finger Circumference at the Distal Interphalangeal Joint (Gordon, Blackwell, et al., 2012 and Dunbar & Chapates, 2019).

Gordon, Blackwell, et al. (2012) used a Poech Sliding Caliper to capture linear measurements of the hand. The Poech Sliding Caliper is a high-cost option (approximately \$2200) (see Figure 11). A more affordable option was chosen, which had similar design features to the Poech Sliding Caliper.

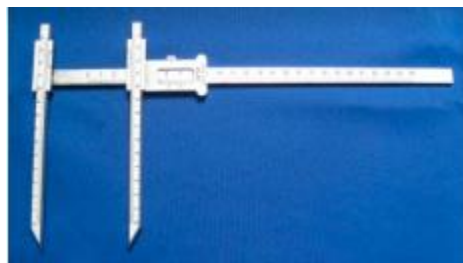





Figure 11. Poech Sliding Caliper (image from Gordon, Blackwell, et al., 2012).

The large bone caliper was used for more extended measurements that were difficult to capture with the small bone caliper, including Hand Length and Palm Length. The small bone caliper was used to obtain Hand Breadth, Index Finger Length, and Index Finger Breadth at the Distal Interphalangeal Joint.

Information on the tools chosen for this data collection method was analyzed before measuring and is located in Table 6.

Table 6. Tools for the traditional method (calipers and tape measure).

Specification	Cescorp Large Bone Caliper	Cescorp Small Bone Caliper	Lufkin Executive Diameter metric tape measure (W606PM)
Image			
Range	600 millimeters	180 millimeters	2 meters
Used for	Hand Length, Palm Length	Hand Breadth, Index Finger Length, Index Finger Breadth at Distal Interphalangeal Joint	Wrist Circumference, Hand Circumference, Index Finger Circumference at Distal Interphalangeal Joint
Cost	\$260.00	\$160.00	\$26.05

Three-Dimensional Scanners

For this study, two (2) full-color hand-held three-dimensional scanners were selected to be validated.

The Occipital Structure Sensor is a full-color hand-held three-dimensional scanner that works with an iPad. It can capture anatomical scans of the hand in roughly 1.5 to 2.5 minutes.

The Artec Leo is a wireless scanner that offers automatic onboarding processing and can capture anatomical scans in roughly 1 minute.

Information on the tools chosen for this data collection method was analyzed before three-dimensional scanning and is located in Table 7. The information in this table has been organized

according to the 3D Hand Scanning Attributes Framework (3DHSAF) by Sokolowski, Griffin, & Chandrasekhar (2018), which provides a checklist of critical three-dimensional scanner attributes needed to collect appropriate hand data, including color capture, file saving, hand-held compatibility, scanning envelope, scanner price, scan resolution, scanner size, scanner weight, and time to scan.

Table 7. Comparison of specification for the full-color hand-held three-dimensional scanners organized following the 3D Hand Scanning Attributes Framework (3DHSAF) by Sokolowski, Griffin, & Chandrasekhar (2018).

Specification	Occipital Structure Sensor	Artec Leo
Image		
Color/Texture Capture	Yes	Yes
File Saving	SDK/OBJ/STL	OBJ/PLY/WRL/STL/AOP/ASCII/PTX/E57/XYZRGB
Hand-held Compatibility	Yes	Yes
Scanner Envelope	400 mm high by 3500 mm wide	244 by 142 mm
Scanner Price	\$527.00	\$25,800.00
Scan Resolution	VGA (640 by 480 pixels)	2.3 megapixels
Scanner Size	119.9 mm L by 29 mm H by 28 mm W (affixes to an iPad)	231 mm H by 162 mm D by 230 mm W
Scan Technology	Structured Light	Structured Light (VCSEL)
Scanner Weight	0.1 kg plus iPad	2.6 kgs (5.7 lbs)
Time to Scan	Approximately 1.5 to 2.5 minutes	Approximately 1 minute

Landmarking

Fourteen (14) total landmarks were placed on the three-dimensional printed hands using blue 0.125" diameter circular dot stickers. The landmarking procedures are adapted from Griffin, Sokolowski, Lee, Seifert, Kim, & Carufel (2018). Landmarks were used to ensure that the

measurement was taken from the same location each time it was measured for each tool (Kouchi, 2020). Landmarks were placed at anatomical locations on the three-dimensional printed hand (see Figure 12 and Table 8).

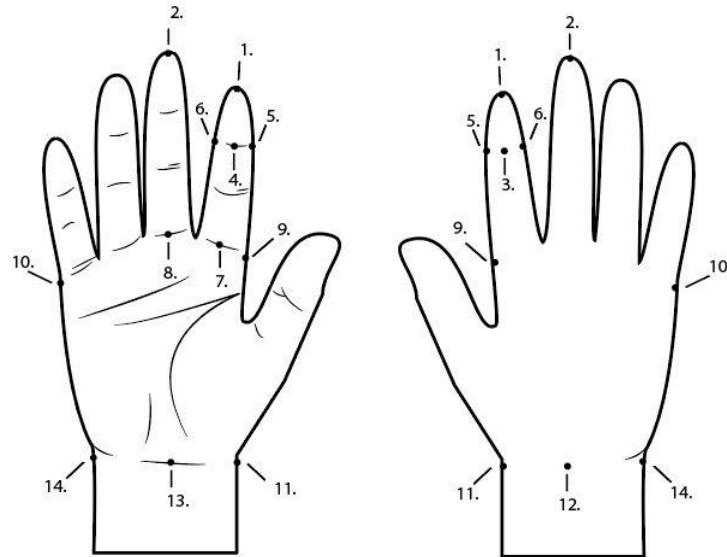


Figure 12. Fully landmarked hand (Palmar and Dorsal side).

Table 8. Landmark Locations and Definitions.

#	Landmark Locations	Used In:	Description
1.	Fingertip of Digit 2	Gordon, Churchill, et al. (1989) and Greiner (1991)	The center of the distal tip of digit 2.
2.	Fingertip of Digit 3	Gordon, Churchill, et al. (1989), Greiner (1991), Robinette, Blackwell, et al. (2002), and Gordon, Blackwell, et al. (2012)	The center of the distal tip of digit 3.
3.	Distal Interphalangeal Joint of Digit 2 (Dorsal side)	Greiner (1991)	The center of the dorsal side of the Distal Interphalangeal Joint of digit 2.
4.	Distal Interphalangeal Joint	Greiner (1991)	The center of the palmar side of the Distal Interphalangeal Joint of digit 2.

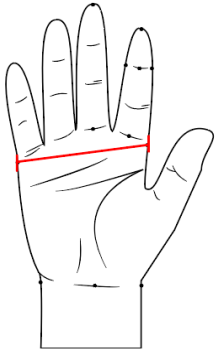
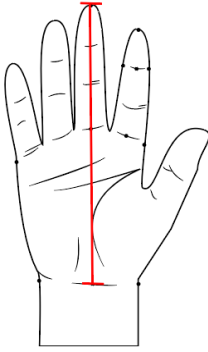
	of Digit 2 (Palmar side)		
5.	Distal Interphalangeal Joint of Digit 2 (Lateral side)	Greiner (1991)	The center of the lateral side of the Distal Interphalangeal Joint of digit 2.
6.	Distal Interphalangeal Joint of Digit 2 (Medial side)	Greiner (1991)	The center of the medial side of the Distal Interphalangeal Joint of digit 2.
7.	Base of Digit 2	Greiner (1991)	The center of the crease at the base of digit 2 on the palmar side.
8.	Base of Digit 3	Greiner (1991) and Gordon, Blackwell, et al. (2012)	The center of the crease at the base of digit 3 on the palmar side.
9.	Metacarpal 2	Gordon, Churchill, et al. (1989), Greiner (1991), Robinette, Blackwell, et al. (2002), and Gordon, Blackwell, et al. (2012)	The center of the lateral point of the Metacarpal Phalangeal Joint 2 (at the base of digit 2, on the outer edge of the three-dimensional printed hand).
10.	Metacarpal 5	Gordon, Churchill, et al. (1989), Greiner (1991), Robinette, Blackwell, et al. (2002), and Gordon, Blackwell, et al. (2012)	The center of the medial point of the Metacarpal Phalangeal Joint 5 (at the base of digit 5, on the outer edge of the three-dimensional printed hand).
11.	Radial Styloid (Lateral side)	Robinette, Blackwell, et al. (2002)	The inferior point of the bottom of the radius.
12.	Radial Styloid (Dorsal side)	Gordon, Churchill, et al. (1989), Greiner (1991), and Gordon, Blackwell, et al. (2012)	Using the inferior point of the bottom of the radius as reference, the extension of this landmark around the wrist to the dorsal side.
13.	Radial Styloid (Palmar side)		Using the inferior point of the bottom of the radius as reference,

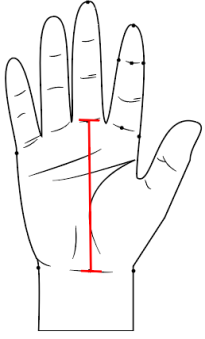
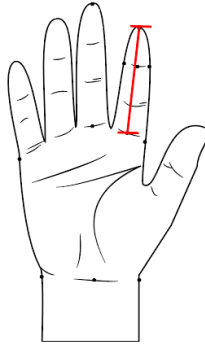
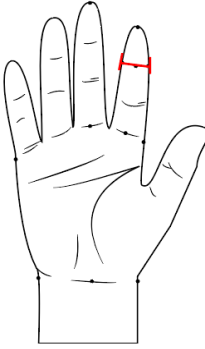
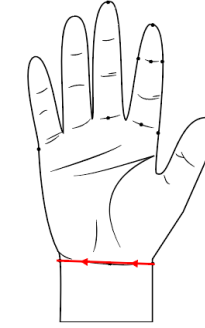
			the extension of this landmark around the wrist to the palmar side.
14.	Radial Styloid (Medial side)	Robinette, Blackwell, et al. (2002)	Using the inferior point of the bottom of the radius as reference, the extension of this landmark around the wrist to the medial side.

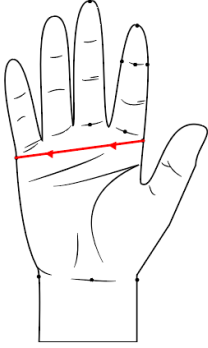
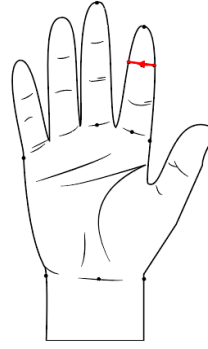
Measurements

The landmarks chosen for this study directly correlate to the eight (8) defined measurements being analyzed in this study (see Table 9). The eight (8) defined measurements for this study were identified through literature and previous anthropometric studies and were chosen to represent lengths, breadths, and circumferences at different areas of the hand.

Table 9. Defined Measurements.

Measurement Name	Used In:	Measurement Definition	Image
Hand Breadth	White (1980), Gordon, Churchill, et al. (1989), Greiner (1991), Gordon, Blackwell, et al. (2012), and International Organization for Standardization (2017)	The hand breadth is the distance from the Metacarpal 2 landmark to the Metacarpal 5 landmark measured perpendicular to the long axis of digit 3.	
Hand Length	White (1980), Greiner (1991), and International Organization for Standardization (2017) took this measurement on the palmar side.	The hand length is the distance from the Fingertip of Digit 3 landmark to the landmark located on the Radial Styloid (Palmar Side).	

<p>Palm Length</p>	<p>White (1980), Greiner (1991), Gordon, Blackwell, et al. (2012), and International Organization for Standardization (2017)</p>	<p>The palm length is the distance between the landmark located at the Base of Digit 3 to the landmark located on the Radial Styloid (Palmar Side).</p>	
<p>Index Finger Length</p>	<p>Greiner (1991), and International Organization for Standardization (2017)</p>	<p>The index finger length distance from the landmark located on the Fingertip of Digit 2 to the landmark located on the Base of Digit 2.</p>	
<p>Index Finger Breadth, Distal Interphalangeal Joint</p>	<p>Greiner (1991), and International Organization for Standardization (2017)</p>	<p>The index finger breadth at the distal interphalangeal joint is the distance between the landmark located on the lateral side of the Distal Interphalangeal Joint to the landmark located on the medial side of the Distal Interphalangeal Joint.</p>	
<p>Wrist Circumference</p>	<p>White (1980), Gordon, Churchill, et al. (1989), Greiner (1991), Gordon, Blackwell, et al. (2012), and International Organization for Standardization (2017)</p>	<p>The circumference of the wrist is measured by passing over the four (4) landmarks located on the Radial Styloid and around the wrist (Dorsal, Palmar, and Medial Side).</p>	

Hand Circumference	White (1980), Gordon, Churchill, et al. (1989), Greiner (1991), Robinette, Blackwell, et al. (2002), Gordon, Blackwell, et al. (2012), and International Organization for Standardization (2017).	The circumference of the hand is measured over the landmarks at Metacarpal 2 and Metacarpal 5.	
Index Finger Circumference, Distal Interphalangeal Joint	Greiner (1991), Robinette, Blackwell, et al. (2002), Yu, Yick, Ng, & Yip (2013), and International Organization for Standardization (2017).	The circumference of the Index Finger at the Distal Interphalangeal Joint is measured by passing over the landmarks located on the Distal Interphalangeal Joint of Digit 2 (Dorsal, Palmar, Lateral, Medial Side).	

Researcher Experience

Since 2016, I have held a position as a research assistant in the Human Dimensioning Lab at the University of Minnesota. This position has provided training and experience working with the tools and methods used in this study for anthropometric data collection for the hand.

I was self-trained in capturing three-dimensional images of the hand using the Occipital Structure Sensor. Since learning how to scan hands with the Occipital Structure Sensor, I have assisted in building methodologies and gathering hand scans for both small- and large-scale anthropometric studies. I have also trained others in the use of this scanner for capturing the hand.

I have attended over eight (8) hours of formal training on the Artec Leo with a trained operator.

Pilot

A pilot study was conducted to refine the methods used in this study with one (1) three-dimensional printed hand and to test a new version of the Occipital Structure Sensor (Mark II) against the original version.

During the pilot study, the scan capture quality for both scanners (the Occipital Structure Sensor and the Artec Leo) was compromised due to visual contrast occurring between the scanning surface (the circular cake stand topper) and the three-dimensional printed hand since both were white. The flat scanning surface (the circular cake stand topper) also had a glossy finish, which created light-refraction when scanning took place using the Artec Leo. A fabric in a darker color was used to create more visual contrast between the flat scanning surface (the circular cake stand topper) and the three-dimensional printed hand.

The scaling needed for the scans taken with the Occipital Structure Sensor and Artec Leo for Anthroscan was determined by scanning a fixed object. An eleven (11) inch by seven (7) inch box was scanned with both scanners (the Occipital Structure Sensor and the Artec Leo) and measured in Anthroscan. The scans from the Occipital Structure Sensor scale correctly into Anthroscan. The scans from the Artec Leo need to be scaled down to 0.001 in Anthroscan.

On occasion, both scanners (the Occipital Structure Sensor and the Artec Leo) had difficulty capturing complete landmarks for the hand in the pilot study. The scanning methods were adjusted to assist with landmark capture.

During the pilot study, extensive testing took place to compare the visual quality of the three-dimensional hand models provided by the Occipital Structure Sensor (Mark II) to the original Occipital Structure Sensor (see Figure 13). Scans capturing using Occipital Structure (Mark II) had significant flaws, including thicker fingers and webbing occurring between the fingers. The visual quality of the newer Occipital Structure Sensor (Mark II) was found not to be sufficient for completing anthropometric measurements of the hand than that of the Occipital Structure Sensor.

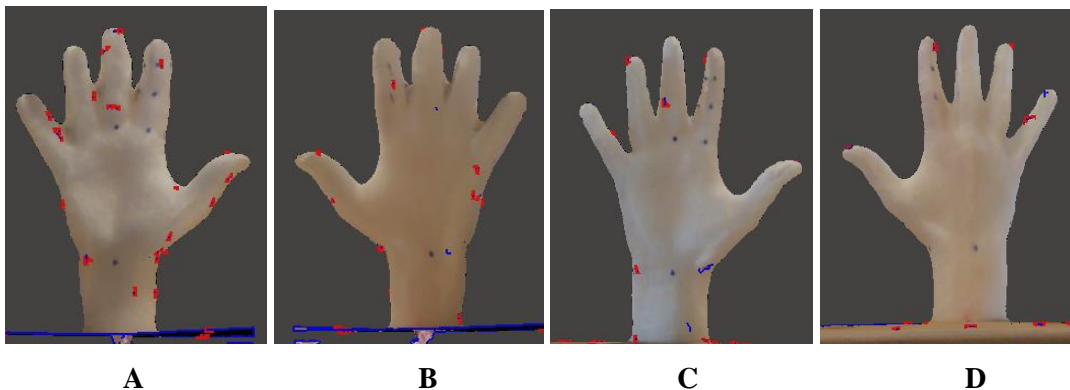


Figure 13. Comparison of visual quality of new Occipital Structure Sensor (Mark II) on the Palmar (A) and Dorsal (B) to the original Structure Sensor Palmar (C) and Dorsal (D).

Data Collection

The data collection for this study included anthropometric measurement processes using traditional methods (caliper and tape measure) and three-dimensional scanning (Occipital Structure Sensor and Artec Leo) (see Figure 14). After landmarking was completed, the traditional measurements took place with the three-dimensional printed hand using caliper and tape measure. The three-dimensional scanning process occurred, which included three-dimensional scanning, editing and processing the three-dimensional scans, and digitally measuring the three-dimensional scans. Two (2) data analysis types took place in this study, which included Measurement Analysis and Three-Dimensional Visual Analysis. Data analysis will be discussed in further detail below

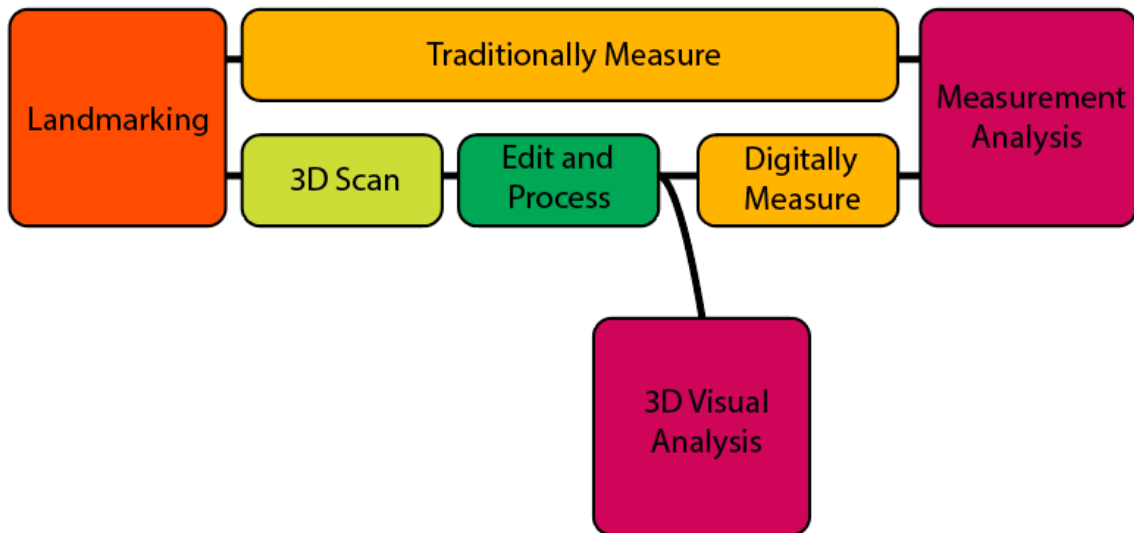









Figure 14. Data Collection Summary.


Traditional Anthropometric Measurement Process

Data collection for the traditional anthropometric measurement process took place with the three-dimensional printed hands for eight (8) defined measurements, which include Hand Breadth, Hand Length, Palm Length, Index Finger Length, Index Finger Breadth at the Distal Interphalangeal Joint, Wrist Circumference, Hand Circumference, and Index Finger Circumference at the Distal Interphalangeal Joint (see Table 10).

Table 10. Defined Measurements Definitions for Manual Measuring.

Measurement Name	Descriptions	Image
Hand Breadth	<p>The three-dimensional printed hand was measured on a flat surface with palm up. One end of the lower jaws of the sliding caliper was lined up on the landmark located at Metacarpal 2 and the other end of the lower jaws of the sliding caliper was lined up with the landmark located at Metacarpal 5.</p>	
Hand Length	<p>The three-dimensional printed hand was measured on a flat surface with palm up. One end of the lower jaws of the sliding caliper was lined up on the landmark located at Fingertip of Digit 3 and the other end of the lower jaws of the sliding caliper was lined up with the landmark located at the Palmar Stylium.</p>	
Palm Length	<p>The three-dimensional printed hand was measured on a flat surface with palm up. One end of the lower jaws of the sliding caliper was lined up on the landmark located at the Base of Digit 3 and the other end of the lower jaws of the sliding caliper was lined up with the landmark located at the Palmar Stylium.</p>	

<p>Index Finger Length</p>	<p>The three-dimensional printed hand was measured on a flat surface with palm up. One end of the lower jaws of the sliding caliper was lined up on the landmark located at the Fingertip of Digit 2 and the other end of the lower jaws of the sliding caliper was lined up with the landmark located at the Base of Digit 2.</p>	
<p>Index Finger Breadth, Distal Interphalangeal Joint</p>	<p>The three-dimensional printed hand was measured on a flat surface with palm up. One end of the lower jaws of the sliding caliper was lined up on the landmark located at Distal Interphalangeal Joint of Digit 2 on the lateral side and the other end of the lower jaws of the sliding caliper was lined up with the landmark located at Distal Interphalangeal Joint of Digit 2 on the medial side.</p>	
<p>Wrist Circumference</p>	<p>The three-dimensional printed hand was measured on a flat surface with palm down. The tape measure passes around the four (4) landmarks located on the Radial Styloid and around the wrist (Dorsal, Palmar, and Medial side) to gather the whole circumference of this area.</p>	
<p>Hand Circumference</p>	<p>The three-dimensional printed hand was measured on a flat surface with palm down. The tape measure passes around the landmark located at Metacarpal 2 and the landmark located at Metacarpal 5 to gather the whole circumference of this area</p>	

Index Finger Circumference, Distal Interphalangeal Joint	The three-dimensional printed hand was measured on a flat surface with palm down. The tape measure passes around all four (4) landmarks located at the Distal Interphalangeal Joint to gather the whole circumference of this area.	
--	---	--

Three-Dimensional Scanning Process

This section will discuss the data collection for the three-dimensional scanning process, including the room set-up for scanning, the scanners' calibration, scanning methods used for both scanners, the number of scans taken with each scanner, and how final scans were chosen.

Room Set-up for Scanning

The scanning room measured twelve (12) feet by nine (9) feet. A platform was placed in the center of the room to ensure a minimum of three (3) feet between them and the three-dimensional printed hand. The platform consisted of a cabinet with the following dimensions: 31.25 inches (H) by 23.7 inches (L) by 11.8 inches (W). A flat scanning surface was created, which raised the flat scanning surface height to 41.25 inches (see Figure 15). A piece of grey jersey fabric was used to cover the flat scanning surface. During the pilot study, placing a piece of fabric in a darker color was found to create more visual contrast between the flat scanning surface (the circular cake stand topper) and the three-dimensional printed hand to assist in scan capture.

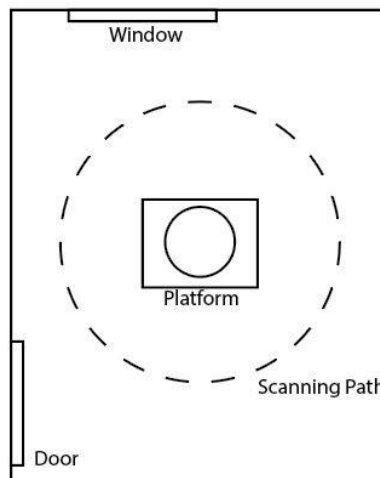


Figure 15. Scanning area diagram.

Calibration of Scanners

Prior to the scanning session, the Occipital Structure Sensor was calibrated using an application provided by Occipital.

The Artec Leo was delivered pre-calibrated.

Scanning using the Occipital Structure Sensor

Each scan was started by standing three (3) feet away from the scanning platform, facing the palm, and with the Occipital Structure Sensor at chest level. The way the Occipital Structure Sensor's software adds color and texture to an image is by capturing keyframes. Keyframes are full-color pictures taken from different angles that are then applied to the mesh afterward. Momentary pauses must take place every 10 to 15 degrees for two (2) to three (3) seconds to trigger a keyframe with the Occipital Structure Sensor. A slow paneling scanning method was used to scan the hand models (see Figure 16). One (1) full rotation was made around the scanning platform.

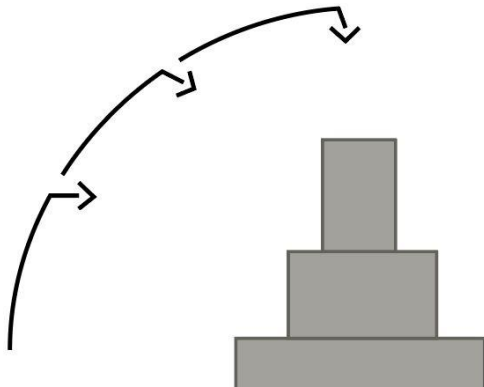


Figure 16. Slow paneling scanning method.

Scanning using the Artec Leo

Each scan was started by standing three (3) feet away from the scanning platform, facing the palm, and with the Artec Leo at chest level. To capture the hand model from all directions with the Artec Leo, a smooth motion scanning method was used (see Figure 17). The scan was complete after one (1) full rotation was made around the scanning platform.

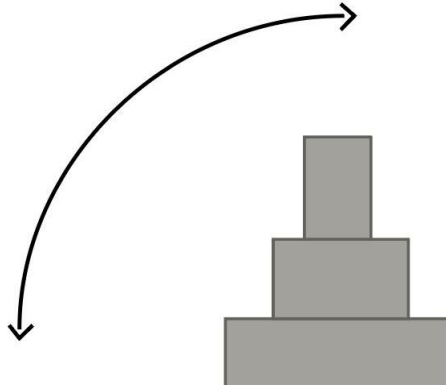


Figure 17. Smooth motion scanning method.

Number of Scans Taken

Three (3) scans were taken using both scanners (the Occipital Structure Sensor and Artec Leo) for each hand model.

Choosing Final Scans

The Visual Analysis Likert Scale results during the Three-Dimensional Visual Reliability Analysis were used to choose which of the three (3) scans taken using both scanners (the Occipital Structure Sensor and Artec Leo) will be the final scan. The Visual Analysis Likert Scale and the Three-Dimensional Visual Reliability Analysis will be discussed in detail below.

Three-Dimensional Scan Processing and Editing

Before measuring the three-dimensional scans, each model goes through processing and editing. The following section describes how processing and editing occur for scans taken with both scanners (the Occipital Structure Sensor and Artec Leo).

Occipital Structure Sensor Three-Dimensional Scan Processing and Editing

The scans taken with the Occipital Structure Sensor went through automatic processing in the SDK scanning application software directly after scanning to add color to the scan. The SDK scanning application does not save the scans, so each scan has to be emailed. All the scans are downloaded onto a computer from the email attachment.

The scans were taken into Meshmixer for minimal editing. The original, unedited scan (see Figure 18) has the entire flat scanning surface visible, which was unnecessary for analyzing the scans.

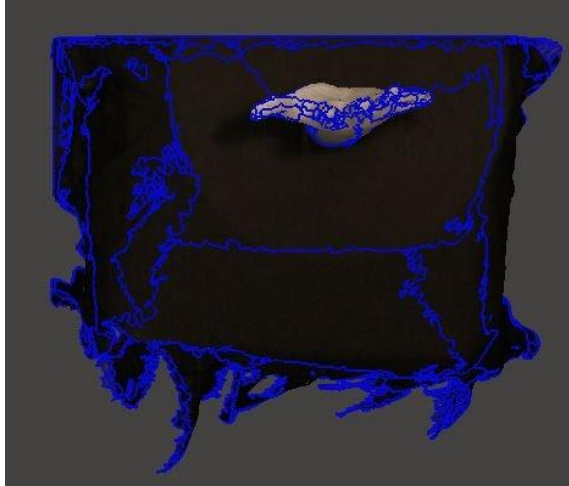


Figure 18. Original, unedited Occipital Structure scan in Meshmixer.

The removal of the base of the flat scanning surface occurred using the Edit function and the Plane Cut tool to create a rectangular base (see Figure 19).

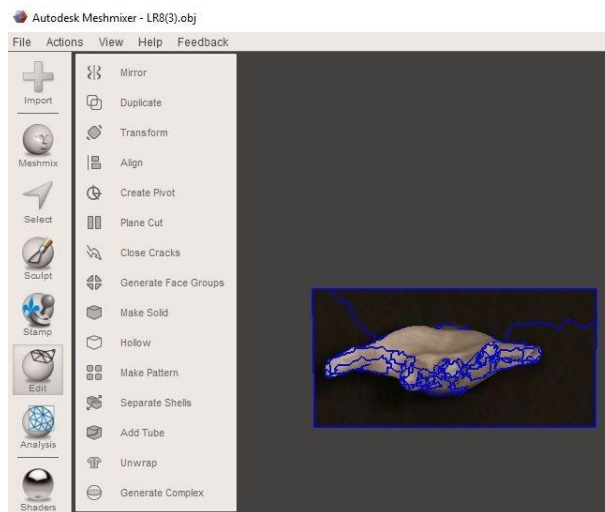


Figure 19. Edited Occipital Structure scan in Meshmixer.

The scans from the Occipital Structure Sensor come into Meshmixer with cracks visible throughout the surface (see Figure 20).

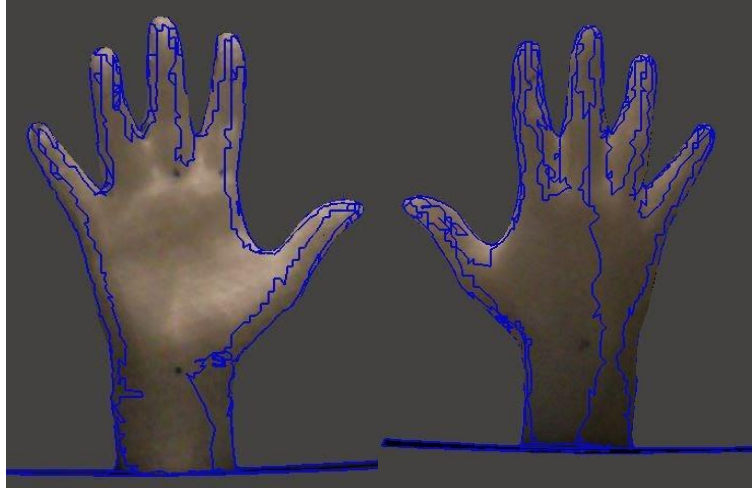


Figure 20. Occipital Structure scan in Meshmixer with visible cracks.

The cracks can be closed by using the Edit function and the Close Cracks tool. The Close Cracks tools weld the cracks together without any movement to the form (see Figure 21).

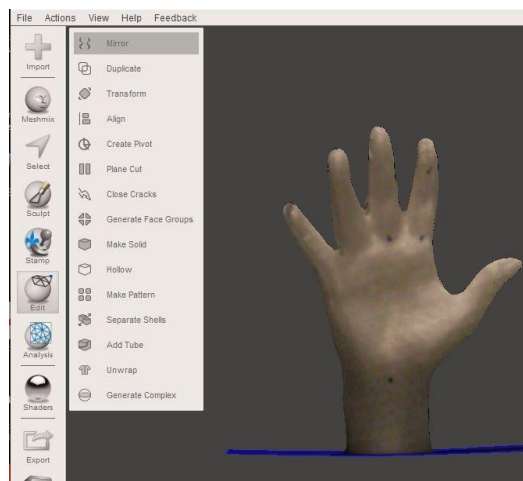


Figure 21. Edited hand with cracks filled.

The final edited files are exported as .obj files, and texture and color files are automatically saved as .jpg files.

Artec Leo Three-Dimensional Scan Processing and Editing

The Artec Leo can save scans under one (1) project on the scanner, which can be exported from the Artec Leo with an SD card onto a desktop computer. These files are imported into Artec Studio 14 Professional Software as Leo Project Package files (.pkg files).

Artec Studio 14 Professional Software was then used for manual processing and minimal editing. Manual processing includes using the following editing tools: Global Registration, Outlier Removal, and Sharp Fusion (Resolution: 1, Fill Holes: Watertight, Remove Targets: On).

Minimal editing occurred by removing the base of the flat scanning surface using the Editor function using the Defeature Brush, and the Rectangular section tool (see Figure 22).

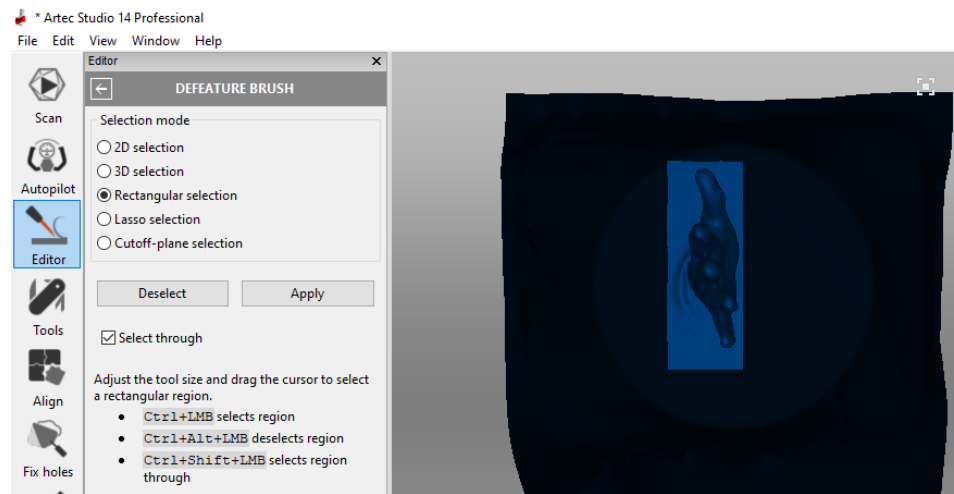


Figure 22. Editing of the Artec Leo scan in Artec Studio 14 Professional Software.

Texture and color were added to the edited hand through the Texture tool. The original scans are chosen, and the texture and color from those scans were applied. No adjustments were made to the texture/color files (see Figure 23).

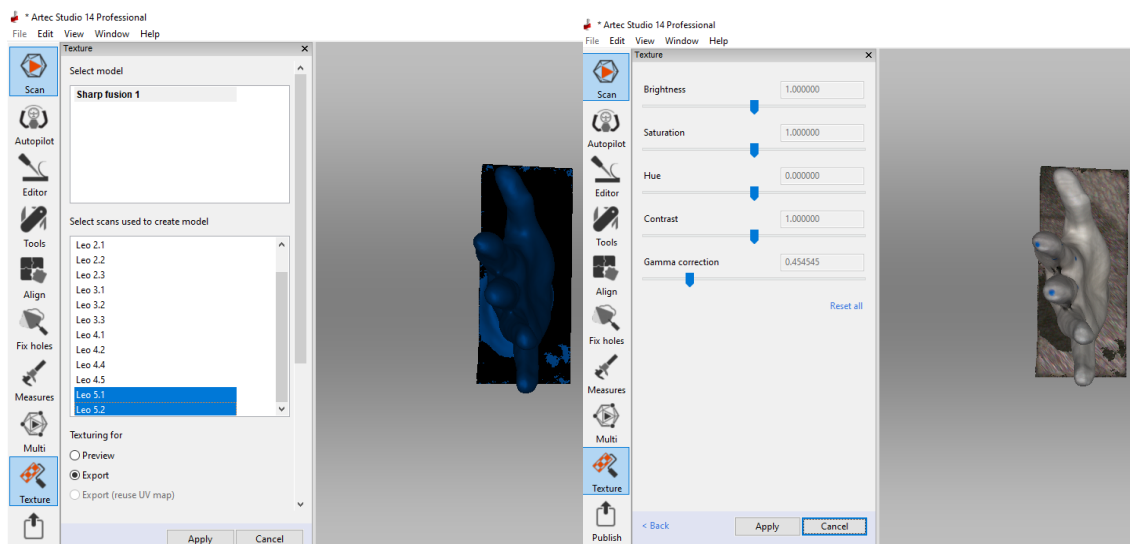


Figure 23. Adding texture/color to the Artec Leo scan in Artec Studio 14 Professional Software.

The scans are then exported as .obj files and the texture files were saved as .jpg files.

Three-Dimensional Anthropometric Measurement Process

The three-dimensional scanners (Occipital Structure Sensor and Artec Leo) used digital measuring using a measuring software called Anthroscan. The process of preparing the scans in Anthroscan by scaling and rotating the three-dimensional scans, digital landmarking, and digital measuring is discussed in the following section.

Scaling and Rotating the Three-dimensional Scans for Measuring

Scaling and rotating occurs prior to measuring the three-dimensional scans using digital measuring through Anthroscan. The amount of scaling needed for scans taken with the Occipital Structure Sensor and Artec Leo was tested in the pilot study. The scans from the Occipital Structure Sensor scale correctly into Anthroscan, while the Artec Leo scans needed to be scaled down to 0.001. Once scaled, the scans can then be rotated for the hand to a 90-degree angle.

Digital Landmarking

Before digital measuring in Anthroscan, digital landmarks are placed on the three-dimensional hand scan's landmark locations. Digital landmarks assist during digital measuring by giving a reference point for the measurement tool to grab onto (see Figure 24).

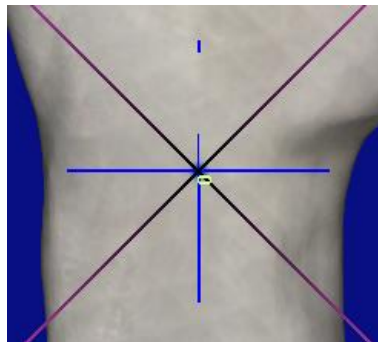


Figure 24. Digital Landmarking in Anthroscan.

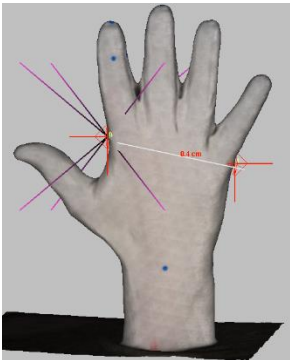
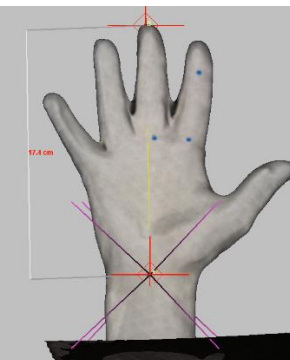
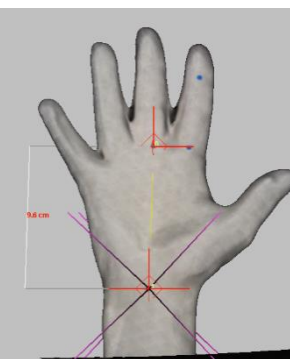
In the pilot study, both scanners (the Occipital Structure Sensor and the Artec Leo) had difficulty capturing complete landmarks in every scan. If a visibility issue was found on the final scans, independent identification of the landmark was completed in Anthroscan. Independent identification of landmarks occurred by choosing the digital landmark location based on estimating the landmark location.

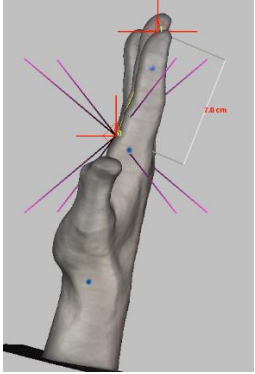
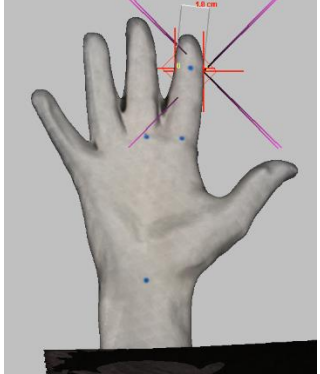
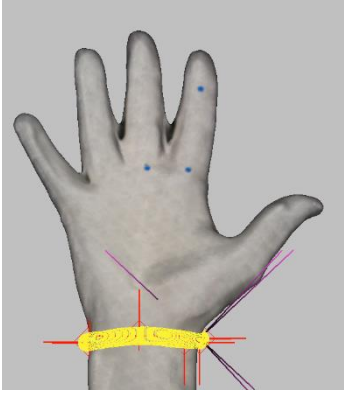
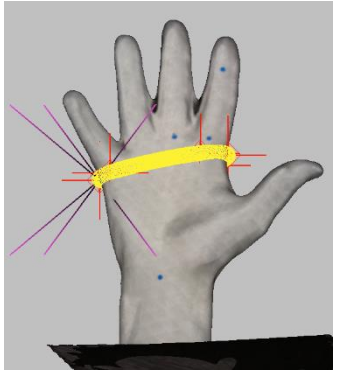
Digital Measuring for Three-Dimensional Scans

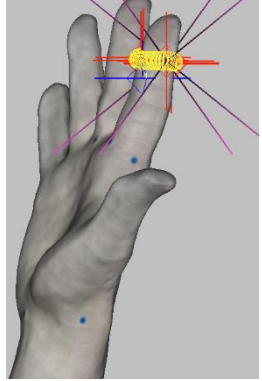
The digital measurement process took place with the three-dimensional printed hands for eight (8) defined measurements, which include Hand Breadth, Hand Length, Palm Length, Index

Finger Length, Index Finger Breadth at the Distal Interphalangeal Joint, Wrist Circumference, Hand Circumference, and Index Finger Circumference at the Distal Interphalangeal Joint (see Table 11).

Table 11. Defined Measurements Definitions for Digital Measuring in Anthroscan.

Measurement Name	Digital Measurement (Anthroscan)	Image
Hand Breadth	Digital landmarks are placed on the landmark located at Metacarpal 2 and Metacarpal 5. The Distance between 2 Positions tool within the Measure three-dimensional toolbox was used to take the linear measurement between these two (2) digital landmarks.	
Hand Length	Digital landmarks are placed on the landmark located at Fingertip of Digit 3 and the Palmar Styliion. The Distance between 2 Positions tool within the Measure three-dimensional toolbox was used to take the linear measurement between these two (2) digital landmarks	
Palm Length	Digital landmarks are placed on the landmark located at the Base of Digit 3 and the Palmar Styliion. The Distance between 2 Positions tool within the Measure three-dimensional toolbox was used to take the linear measurement between these two (2) digital landmarks.	

<p>Index Finger Length</p>	<p>Digital landmarks are placed on the landmark located at the Fingertip of Digit 2 and the Base of Digit 2. The Distance between 2 Positions tool within the Measure three-dimensional toolbox was used to take the linear measurement between these two (2) digital landmarks.</p>	
<p>Index Finger Breadth, Distal Interphalangeal Joint</p>	<p>Digital landmarks are placed on the landmark located at the Distal Interphalangeal Joint of Digit 2 on the lateral side and the Distal Interphalangeal Joint of Digit 2 on the medial side. The Distance between 2 Positions tool within the Measure three-dimensional toolbox was used to take the linear measurement between these two (2) digital landmarks.</p>	
<p>Wrist Circumference</p>	<p>Digital landmarks are placed on the four (4) landmarks located on the Radial Styloid and around the wrist (Dorsal, Palmar, and Medial side). The Curved Length (Closed) tool within the Measure three-dimensional toolbox was used to take the circumference measurement on the surface of the scan.</p>	
<p>Hand Circumference</p>	<p>Digital landmarks are placed on the two (2) landmarks located on the Metacarpal 2 and Metacarpal 5 landmarks. The Curved Length (Closed) tool within the Measure three-dimensional toolbox was used to take the circumference measurement on the surface of the scan.</p>	

<p>Index Finger Circumference, Distal Interphalangeal Joint</p>	<p>Digital landmarks are placed on the four (4) landmarks located on the Distal Interphalangeal Joint. The Curved Length (Closed) tool within the Measure three-dimensional toolbox was used to take the circumference measurement on the surface of the scan.</p>	
---	--	---

Data Analysis

Two (2) types of data analysis took place after the data collection process in this study, Measurement Analysis and Three-Dimensional Visual Analysis (see Figure 25). The Anthropometric Tool Reliability Analysis and Anthropometric Tool Precision Analysis took place during the Measurement Analysis for traditional methods (caliper and tape measure) and three-dimensional scanning (the Occipital Structure Sensor and Artec Leo). The Three-Dimensional Visual Reliability and Three-Dimensional Visual Precision Analyses took place during the Three-Dimensional Visual Analysis in the post-processing stage of data collection.

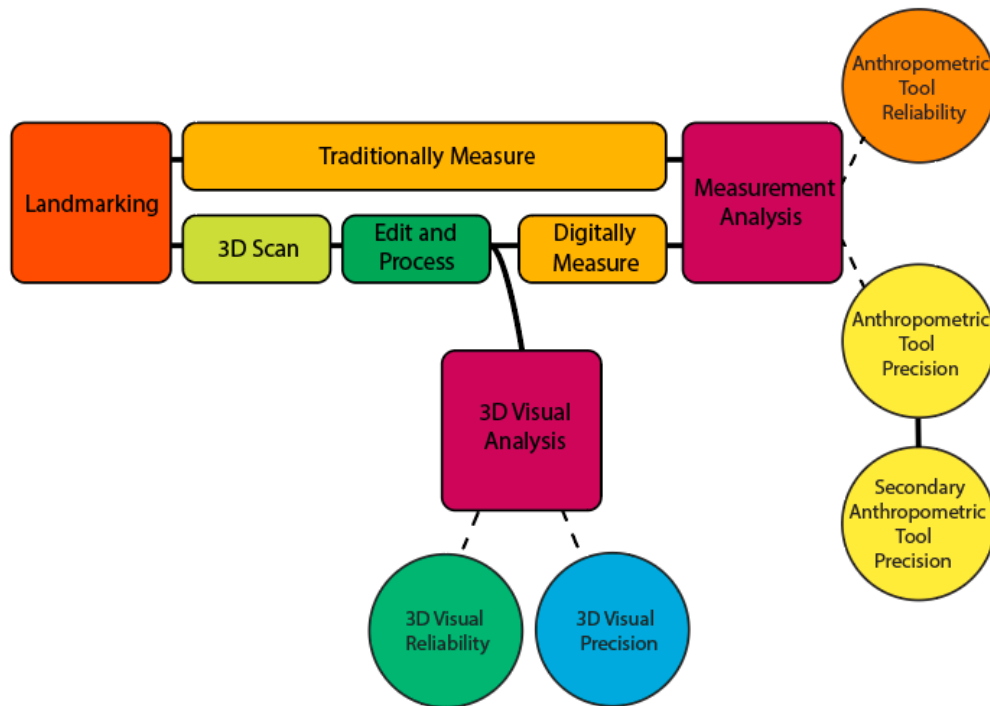


Figure 25. Interaction between Data Collection and Data Analysis.

This study's data analysis focuses on four (4) different areas of analysis: Anthropometric Tool Reliability Analysis, Anthropometric Tool Precision Analysis, Three-Dimensional Visual Reliability Analysis, and Three-Dimensional Visual Precision Analysis.

The Anthropometric Tool Reliability Analysis examines the ability of each anthropometric tool to measure and collect data consistently. Many factors could influence the reliability of a tool for capturing measurements; however, the leading cause of measurement error within anthropometric data collection is intra-observer reliability (Kouchi, 2020). Intra-observer reliability is the ability of the same observer to obtain consistent measurements. Reliability has previously been assessed through repeatability (Li, Chang, Dempsey, Ouyang, & Duan, 2008 and Dunbar & Chapates, 2019).

The Anthropometric Tool Precision Analysis examines the exactness and accuracy of the measurement technique. Anthropometric Tool Precision Analysis has been previously validated through evaluation of statistical significance. The ISO 20685:2018 standard has previously been used to validate tools' precision (Li, Chang, Dempsey, Ouyang, & Duan, 2008). The ISO 20685:2018 standard sets a maximum difference between measurements observed using traditional methods (caliper and tape measure) and a three-dimensional scanner for hand measurements, which was 1 mm (International Organization for Standardization, 2018).

Three-Dimensional Visual Analysis has not been analyzed previously for comparison studies. For this study, Three-Dimensional Visual Analysis was split into two categories, Three-Dimensional Visual Reliability and Three-Dimensional Visual Precision. The Three-Dimensional Visual Reliability examines the ability of each scanner to capture the three-dimensional scan consistently. The Three-Dimensional Visual Precision examines the exactness and accuracy of the final scans used for digital measuring.

Evaluation and Statistical Analysis

The evaluation and statistical analysis will discuss each component of the analysis:

Anthropometric Tool Reliability Analysis, Anthropometric Tool Precision Analysis, Three-Dimensional Visual Reliability Analysis, and Three-Dimensional Visual Precision Analysis (see Figure 26). The statistical analysis consists of descriptive statistics, One-Way ANOVA, and Post-Hoc Analysis (Tukey Honestly Significant Difference (HSD)). The descriptive statistics included the mean (M) and standard deviations (SD). The mean (M) is the average value of the data. Standard deviation (SD) describes the amount of variation in the data. Higher standard deviations (equal to or greater than 1) indicate the data has more variation, which means it is less reliable. A lower standard deviation (less than 1) indicates that the data has less variation, which means it is

more reliable (Lane, 2003). A One-Way ANOVA is used to determine whether there is any significant difference within the data collected. The One-way ANOVA included the degrees of freedom (DF), f-statistic (F), and p-value. Two degrees of freedom (Df) are reported: one for the numerator (between groups) and one for the denominator (within group). The f-statistic (F) is the ratio of two variances and gives information on how far the data are scattered from the mean. If there is a larger value, there is a greater dispersion. The p-value is the probability that the group means are unequal (Lane, 2003). For this study, statistically significant differences are reported as a p-value of less than 0.05. If a statistically significant difference occurred, then a Post-Hoc Pairwise Analysis (Tukey Honestly Significant Difference (HSD) Method) took place to find out which differences between pairs of means are significant within the measurements showing statistical significance. The p-adj is the adjusted p-value, which occurs due to multiple testing. The confidence interval is a range of values likely to include a population with a certain degree of confidence (95%) (Lane, 2003).

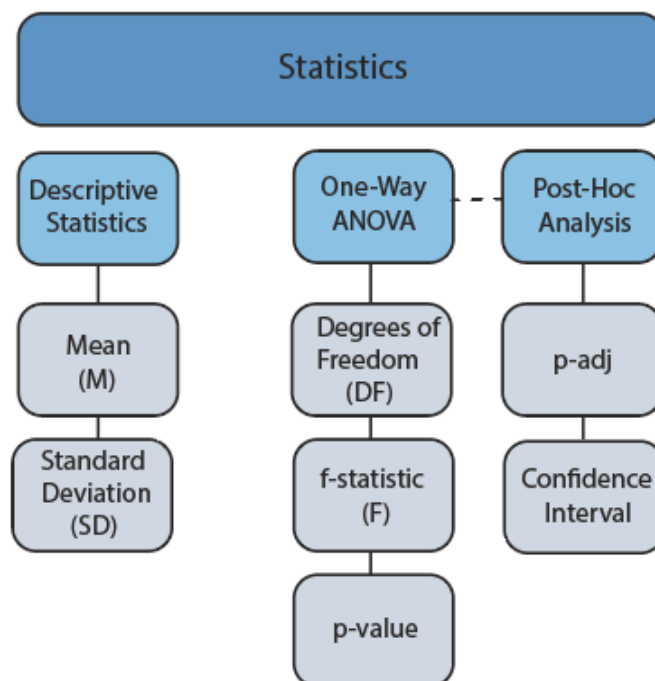


Figure 26. Statistical Analysis.

Anthropometric Tool Reliability Analysis

The Anthropometric Tool Reliability Analysis examines the ability of each anthropometric tool to measure and collect data consistently. For the Anthropometric Tool Reliability Analysis, the defined measurements were taken with each tool taken five (5) times for one (1) participant in order to evaluate the repeatability of the three (3) tools.

Anthropometric Tool Reliability Analysis helps answer research question one (RQ1), which asks how reliable traditional methods (caliper and tape measure), the Occipital Structure Sensor, and the Artec Leo are for gathering hand anthropometric data.

The Anthropometric Tool Reliability Analysis's statistical analysis will include descriptive statistics, including mean and standard deviation. The Mean of the Absolute Difference Values will be compared to ISO 20685:2018 standard. The ISO 20685:2018 standard sets a maximum difference between measurements observed using traditional methods (caliper and tape measure) and a three-dimensional scanner for hand measurements, which was 1 mm (International Organization for Standardization, 2018). One-sample t-tests will be performed on the Mean of the Absolute Difference Values from the two (2) three-dimensional scanners (Occipital Structure Sensor and Artec Leo) for the Anthropometric Tool Reliability Analysis to see if they were significantly different from a mean of one (1). The significance of the differences among the different means of each hand measurement from the three (3) methods will be reported via One-Way ANOVA ($p < 0.05$). Post-Hoc Pairwise Analysis will take place for the measurements showing statistical significance from the One-Way ANOVA using Tukey Honestly Significant Difference (HSD) Method.

Anthropometric Tool Precision Analysis

The Anthropometric Tool Precision Analysis examines the exactness and accuracy of the measurement technique. For the Anthropometric Tool Precision Analysis in this study, each measurement for each tool that was used for gathering the anthropometric measurements was taken one (1) time for twelve (12) participants in order to evaluate the precision of the three (3) tools (traditional methods (caliper and tape measure), the Occipital Structure Sensor, and the Artec Leo).

The Anthropometric Tool Precision Analysis included independent identification of landmarks at Fingertips of Digit 2 and 3 for six (6) out of twelve (12) Occipital Structure scans, which impacted two (2) measurements, Hand Length and Index Finger Length. A secondary Anthropometric Tool Precision Analysis took place for the two (2) impacted hand anthropometric measurements (Hand Length and Index Finger Length) for the six (6) participants that had complete landmarks.

For the Secondary Anthropometric Tool Precision Analysis in this study, the two (2) impacted hand anthropometric measurements (Hand Length and Index Finger Length) are taken one (1) time for the six (6) participants that had complete landmarks with all three (3) measurement tools

(traditional methods (caliper and tape measure), the Occipital Structure Sensor, and the Artec Leo).

The Anthropometric Tool Precision Analysis helps answer research question two, part A (RQ2a), and research question two, part B (RQ2b). Research Question Two, part A (RQ2a) asks how precise the three (3) tools (traditional methods (caliper and tape measure), the Occipital Structure Sensor, and the Artec Leo) are for collecting hand anthropometric measurements. Research Question Two, part B (RQ2b) asks how the inclusion of complete landmarking, which does not rely on independent identification of landmarks, impacts the three-dimensional scans' precision.

The Anthropometric Tool Precision Analysis's statistical analysis will include descriptive statistics, including mean and standard deviation. The Mean of the Absolute Difference Values will be compared to ISO 20685:2018 standard. One-sample t-tests will be performed on the Mean of the Absolute Difference Values from the two (2) three-dimensional scanners (Occipital Structure Sensor and Artec Leo) for the Anthropometric Tool Precision Analysis to see if they were significantly different from a mean of one (1). The significance of the differences among the different means of each hand measurement from the three (3) methods will be reported via One-Way ANOVA ($p < 0.05$). Post-Hoc Pairwise Analysis will take place for the measurements showing statistical significance from the One-Way ANOVA using Tukey Honestly Significant Difference (HSD) Method.

Three-Dimensional Visual Analysis

The Three-Dimensional Visual Analysis of the three-dimensional models provided from the two (2) full-color hand-held three-dimensional scanners (the Occipital Structure Sensor and Artec Leo) occurred in the post-processing stage of data collection to determine the Three-Dimensional Visual Reliability Analysis and Three-Dimensional Visual Precision Analysis of the three-dimensional scanners using a Post-processing Visual Analysis Likert Scale (Juhnke, Pokorny, and Griffin, 2021) discussed below.

Post-Processing Visual Analysis Likert Scale

The Post-Processing Visual Analysis Likert Scale, developed by Juhnke, Pokorny, and Griffin (2021), was modified and used to compare the scans for Three-Dimensional Visual Reliability Analysis and Three-Dimensional Visual Precision Analysis. The Post-Processing Visual Analysis Likert Scale (Juhnke, Pokorny, and Griffin, 2021) provided clear definitions for each location to quantify the scans' overall quality within the visual assessment. Quantification occurs in this

Likert scale through rating the hand one (1) to five (5), with one (1) being the lowest quality and five (5) being the highest quality. There are three (3) areas of interest when assessing a three-dimensional scan: hand visibility, webbing, and landmarking. Each of these areas was then split up into locations when evaluating the quality of the three-dimensional hand scan for digital measuring. Detailed descriptions of each quantification measurement are listed for each location in Table 12.

Table 12. Post-Processing Visual Analysis Likert Scale (modified via Juhnke, Pokorny, and Griffin (2021)).

Visual Analysis	Location	1	2	3	4	5
Hand Visibility	Dorsal Side of Hand	The entire dorsal side of the hand is distorted	75% of the dorsal side of the hand is distorted	50% of the dorsal side of the hand is distorted	25% of the dorsal side of the hand is distorted	The dorsal side of the hand is clear of any distortions and appears realistic to the human hand
	Palmar Side of Hand	The entire palmar side of the hand is distorted	75% of the palmar side of the hand is distorted	50% of the palmar side of the hand is distorted	25% of the palmar side of the hand is distorted	The palmar side of hand is clear of any distortions and appears realistic to the human hand
	Clarity of Digit Shape	5 digits are distorted	4 digits are distorted	2-3 digits are distorted	1 digit is distorted	No digits are distorted
Webbing	Quantity of Digits	Webbing is present	Webbing is present	Webbing is present	Webbing is present	Webbing between digits

	with Webbing	between all digits	between 3 sets of digits	between 2 sets of digits	between 1 set of digits	appears realistic to the human hand
	Amount of Webbing between Digits 1 and 2	Webbing extends past the proximal interphalangeal joint	Webbing exists at or near the proximal interphalangeal joint	Webbing exists between the metacarpal phalangeal joint and proximal interphalangeal joint	Webbing exists near the metacarpal phalangeal joint	Webbing between digits appears realistic to the human hand
	Amount of Webbing between Digits 2 and 3	Webbing extends past the distal interphalangeal joint	Webbing between proximal and distal interphalangeal joint	Webbing exists at or near the proximal interphalangeal joint	Webbing exists between the metacarpal phalangeal joint and proximal interphalangeal joint	Webbing between digits appears realistic to the human hand
	Amount of Webbing between Digits 3 and 4	Webbing extends past the distal interphalangeal joint	Webbing between proximal and distal interphalangeal joint	Webbing exists at or near the proximal interphalangeal joint	Webbing exists between the metacarpal phalangeal joint and proximal interphalangeal joint	Webbing between digits appears realistic to the human hand
	Amount of Webbing between Digits 4 and 5	Webbing extends at or past the distal interphalangeal joint	Webbing between proximal and distal interphalangeal joint	Webbing exists at or near the proximal interphalangeal joint	Webbing exists between the metacarpal phalangeal joint and proximal interphalangeal joint	Webbing between digits appears realistic to the human hand
Landmark (*)	Visibility of Landmarks	7 of the landmarks are visible	8 or 9 of the landmarks are visible	11 or 10 of the landmarks are visible	12 or 13 of the landmarks are visible	All 14 of the landmarks are visible
	Clarity of Visible	6 or more of the visible	4-5 of the visible	2-3 of the visible	1 of the visible	No distortion

	Landmarks	landmarks are distorted	landmarks are distorted	landmarks are distorted	landmarks is distorted	seen in visible landmarks
--	-----------	-------------------------	-------------------------	-------------------------	------------------------	---------------------------

(*) Not a form of measurement for the original three-dimensional scan.

Three-Dimensional Visual Reliability Analysis

The Three-Dimensional Visual Reliability Analysis examines the ability of each scanner to capture the three-dimensional scan consistently. The Three-Dimensional Visual Reliability Analysis consisted of assessing three (3) scans taken with the Occipital Structure Sensor and three (3) scans taken with the Artec Leo for each participant using the Post-Processing Visual Analysis Likert Scale (Juhnke, Pokorny, and Griffin, 2021).

The Three-Dimensional Visual Reliability Analysis assists with answering research question three (RQ3), which asks how reliable the quality of the scans from the three-dimensional scanners is (the Occipital Structure Sensor and the Artec Leo) for use in collecting hand anthropometric data.

The Three-Dimensional Visual Reliability Analysis's statistical analysis assists will include descriptive statistics, including mean and standard deviation. The significance of the differences among the different means of each hand measurement from the two (2) methods (Occipital Structure Sensor and Artec Leo) will be reported via One-Way ANOVA ($p < 0.05$). Post-Hoc Pairwise Analysis will take place for the measurements showing statistical significance from the One-Way ANOVA using Tukey Honestly Significant Difference (HSD) Method.

Three-Dimensional Visual Precision Analysis

The Three-Dimensional Visual Precision Analysis examines the exactness and accuracy of the final scans used for digital measuring. The Three-Dimensional Visual Precision Analysis was assessed by comparing the original three-dimensional scan used to create the three-dimensional printed model, the final scans taken with the Occipital Structure Sensor, and the final scans taken with the Artec Leo using the Post-Processing Visual Analysis Likert Scale (Juhnke, Pokorny, and Griffin, 2021).

Three-Dimensional Visual Precision Analysis assists with answering research question four (RQ4), which asks how precise the quality of the scans from the three-dimensional scanners (the Occipital Structure Sensor and Artec Leo) compare to each other and the original three-dimensional scan for use in collecting hand anthropometric data.

The Three-Dimensional Visual Precision Analysis's statistical analysis will include descriptive statistics, including mean and standard deviation. The significance of the differences among the different means of each hand measurement from the three (3) methods will be reported via One-Way ANOVA ($p < 0.05$). Post-Hoc Pairwise Analysis will take place for the measurements showing statistical significance from the One-Way ANOVA using Tukey Honestly Significant Difference (HSD) Method.

Hypotheses and Null Hypotheses

The hypotheses and null hypothesis created for this study and are listed below.

Hypothesis One (H1): The measurements from each measurement tool from one (1) participant will not be statistically identical at each measurement location based on a One-Way ANOVA.

Null Hypothesis One (H0(1)): The measurements from each measurement tool from one (1) participant will be statistically identical at each measurement location based on a One-Way ANOVA.

Hypothesis Two, Part A (H2a): The measurements from each measurement tool across twelve (12) participants will not be statistically identical at each measurement location based on a One-Way ANOVA.

Null Hypothesis Two, Part A (H0(2a)): The measurements from each measurement tool across twelve (12) participants will be statistically identical at each measurement location based on a One-Way ANOVA.

Hypothesis Two, Part B (H2b): The measurements impacted by independent landmarking from each measurement tool across twelve (12) participants will not be statistically identical at each measurement location based on a One-Way ANOVA.

Null Hypothesis Two, Part B (H0(2b)): The measurements impacted by independent landmarking from each measurement tool across twelve (12) participants will be statistically identical at each measurement location based on a One-Way ANOVA.

Hypothesis Three (H3): The final scans from each three-dimensional scanner across twelve (12) participants will not be statistically identical at each location of the Post-Processing Visual Analysis Likert Scale (Juhnke, Pokorny, and Griffin, 2021).

Null Hypothesis Three (H0(3)): The final scans from each three-dimensional scanner across twelve (12) participants will be statistically identical at each location of the Post-Processing Visual Analysis Likert Scale (Juhnke, Pokorny, and Griffin, 2021).

Hypothesis Four (H4): The final scans from each three-dimensional scanner and the original three-dimensional scan (used to create the three-dimensional printed model) across twelve (12) participants will not be statistically identical at each location of the Post-Processing Visual Analysis Likert Scale (Juhnke, Pokorny, and Griffin, 2021).

Null Hypothesis Four (H0(4)): The final scans from each three-dimensional scanner and the original three-dimensional scan (used to create the three-dimensional printed model) across twelve (12) participants will be statistically identical at each location of the Post-Processing Visual Analysis Likert Scale (Juhnke, Pokorny, and Griffin, 2021).

Summary

Twelve (12) three-dimensional hand scans, from a more extensive database taken by the Human Dimensioning Lab at the University of Minnesota, were three-dimensionally printed. Fourteen (14) landmarks were placed on the three-dimensional printed hands, which correlated with the eight (8) defined measurements being analyzed. The three-dimensional printed hands were first measured using traditional methods (caliper and tape measure). The three-dimensional printed hands were then scanned three (3) times with each of the three-dimensional scanners (the Occipital Structure Sensor and the Artec Leo). The scans provided by the scanners go through processing and minimal editing. During the post-processing stage, the scans provided by the scanner were analyzed for visual quality using a Post-Processing Visual Analysis Likert Scale (Juhnke, Pokorny, and Griffin, 2021). Once the visual analysis was complete, final scans for each of the three-dimensional printed hands were brought into Anthroscan to measure. The data analysis for this study focuses on four (4) different areas: Anthropometric Tool Reliability Analysis, Anthropometric Tool Precision Analysis, Three-Dimensional Visual Reliability Analysis, and Three-Dimensional Visual Precision Analysis.

Chapter 4. Results for Anthropometric Tool Reliability Analysis and Anthropometric Tool Precision Analysis

This chapter presents the data analysis results for the Anthropometric Tool Reliability Analysis and Anthropometric Tool Precision Analysis (see Figure 27). Anthropometric Tool Reliability Analysis took place with one (1) participant for the eight (8) defined measurements. Each measurement was repeated five (5) times for the tools used within this study (traditional methods (caliper and tape measure), Occipital Structure Sensor, and Artec Leo). Anthropometric Tool Precision Analysis took place with the twelve (12) participants for the eight (8) defined measurements. Each measurement was taken one (1) time for the tools used within this study (traditional methods (caliper and tape measure), Occipital Structure Sensor, and Artec Leo).

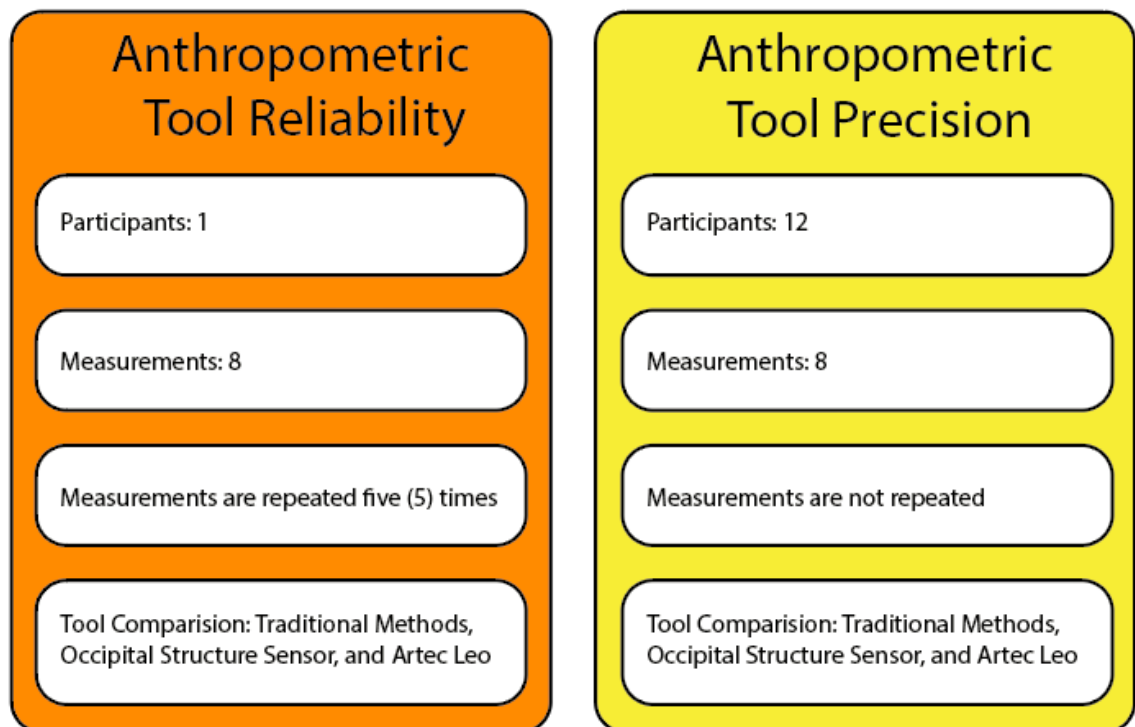


Figure 27. Overview of Anthropometric Tool Reliability Analysis and Anthropometric Tool Precision Analysis.

Anthropometric Tool Reliability Analysis

The statistical analysis for the Anthropometric Tool Reliability Analysis included descriptive statistics, including mean and standard deviation. The Mean of the Absolute Difference Values were compared to ISO 20685:2018 standard. The ISO 20685:2018 standard sets a maximum difference between measurements of 1 mm observed using traditional methods (caliper and tape measure) and a three-dimensional scanner for hand measurements (International Organization for

Standardization, 2018). One-sample t-tests were performed on the Mean of the Absolute Difference Values from the two (2) three-dimensional scanners (Occipital Structure Sensor and Artec Leo) for the Anthropometric Tool Reliability Analysis to see if they were significantly different from a mean of one (1). The significance of the differences among the different means of each hand measurement from the three (3) methods was reported via One-Way ANOVA ($p < 0.05$). Post-Hoc Pairwise Analysis took place for the measurements showing statistical significance from the One-Way ANOVA using Tukey Honestly Significant Difference (HSD) Method.

Descriptive Statistics for the Anthropometric Tool Reliability Analysis

The information provided by the descriptive statistics for the Anthropometric Tool Reliability Analysis (see Table 13) was used to assess data before running the One-Way ANOVA. The descriptive statistics for the Anthropometric Tool Reliability Analysis included the mean (M) and standard deviations (SD) from traditional methods (caliper and tape measure) (T), the Occipital Structure Sensor (O), and Artec Leo (A).

Table 13. Descriptive Statistics for Anthropometric Tool Reliability Analysis (mm).

Defined Measurement	T		O		A	
	Mean	SD	Mean	SD	Mean	SD
Hand Breadth	79.8	2.49	82	0	83.6	0.89
Hand Length	173.6	0.55	168	0	174	0
Palm Length	96.2	1.3	94	0	96	0
Index Finger Length	72.8	0.84	67	0	72	0
Index Finger Breadth at the Distal Interphalangeal Joint	19.2	0.45	16	0	19	0
Wrist Circumference	167.6	2.7	166	1	166.2	0.84
Hand Circumference	194.8	1.3	187.4	1.82	193	1.73
Index Finger Circumference at the Distal Interphalangeal Joint	56.8	1.3	46.2	0.45	55	0

Lower standard deviations are seen within the two (2) three-dimensional scanners (the Occipital Structure Sensor (O) and Artec Leo (A)) at all measurement locations, except for the Hand Circumference measurement. The results indicated that the three-dimensional scanners were more reliable at more measurement locations than traditional methods (caliper and tape measure).

The Occipital Structure Sensor's mean values were lower at more measurement locations than traditional methods (caliper and tape measure) and the Artec Leo. Disproportionate mean differences occur at several locations for the Occipital Structure Sensor, most notably the Interphalangeal Finger Circumference at the Distal Interphalangeal Joint, Hand Circumference, Hand Length, and Index Finger Length compared to the traditional methods (caliper and tape measure) and the Artec Leo.

Unlike the Occipital Structure Sensor, the averages were similar at most locations between traditional methods (caliper and tape measure) and the Artec Leo.

Comparison of the Mean of the Absolute Difference Values to ISO 20685:2018 for the Anthropometric Tool Reliability Analysis

The Mean of the Absolute Difference Values for the Anthropometric Tool Reliability Analysis were assessed to compare the results to the ISO 20685:2018 standard (1 mm) (see Table 14).

Table 14. Mean of the Absolute Difference Values of the Differences for the Anthropometric Tool Reliability Analysis (mm).

Defined Measurement	Mean of the Absolute Difference Values	
	T vs O	T vs A
Hand Breadth	2.2	3.8
Hand Length	5.6	0.4
Palm Length	2.2	0.2
Index Finger Length	5.8	0.8
Index Finger Breadth at the Distal Interphalangeal Joint	3.2	0.2
Wrist Circumference	1.6	1.4
Hand Circumference	7.4	1.8

Index Finger Circumference at the Distal Interphalangeal Joint	10.6	1.8
--	------	-----

All the defined measurements were above the maximum allowable error according to ISO 20685:2018 standard (1 mm) when comparing traditional methods (caliper and tape measure) to the Occipital Structure Sensor (T vs O). The defined measurements that were above the maximum allowable error according to ISO 20685:2018 standard (1 mm) when comparing traditional methods (caliper and tape measure) to the Artec Leo (T vs A) were Hand Breadth (3.8 mm), Wrist Circumference (1.4 mm), Hand Circumference (1.8 mm), and Index Finger Circumference at the Distal Interphalangeal Joint (1.8 mm).

None of the defined measurements would pass the maximum allowable error according to ISO 20685:2018 standard (1 mm) when comparing traditional methods (caliper and tape measure) to the Occipital Structure Sensor (T vs O). The measurements that would pass the maximum allowable error according to ISO 20685:2018 standard (1 mm) when comparing traditional methods (caliper and tape measure) to the Artec Leo (T vs A) were Hand Length (0.4 mm), Palm Length (0.2 mm), Index Finger Length (0.8 mm), and Index Finger Breadth at the Distal Interphalangeal Joint (0.2 mm).

One-sample t-tests were performed on the Mean of the Absolute Difference Values from the two (2) three-dimensional scanners (Occipital Structure Sensor and Artec Leo) for the Anthropometric Tool Reliability Analysis to see if they were significantly different from a mean of one (1) (see Table 15). One (1) mm is the maximum allowable error allowed by the ISO 20685:2018 standard for hand measurements observed using traditional methods (caliper and tape measure) and three-dimensional scanner (International Organization for Standardization, 2018).

Table 15. One-sample t-tests to assess significant difference from one (1) for the Mean of the Absolute Difference Values for the Anthropometric Tool Reliability Analysis.

Three-Dimensional Scanner	t-value	p-value	Statistical different from 1 (Yes/No)
Occipital Structure Sensor	3.4621	0.01052*	Yes
Artec Leo	0.70156	0.5056	No

*Significant at the .05 level

The one-sample t-tests from the Mean of the Absolute Difference Values for the Anthropometric Tool Reliability Analysis revealed that the Occipital Structure Sensor ($t = 3.4621$, $p = 0.01052$) was statistically different from a mean of one (1) and the Artec Leo ($t = 0.70156$, $p = 0.5056$) was not statistically different from a mean of one (1).

One-Way ANOVA and Post-Hoc Analysis for the Anthropometric Tool Reliability Analysis

The One-Way ANOVA for the Anthropometric Tool Reliability Analysis (see Table 16) was used to assess hypothesis one (H1) and null hypothesis one (H0(1)). The information presented in the One-Way ANOVA includes the degrees of freedom (DF), f-statistic (F), and p-value.

Table 16. Anthropometric Tool Reliability Analysis One-Way ANOVA.

Defined Measurement	Df	F	P-value
Hand Breadth	2, 12	7.8	0.00676 **
Hand Length	2, 12	562.7	1.38e-12 ***
Palm Length	2, 12	13.06	0.000973 ***
Index Finger Length	2, 12	211.7	4.38e-10 ***
Index Finger Breadth at the Distal Interphalangeal Joint	2, 12	241	2.05e-10 ***
Wrist Circumference	2, 12	1.267	0.317
Hand Circumference	2, 12	27.93	3.06e-05 ***
Index Finger Circumference at the Distal Interphalangeal Joint	2, 12	254	1.51e-10 ***

*Significant at the .05 level

** Significant at the .01 level

*** Significant at the .00 level

The One-Way ANOVA revealed statistically significant differences occurred at the Hand Breadth ($F(2, 12) = 7.8$, $p = 0.00676$), Hand Length ($F(2, 12) = 562.7$, $p = 1.38e-12$), Palm Length ($F(2,$

12) = 13.06, $p = 0.000973$), Index Finger Length ($F(2, 12) = 211.7$, $p = 4.38e-10$), Index Finger Breadth at the Distal Interphalangeal Joint ($F(2, 12) = 241$, $p = 2.05e-10$), Hand Circumference ($F(2, 12) = 27.93$, $p = 3.06e-05$), and Index Finger Circumference at the Distal Interphalangeal Joint ($F(2, 12) = 254$, $p = 1.51e-10$) measurements.

The One-Way ANOVA does not identify which differences between pairs of means are significant. To determine which differences between pairs of means are significant, a Post-Hoc Pairwise Analysis took place using Tukey Honestly Significant Difference (HSD) Method (see Table 17).

Table 17. Anthropometric Tool Reliability Analysis Post-Hoc Pairwise Analysis using Tukey Honestly Significant Difference (HSD) Method.

Hand Breadth	P-Adj	95% Confidence Interval	
		Lower Bound	Upper Bound
T vs O	0.0980553	-4.777401	0.3774012
T vs A	0.0052135**	-6.377401	-1.2225988
O vs A	0.2612361	-4.177401	0.9774012
Hand Length	P-Adj	95% Confidence Interval	
		Lower Bound	Upper Bound
T vs O	0.0000000***	5.0664273	6.1335727
T vs A	0.15458	-0.9335727	0.1335727
O vs A	0.0000000***	-6.5335727	-5.4664273
Palm Length	P-Adj	95% Confidence Interval	
		Lower Bound	Upper Bound
T vs O	0.0015770**	0.9298428	3.4701572
T vs A	0.9080353	-1.0701572	1.4701572
O vs A	0.0032562**	-3.2701572	-0.7298428
Index Finger Length	P-Adj	95% Confidence Interval	
		Lower Bound	Upper Bound
T vs O	0.0000000***	4.98495419	6.615046
T vs A	0.0545125	-0.01504581	1.615046
O vs A	0.0000000***	-5.81504581	-4.184954
	P-Adj	95% Confidence Interval	

Index Finger Breadth at the Distal Interphalangeal Joint		Lower Bound	Upper Bound
T vs O	0.0000000***	2.7643397	3.6356603
T vs A	0.4618859	-0.2356603	0.6356603
O vs A	0.0000000***	-3.4356603	-2.5643397
Hand Circumference	P-Adj	95% Confidence Interval	
		Lower Bound	Upper Bound
T vs O	0.0000315**	4.6446423	10.155358
T vs A	0.2300146	-0.9553577	4.555358
O vs A	0.0004194**	-8.3553577	-2.844642
Index Finger Circumference at the Distal Interphalangeal Joint	P-Adj	95% Confidence Interval	
		Lower Bound	Upper Bound
T vs O	0.0000000***	9.2572047	11.942795
T vs A	0.0098537	0.4572047	3.142795
O vs A	0.0000000***	-10.1427953	-7.457205

*Significant at the .05 level

** Significant at the .01 level

*** Significant at the .00 level

The post-hoc comparison revealed that statistically significant differences occurred more often between the traditional methods (caliper and tape measure) and Occipital Structure Sensor (T vs O) and between the Occipital Structure Sensor and Artec Leo (O vs A) than between traditional methods (caliper and tape measure) and Artec Leo (T vs A).

Results from for the Anthropometric Tool Reliability Analysis

This analysis showed that the Artec Leo was more reliable than traditional methods (caliper and tape measure) when examining the standard deviations. The Artec Leo had similar mean values and less statistically significant differences to traditional methods (caliper and tape measure) than the Occipital Structure Sensor. Half (four (4) out of eight (8)) of the defined measurements from the Artec Leo passed the ISO 20685: 2018 standard when comparing to traditional methods. The Artec Leo did not have significant differences from a mean of one (1) in the one-sample t-test.

Traditional methods (caliper and tape measure) were less reliable when examining the standard deviations than the Occipital Structure Sensor and Artec Leo.

The Occipital Structure Sensor was more reliable than traditional methods (caliper and tape measure) when examining the standard deviations. However, low mean values caused more statistically significant differences compared to traditional methods (caliper and tape measure) and the Artec Leo. None of the defined measurements from the Occipital Structure Sensor passed the ISO 20685: 2018 standard compared to traditional methods. The Occipital Structure Sensor had significant differences from a mean of one (1) in the one-sample t-test.

The hypothesis was confirmed. The hypothesis was accepted based on the statistically significant differences found within the One-Way ANOVA (see Table 16), and the null hypothesis was rejected (see Table 18).

Table 18. Anthropometric Tool Reliability Analysis Results Summary.

Anthropometric Tool Reliability Analysis	
<p><i>Research Question One (RQ1):</i> How reliable are traditional methods (caliper and tape measure), the Occipital Structure Sensor, and the Artec Leo are for gathering hand anthropometric data?</p>	<p>The Artec Leo was more reliable than traditional methods (caliper and tape measure) and Occipital Structure Sensor. Half (four (4) out of eight (8)) of the defined measurements from the Artec Leo passed the ISO 20685: 2018 standard compared to traditional methods. The Artec Leo did not have significant differences from a mean of one (1) in the one-sample t-test.</p> <p>Traditional methods (caliper and tape measure) were less reliable than the Occipital Structure Sensor and Artec Leo.</p> <p>The Occipital Structure Sensor was more reliable than traditional methods (caliper and tape measure) and less reliable than the Artec Leo. None of the defined measurements from the Occipital Structure Sensor passed the ISO 20685: 2018 standard when comparing to</p>

	traditional methods. The Occipital Structure Sensor had significant differences from a mean of one (1) in the one-sample t-test.
<i>Hypothesis One (H1):</i> The measurements from each measurement tool from one (1) participant will not be statistically identical at each measurement location based on a One-Way ANOVA.	Accepted
<i>Null Hypothesis One (H0(1)):</i> The measurements from each measurement tool from one (1) participant will be statistically identical at each measurement location based on a One-Way ANOVA.	Rejected.

Anthropometric Tool Precision

The statistical analysis for the Anthropometric Tool Precision Analysis included descriptive statistics, including mean and standard deviation. The Mean of the Absolute Difference Values will be compared to ISO 20685:2018 standard. The ISO 20685:2018 standard sets a maximum difference between measurements of 1 mm observed using traditional methods (caliper and tape measure) and a three-dimensional scanner for hand measurements (International Organization for Standardization, 2018). One-sample t-tests were performed on the Mean of the Absolute Difference Values from the two (2) three-dimensional scanners (Occipital Structure Sensor and Artec Leo) for the Anthropometric Tool Precision Analysis to see if they were significantly different from a mean of one (1). The significance of the differences among the different means of each hand measurement from the three (3) methods were reported via One-Way ANOVA ($p < 0.05$). Post-Hoc Pairwise Analysis took place for the measurements showing statistical significance from the One-Way ANOVA using Tukey Honestly Significant Difference (HSD) Method.

Descriptive Statistics for the Anthropometric Tool Precision Analysis

The information provided by the descriptive statistics for the Anthropometric Tool Precision Analysis (see Table 19) was used to assess data before running the One-Way ANOVA. The descriptive statistics for the Anthropometric Tool Precision Analysis includes the mean (M) and

standard deviations (SD) from traditional methods (caliper and tape measure) (T), the Occipital Structure Sensor (O), and Artec Leo (A).

Table 19. Anthropometric Tool Precision Analysis Descriptive Statistics (mm).

Defined Measurement	T		O		A	
	Mean	SD	Mean	SD	Mean	SD
Hand Breadth	83.7	0.93	84.6	0.95	85.2	0.96
Hand Length [^]	182.7	0.95	177.8	1	181.8	0.92
Palm Length	106.6	0.59	105.6	0.73	105.7	0.69
Index Finger Length [^]	71.2	0.3	65.5	0.41	69.8	0.35
Index Finger Breadth at the Distal Interphalangeal Joint	18.9	0.17	17.3	0.23	19.2	0.25
Wrist Circumference	166.2	1.81	164.3	1.89	164.9	1.71
Hand Circumference	202.7	2.31	194.3	2.31	199.1	2.23
Index Finger Circumference at the Distal Interphalangeal Joint	56.3	0.66	48.3	0.57	54.9	0.54

[^]*This data includes independent identification of landmarks at Fingertips of Digit 2 and 3 for six (6) out of twelve (12) Occipital Structure scans.*

The Occipital Structure Sensor, Artec Leo, and traditional methods (caliper and tape measure) had standard deviations of less than 1 mm at all measurement locations, except Wrist Circumference and Hand Circumference. High mean differences occur at several locations for the Occipital Structure Sensor, most notably at the Interphalangeal Finger Circumference at the Distal Interphalangeal Joint, Hand Circumference, Hand Length, and Index Finger Length compared to the traditional methods (caliper and tape measure) and the Artec Leo. The averages were similar at most locations between traditional methods (caliper and tape measure) and the Artec Leo than the Occipital Structure Sensor.

Comparison of the Mean of the Absolute Difference Values to ISO 20685:2018 for the Anthropometric Tool Precision Analysis

The Mean of the Absolute Difference Values for the Anthropometric Tool Precision Analysis were assessed to compare the results to the ISO 20685:2018 standard (1 mm) (see Table 20).

Table 20. Mean of the Absolute Difference Values of the Differences for the Anthropometric Tool Precision Analysis (mm).

Defined Measurement	Mean Absolute Difference	
	T vs O	T vs A
Hand Breadth	0.9	1.5
Hand Length	4.9	0.9
Palm Length	1.0	0.9
Index Finger Length	5.7	1.4
Index Finger Breadth at the Distal Interphalangeal Joint	1.6	0.3
Wrist Circumference	1.9	1.3
Hand Circumference	8.4	3.6
Index Finger Circumference at the Distal Interphalangeal Joint	8.0	1.4
Average Difference	4.0	1.4
Standard Deviation	3.1	1.0
Standard Error of Means	1.1	0.3

The defined measurements that were above the maximum allowable error according to ISO 20685:2018 standard (1 mm) when comparing traditional methods (caliper and tape measure) to the Occipital Structure Sensor (T vs O) were Hand Length (4.9 mm), Index Finger Length (5.7 mm), Index Finger Breadth at the Distal Interphalangeal Joint (1.6 mm), Wrist Circumference (1.9 mm), Hand Circumference (8.4 mm), and Index Finger Circumference at the Distal Interphalangeal Joint (8 mm).

The defined measurements that were above the maximum allowable error according to ISO 20685:2018 standard (1 mm) when comparing traditional methods (caliper and tape measure) to

the Artec Leo (T vs A) were Hand Breadth (1.5 mm), Index Finger Length (1.4 mm), Wrist Circumference (1.3 mm), Hand Circumference (3.6 mm), and Index Finger Circumference at the Distal Interphalangeal Joint (1.4 mm).

The measurements that would pass the maximum allowable error according to ISO 20685:2018 standard (1 mm) when comparing traditional methods (caliper and tape measure) to the Occipital Structure Sensor (T vs O) were Hand Breadth (0.9 mm) and Palm Length (1 mm).

The measurements that would pass the maximum allowable error according to ISO 20685:2018 standard (1 mm) when comparing traditional methods (caliper and tape measure) to the Artec Leo (T vs A) were Hand Length (0.9 mm), Palm Length (0.9 mm), and Index Finger Breadth at the Distal Interphalangeal Joint (0.3 mm).

One-sample t-tests were performed on the Mean of the Absolute Difference Values from the two (2) three-dimensional scanners (Occipital Structure Sensor and Artec Leo) for the Anthropometric Tool Precision Analysis to see if they were significantly different from one (1) (see Table 21). One (1) mm is the maximum allowable error allowed by the ISO 20685:2018 standard for hand measurements observed using traditional methods (caliper and tape measure) and three-dimensional scanner (International Organization for Standardization, 2018).

Table 21. One-sample t-tests to assess significant difference from one (1) for the Mean of the Absolute Difference Values for the Anthropometric Tool Precision Analysis.

Three-dimensional Scanner	t-value	p-value	Statistical different from 1 (Yes/No)
Occipital Structure Sensor	2.7715	0.02763*	Yes
Artec Leo	1.2044	0.2676	No

*Significant at the .05 level

The one-sample t-tests from the Mean of the Absolute Difference Values for the Anthropometric Tool Precision Analysis revealed that the Occipital Structure Sensor ($t = 2.7715$, $p = 0.02763$) was statistically different from 1 and the Artec Leo ($t = 1.2044$, $p = 0.2676$) was not statistically different from 1.

One-Way ANOVA and Post-Hoc Analysis for the Anthropometric Tool Precision Analysis

The One-way ANOVA for the Anthropometric Tool Precision Analysis (see Table 22) was used to assess hypothesis two, part A (H2a) and null hypothesis two, part B (H0(2a)). The information presented in the One-Way ANOVA includes the degrees of freedom (DF), f-statistic (F), and p-value.

Table 22. Anthropometric Tool Precision Analysis One-Way ANOVA.

Defined Measurement	Df	F	P-Value
Hand Breadth	2, 33	0.077	0.926
Hand Length [^]	2, 33	0.861	0.432
Palm Length	2, 33	0.082	0.922
Index Finger Length [^]	2, 33	8.325	0.00118 **
Index Finger Breadth at the Distal Interphalangeal Joint	2, 33	2.707	0.0816
Wrist Circumference	2, 33	0.036	0.965
Hand Circumference	2, 33	0.411	0.667
Index Finger Circumference at the Distal Interphalangeal Joint	2, 33	6.361	0.00461 **

[^]This data includes independent identification of landmarks at Fingertips of Digit 2 and 3 for six (6) out of twelve (12) Occipital Structure scans.

*Significant at the .05 level

** Significant at the .01 level

*** Significant at the .00 level

The One-Way ANOVA revealed statistically significant differences occurred at the Index Finger Length ($F(2, 33) = 8.325$, $p = 0.00118$) and Index Finger Circumference at the Distal Interphalangeal Joint ($F(2, 33) = 6.361$, $p = 0.00461$) measurements.

The One-Way ANOVA does not identify which differences between pairs of means are significant. To determine which differences between pairs of means are significant, a Post-Hoc

Pairwise Analysis for Anthropometric Tool Precision Analysis took place for the measurements showing statistical significance from the One-Way ANOVA using Tukey Honestly Significant Difference (HSD) Method (see Table 23).

Table 23. Anthropometric Tool Precision Analysis Post-Hoc Pairwise Analysis using Tukey Honestly Significant Difference (HSD) Method.

Index Finger Length [^]	P-Adj	95% Confidence Interval	
		Lower Bound	Upper Bound
T vs O	0.0012114	2.146893	9.3531069
T vs A	0.6038889	-2.186440	5.0197736
O vs A	0.0155555	-7.936440	-0.7302264
Index Finger Circumference at the Distal Interphalangeal Joint	P-Adj	95% Confidence Interval	
		Lower Bound	Upper Bound
T vs O	0.0057735	2.144469	14.0221975
T vs A	0.8288809	-4.522197	7.3555308
O vs A	0.0250529	-12.605531	-0.7278025

[^]This data includes independent identification of landmarks at Fingertips of Digit 2 and 3 for six (6) out of twelve (12) Occipital Structure scans.

*Significant at the .05 level

** Significant at the .01 level

*** Significant at the .00 level

The post-hoc comparison revealed that statistically significant differences occurred between the Index Finger Length (IFL) and Index Finger Circumference at the Distal Interphalangeal Joint (IFC) measurements between the traditional methods (caliper and tape measure) and Occipital Structure Sensor (T vs O) and between the Occipital Structure Sensor and Artec Leo (O vs A).

No statistically significant difference occurred between traditional methods (caliper and tape measure) and Artec Leo (T vs A).

Results for the Anthropometric Tool Precision Analysis

The Artec Leo did not have statistically significant differences for the defined measurements when compared to those collected using traditional methods (caliper and tape measure), implying that traditional methods (caliper and tape measure) and measurements from the Artec Leo scans are at a similar precision level. Three (3) out of eight (8) of the defined measurements from the

Artec Leo passed the ISO 20685: 2018 standard when comparing to traditional methods. The Artec Leo did not have significant differences from a mean of one (1) in the one-sample t-test.

The Occipital Structure Sensor did not have statistically significant differences for the defined measurements, except Index Finger Length (IFL) and Index Finger Circumference at the Distal Interphalangeal Joint (IFC) measurements when compared to both traditional methods (caliper and tape measure) and the Artec Leo. Two (2) out of eight (8) of the defined measurements from the Artec Leo passed the ISO 20685: 2018 standard when comparing to traditional methods. The Occipital Structure Sensor had significant differences from a mean of one (1) in the one-sample t-test.

The hypothesis was confirmed. The hypothesis was accepted based on the statistically significant differences found within the One-Way ANOVA (see Table 22) and the null hypothesis was rejected (see Table 24).

Table 24. Anthropometric Tool Precision Analysis Results Summary.

Anthropometric Tool Precision Analysis	
<p><i>Research Question Two, Part A (RQ2a):</i> How precise are the three (3) tools (traditional methods (caliper and tape measure), the Occipital Structure Sensor, and the Artec Leo) are for collecting hand anthropometric measurements?</p>	<p>The Artec Leo was able to capture comparable measurements to those collected using traditional methods (caliper and tape measure). Three (3) out of eight (8) of the defined measurements from the Artec Leo passed the ISO 20685: 2018 standard when comparing to traditional methods. The Artec Leo did not have significant differences from a mean of one (1) in the one-sample t-test.</p> <p>The Occipital Structure Sensor was able to capture comparable measurements except Index Finger Length (IFL) and Index Finger Circumference at the Distal Interphalangeal Joint (IFC) measurements when compared to both traditional methods (caliper and tape measure) and the Artec Leo. Two (2) out of eight (8) of the defined measurements from the</p>

	Artec Leo passed the ISO 20685: 2018 standard when comparing to traditional methods. The Occipital Structure Sensor had significant differences from a mean of one (1) in the one-sample t-test.
<i>Hypothesis Two, Part A (H2a):</i> The measurements from each measurement tool across twelve (12) participants will not be statistically identical at each measurement location based on a One-Way ANOVA.	Accepted.
<i>Null Hypothesis Two, Part A (H2a):</i> The measurements from each measurement tool across twelve (12) participants will be statistically identical at each measurement location based on a One-Way ANOVA.	Rejected.

Secondary Anthropometric Tool Precision Analysis

The Anthropometric Tool Precision Analysis included independent identification of landmarks at Fingertips of Digit 2 and 3 for six (6) out of twelve (12) Occipital Structure scans which impacted two (2) measurements, Hand Length and Index Finger Length, due to this a Secondary Anthropometric Tool Precision Analysis took place for the six (6) participants that had complete landmarks. Eliminating the scans that needed independent landmarking allows for the comparison of similar datasets.

Descriptive Statistics for Secondary Anthropometric Tool Precision Analysis

The information provided by the descriptive statistics for the Secondary Anthropometric Tool Precision Analysis (see Table 25) included the mean (M) and standard deviations (SD) from traditional methods (caliper and tape measure) (T), the Occipital Structure Sensor (O), and Artec Leo (A). The information provided by the descriptive statistics for the Secondary Anthropometric Tool Precision Analysis used to assess data before running the One-Way ANOVA.

Table 25. Secondary Anthropometric Tool Analysis Descriptive Statistics.

Defined Measurement	T		O		A	
	Mean	SD	Mean	SD	Mean	SD
Hand Length	186	1.14	181.8	1.35	185	1.11
Index Finger Length	71.0	0.33	67.2	0.39	70.5	0.40

T= Traditional Methods, O = Occipital Structure Sensor, A = Artec Leo

The Occipital Structure Sensor, Artec Leo, and traditional methods (caliper and tape measure) had lower standard deviations at the Index Finger Length and high standard deviations at the Hand Length.

One-way ANOVA for the Secondary Anthropometric Tool Precision Analysis

The One-way ANOVA for the Secondary Anthropometric Tool Precision Analysis (see Table 22) was used to assess hypothesis two, part B (H2b) and null hypothesis two, part B (H0(2b)).

The information presented in Table 26 includes the degrees of freedom (DF), f-statistic (F), and p-value. The significance of the differences among the different means of each hand measurement from the three (3) methods for the secondary analysis for anthropometric tool precision was reported via One-Way ANOVA ($p < 0.05$).

Table 26. Secondary Anthropometric Tool Precision Analysis One-Way ANOVA.

Defined Measurement	Df	F	P-value
Hand Length	2, 15	0.224	0.802
Index Finger Length	2, 15	1.858	0.19

The One-Way ANOVA results showed no statistically significant differences occurred at the Hand Length ($F(2, 15) = 0.224, p = 0.802$) and Index Finger Length ($F(2, 15) = 1.858, p = 0.19$).

A comparison of the results from the Anthropometric Tool Precision Analysis and Secondary Anthropometric Tool Precision Analysis One-Way ANOVAs (see Table 27).

Table 27. Comparison of Results from the Anthropometric Tool Precision and Secondary Anthropometric Tool Precision Analysis One-Way ANOVA.

Defined Measurement	Anthropometric Tool Precision Analysis P-Value	Secondary Anthropometric Tool Precision Analysis P-value
Hand Length	0.432	0.802
Index Finger Length	0.00118 **	0.19

P-values increased within the Secondary Anthropometric Tool Precision Analysis analysis for both the Hand Length and Index Finger Length compared to the Anthropometric Tool Precision Analysis.

Results for the Secondary Anthropometric Tool Precision Analysis

Within the Secondary Anthropometric Tool Precision Analysis, the p-values increased to the point where no statistical significance was found when comparing scans that did not require independent identification of landmarks.

The hypothesis was not confirmed. The hypothesis was rejected based on the One-Way ANOVA results (see Table 26) and the null hypothesis was accepted (see Table 28).

Table 28. Secondary Anthropometric Tool Precision Analysis Results Summary.

Secondary Anthropometric Tool Precision Analysis	
<i>Research Question Two, Part B (RQ2b):</i> How does the inclusion of complete landmarking, that does not rely on independent identification of landmarks, impact the precision of the three-dimensional scans?	P-values increased to the point where no statistical significance was found when comparing scans that did not require independent identification of landmarks.
<i>Hypothesis Two, Part B (H2b):</i> The measurements impacted by independent landmarking from each measurement tool across twelve (12) participants will not be statistically identical at each measurement location based on a One-Way ANOVA.	Rejected.
<i>Null Hypothesis Two, Part B (H2b):</i> The measurements impacted by independent	Accepted.

landmarking from each measurement tool across twelve (12) participants will be statistically identical at each measurement location based on a One-Way ANOVA.	
---	--

Summary

The results from the Anthropometric Tool Reliability Analysis found that the Artec Leo was more reliable than traditional methods (caliper and tape measure) had similar mean values and less statistically significant differences to traditional methods (caliper and tape measure) compared to the Occipital Structure Sensor. Traditional methods (caliper and tape measure) were less reliable than the Occipital Structure Sensor and Artec Leo. The Occipital Structure Sensor was more reliable than traditional methods (caliper and tape measure). However, lower mean values caused statistically significant differences at more locations than traditional methods (caliper and tape measure) and the Artec Leo.

Anthropometric Tool Precision Analysis found that the Artec Leo was able to capture comparable measurements to those collected using traditional methods (caliper and tape measure). The Occipital Structure Sensor was able to capture precise for all of the defined measurements, except Index Finger Length (IFL) and Index Finger Circumference at the Distal Interphalangeal Joint (IFC) measurements when compared to both traditional methods (caliper and tape measure) and the Artec Leo.

Secondary Anthropometric Tool Precision Analysis found that p-values increased to the point where no statistical significance was found when comparing scans that did not require independent identification of landmarks.

Chapter 5. Three-Dimensional Visual Reliability and Three-Dimensional Visual Precision

This chapter presents the results from the data analysis for the Three-Dimensional Visual Reliability Analysis and Three-Dimensional Visual Precision Analysis (see Figure 28). The Three-Dimensional Visual Reliability Analysis took place with the twelve (12) participants using the Post-Processing Visual Analysis Likert Scale (Juhnke, Pokorny, and Griffin, 2021). Three (3) scans were taken for each participant using the Occipital Structure Sensor and Artec Leo. The Three-Dimensional Visual Precision Analysis took place with the twelve (12) participants using the Post-Processing Visual Analysis Likert Scale (Juhnke, Pokorny, and Griffin, 2021). One (1) scan was chosen for each participant from the Three-Dimensional Visual Reliability Analysis from each scanner and they were compared against each other and the original three-dimensional scan used to create the three-dimensional hand model.

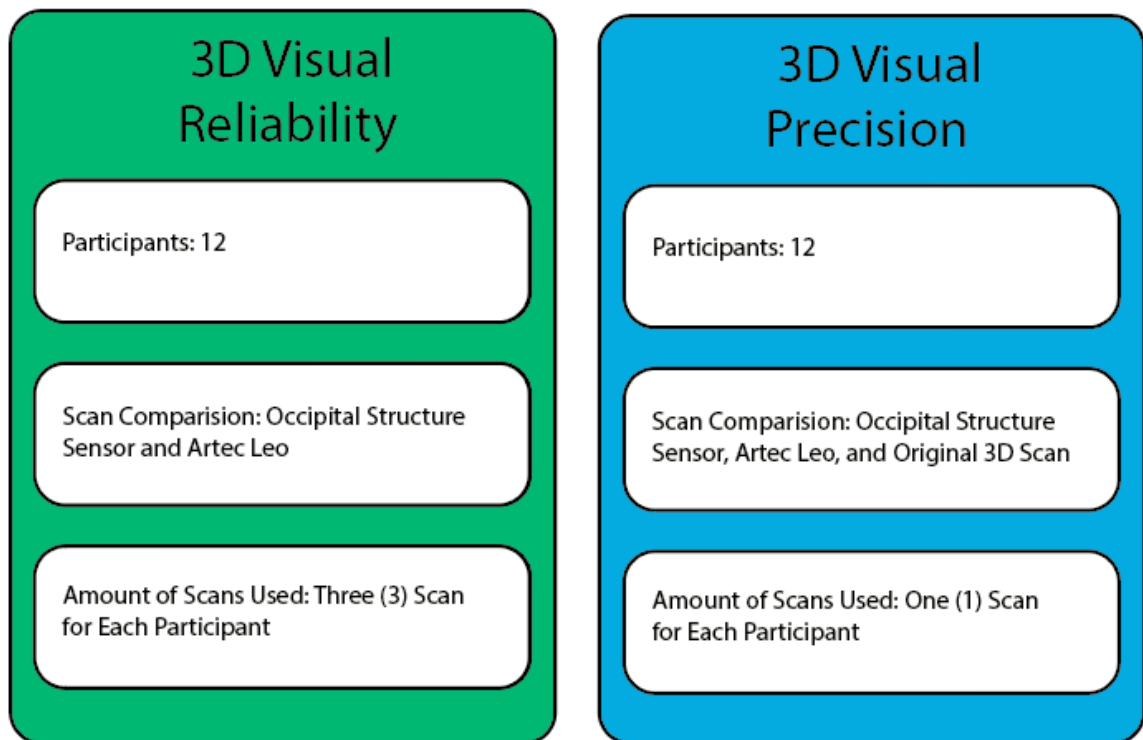


Figure 28. Overview of Visual Analysis.

The visual analysis occurred at the post-processing stage using the Post-Processing Visual Analysis Likert Scale (Juhnke, Pokorny, and Griffin, 2021) (see Table 12).

Table 12. Post-Processing Visual Analysis Likert Scale (modified via Juhnke, Pokorny, & Griffin (2021)).




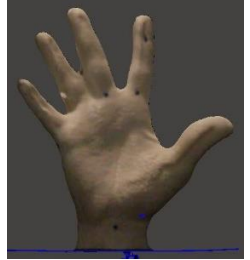







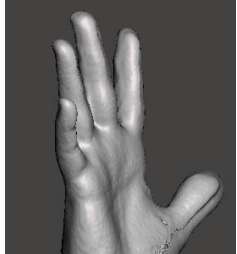


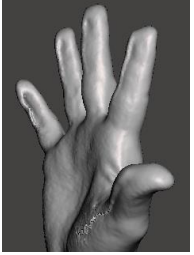
Visual Analysis	Location	1	2	3	4	5
Hand Visibility	Dorsal Side of Hand	The entire dorsal side of the hand is distorted	75% of the dorsal side of the hand is distorted	50% of the dorsal side of the hand is distorted	25% of the dorsal side of the hand is distorted	The dorsal side of the hand is clear of any distortions and appears realistic to the human hand
	Palmar Side of Hand	The entire palmar side of the hand is distorted	75% of the palmar side of the hand is distorted	50% of the palmar side of the hand is distorted	25% of the palmar side of the hand is distorted	The palmar side of hand is clear of any distortions and appears realistic to the human hand
	Clarity of Digit Shape	5 digits are distorted	4 digits are distorted	2-3 digits are distorted	1 digit is distorted	No digits are distorted
Webbing	Quantity of Digits with Webbing	Webbing is present between all digits	Webbing is present between 3 sets of digits	Webbing is present between 2 sets of digits	Webbing is present between 1 set of digits	Webbing between digits appears realistic to the human hand
	Amount of Webbing between Digits 1 and 2	Webbing extends past the proximal interphalangeal joint	Webbing exists at or near the proximal interphalangeal joint	Webbing exists between the metacarpal phalangeal joint and proximal interphalangeal joint	Webbing exists near the metacarpal phalangeal joint	Webbing between digits appears realistic to the human hand
	Amount of Webbing between Digits 2 and 3	Webbing extends past the distal interphalangeal joint	Webbing between proximal and distal interphalangeal joint	Webbing exists at or near the proximal interphalangeal joint	Webbing exists between the metacarpal phalangeal joint and proximal	Webbing between digits appears realistic to the human hand


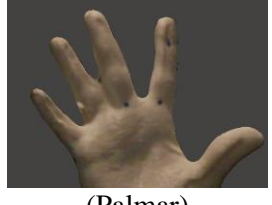
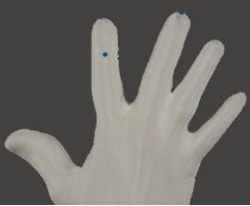
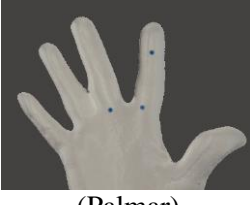





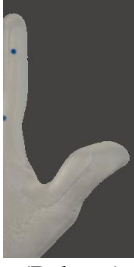



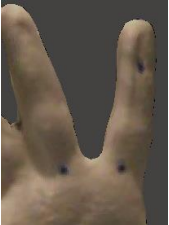




					interphalangeal joint	
	Amount of Webbing between Digits 3 and 4	Webbing extends past the distal interphalangeal joint	Webbing between proximal and distal interphalangeal joint	Webbing exists at or near the proximal interphalangeal joint	Webbing exists between the metacarpal phalangeal joint and proximal interphalangeal joint	Webbing between digits appears realistic to the human hand
	Amount of Webbing between Digits 4 and 5	Webbing extends at or past the distal interphalangeal joint	Webbing between proximal and distal interphalangeal joint	Webbing exists at or near the proximal interphalangeal joint	Webbing exists between the metacarpal phalangeal joint and proximal interphalangeal joint	Webbing between digits appears realistic to the human hand
Landmarks (^)	Visibility of Landmarks	7 of the landmarks are visible	8 or 9 of the landmarks are visible	11 or 10 of the landmarks are visible	12 or 13 of the landmarks are visible	All 14 of the landmarks are visible
	Clarity of Visible Landmarks	6 or more of the visible landmarks are distorted	4-5 of the visible landmarks are distorted	2-3 of the visible landmarks are distorted	1 of the visible landmarks is distorted	No distortion seen in visible landmarks













(^) Not a form of measurement for the original three-dimensional scan.










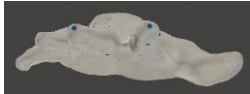
An example of the areas viewed for each location of the Post-Processing Visual Analysis Likert Scale (Juhnke, Pokorny, and Griffin, 2021) (see Table 12) is shown in Table 29 from one (1) of the participants. The Three-Dimensional Visual Reliability Analysis examined scans taken by the two (2) different scanners (the Occipital Structure Sensor and the Artec Leo). The Three-Dimensional Visual Precision Analysis examined the original three-dimensional scan used to create the three-dimensional printed model and the two (2) different scanners (the Occipital Structure Sensor and the Artec Leo). The original three-dimensional scan used to create the three-dimensional printed model did not have landmarks. Only the final scans taken with the Occipital Structure Sensor and the final scans taken with the Artec Leo were analyzed for the Landmarks locations.

Table 29. Example of areas viewed for each location of the Post-Processing Visual Analysis Likert Scale (modified via Juhnke, Pokorny, & Griffin (2021)).

Visual Analysis	Location	Occipital	Artec	Original Three-Dimensional Scan
Hand Visibility	Dorsal Side of the Hand			
	Palmar Side of the Hand			
Clarity of Finger Shape				
		(Dorsal)	(Dorsal)	(Dorsal)
				
	(Side One)	(Side One)	(Side One)	
				
	(Side Two)	(Side Two)	(Side Two)	

<p>Quantity of Fingers with Webbing</p>	 <p>(Dorsal)</p>  <p>(Palmar)</p>	 <p>(Dorsal)</p>  <p>(Palmar)</p>	 <p>(Dorsal)</p>  <p>(Palmar)</p>
<p>Amount of Webbing between Digits 1 and 2</p>	 <p>(Dorsal)</p>  <p>(Palmar)</p>	 <p>(Dorsal)</p>  <p>(Palmar)</p>	 <p>(Dorsal)</p>  <p>(Palmar)</p>
<p>Amount of Webbing between Digits 2 and 3</p>	 <p>(Dorsal)</p>  <p>(Palmar)</p>	 <p>(Dorsal)</p>  <p>(Palmar)</p>	 <p>(Dorsal)</p>  <p>(Palmar)</p>

<p>Amount of Webbing between Digits 3 and 4</p>	 <p>(Dorsal)</p>  <p>(Palmar)</p>	 <p>(Dorsal)</p>  <p>(Palmar)</p>	 <p>(Dorsal)</p>  <p>(Palmar)</p>
<p>Amount of Webbing between Digits 4 and 5</p>	 <p>(Dorsal)</p>  <p>(Palmar)</p>	 <p>(Dorsal)</p>  <p>(Palmar)</p>	 <p>(Dorsal)</p>  <p>(Palmar)</p>

Landmarks ([^])	Visibility of Landmarks	 (Dorsal)	 (Dorsal)	N/A
	Clarity of Visible Landmarks	 (Palmar)	 (Palmar)	
		 (Side One)	 (Side One)	
		 (Side Two)	 (Side Two)	
		 (Fingertips)	 (Fingertips)	

([^]) Not a form of measurement for the original three-dimensional scan.

The evaluation of the scan quality is essential to the success of measuring within digital measuring software. Visual analysis within three-dimensional scanning has mostly been referenced in passing within past research studies. Although visual analysis takes place within three-dimensional scanning, it has yet to be analyzed in comparison studies.

Three-Dimensional Visual Reliability Analysis

Images of the three (3) scans taken with the Occipital Structure Sensor (see Figure 29) and three (3) scans taken with the Artec Leo (see Figure 30) for each participant are seen below.

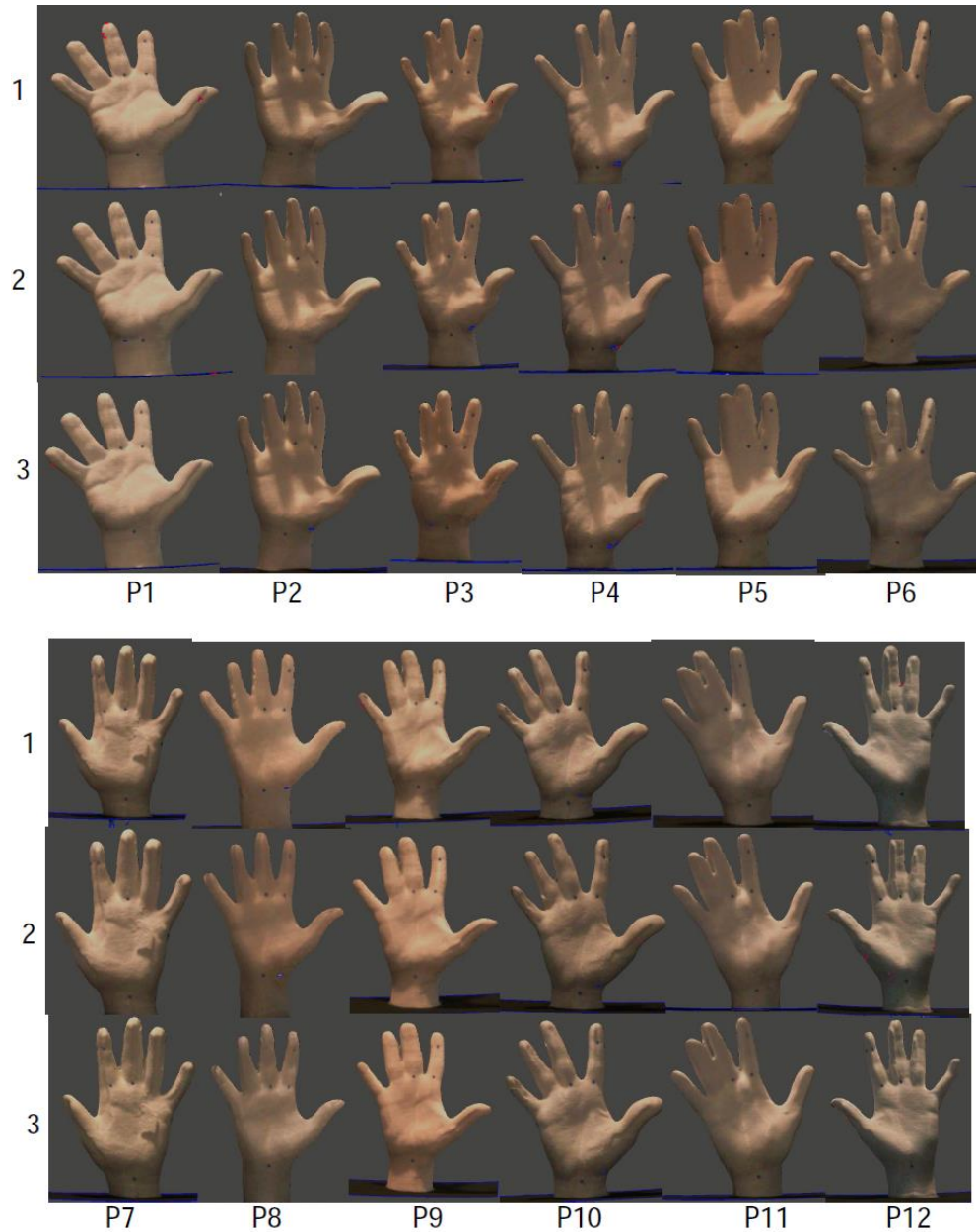


Figure 29. The three (3) scans taken with the Occipital Structure Sensor for each participant.

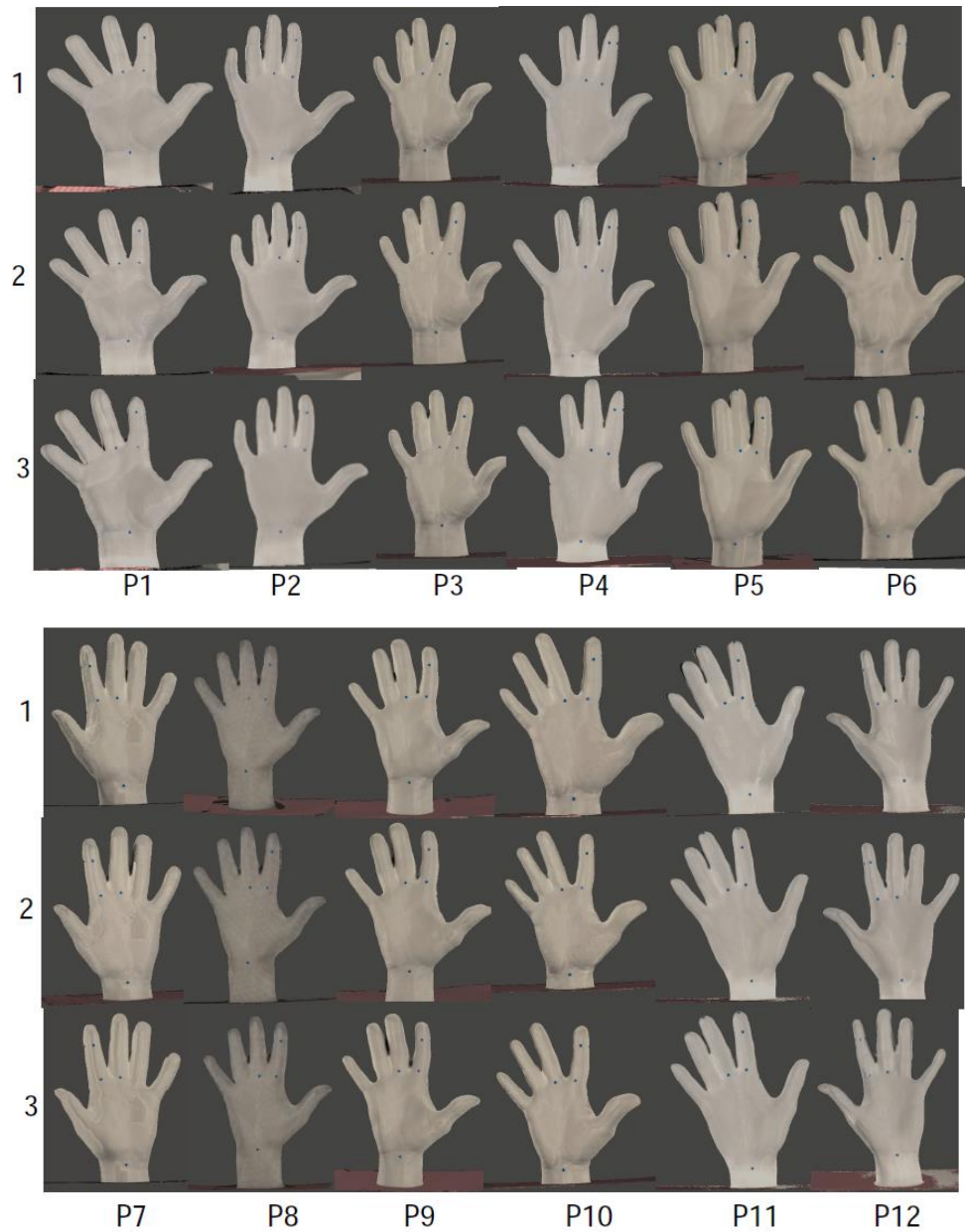


Figure 30. The three (3) scans taken with the Artec Leo for each participant.

Descriptive Statistics for Three-Dimensional Visual Reliability Analysis

The information provided by the descriptive statistics for the Three-Dimensional Visual Reliability Analysis was used to assess data prior to running the One-Way ANOVA. The descriptive statistics for the Three-Dimensional Visual Reliability Analysis (see Table 30) includes the mean (M) and standard deviations (SD) from the Occipital Structure Sensor (O) and Artec Leo (A).

Table 30. Three-dimensional Visual Reliability Analysis Descriptive Statistics.

Visual Analysis	Location	O		A	
		Mean	SD	Mean	SD
Hand Visibility	Dorsal Side of Hand	5	0	4.97	0.17
	Palmar Side of Hand	4.18	0.95	3.96	0.94
	Clarity of Finger Shape	2.58	0.77	2.53	0.74
Webbing	Quantity of Fingers with Webbing	3.25	0.6	3.17	0.56
	Amount of Webbing between Digits 1 and 2	4.92	0.28	4.92	0.28
	Amount of Webbing between Digits 2 and 3	3.89	0.89	3.81	0.98
	Amount of Webbing between Digits 3 and 4	2.47	1.13	2.64	1.2
	Amount of Webbing between Digits 4 and 5	5	0	5	0
Landmarks (^)	Visibility of Landmarks	4.03	0.65	4.81	0.4
	Clarity of Visible Landmarks	3.5	1.21	3.94	0.89

(^) Not a form of measurement for the original three-dimensional scan.

On average, the scores for the Occipital Structure Sensor (O) were higher at the Hand Visibility and Webbing locations compared to the Artec Leo (A).

The greatest differences between the two (2) three-dimensional scanners (Occipital Structure Sensor (O) and Artec Leo (A)) occurred at the Landmark locations. The Artec Leo (A) scored higher on average for both Landmark locations compared to the Occipital Structure Sensor (O).

One-Way ANOVA and Post Hoc Analysis for Three-Dimensional Visual Reliability Analysis

The One-Way ANOVA for the Three-Dimensional Visual Reliability Analysis was used to assess hypothesis three (H3) and null hypothesis three (H0(3)). The significance of the differences among the different means of each hand measurement from the three (3) methods for the Three-Dimensional Visual Reliability Analysis was reported via One-Way ANOVA ($p < 0.05$) (see Table 31). The information includes the degrees of freedom (DF), f-statistic (F), and p-value.

Table 31. Three-Dimensional Visual Reliability Analysis One-Way ANOVA.

Visual Analysis	Location	Df	F	Sig.
Hand Visibility	Dorsal Side of the Hand	2, 81	0.661	0.519
	Palmar Side of the Hand	2, 81	0.974	0.382
	Clarity of Finger Shape	2, 81	0.07	0.933
Webbing	Quantity of Fingers with Webbing	2, 81	0.407	0.667
	Amount of Webbing between Digits 1 and 2	2, 81	0	1
	Amount of Webbing between Digits 2 and 3	2, 81	1.571	0.214
	Amount of Webbing between Digits 3 and 4	2, 81	0.956	0.389
	Amount of Webbing between Digits 4 and 5	2, 81	0.661	0.519
Landmarks (^)	Visibility of Landmarks	1, 70	36.98	5.63e-08 ***
	Clarity of Visible Landmarks	1, 70	3.155	0.08

(^) Not a form of measurement for the original three-dimensional scan.

*Significant at the .05 level

** Significant at the .01 level

*** Significant at the .00 level

The One-Way ANOVA revealed statistically significant between group differences occurred at the Visibility of Landmarks ($F(1,70) = 36.98, p = 5.63e-08$) location. A Post-Hoc Pairwise Analysis took place for the Visibility of Landmarks location from the Three-Dimensional Visual Reliability Analysis using Tukey Honestly Significant Difference (HSD) Method (see Table 32).

Table 32. Three-dimensional Visual Reliability Analysis Post-Hoc Pairwise Analysis using Tukey Honestly Significant Difference (HSD) Method.

Visibility of Landmarks	Sig.	95% Confidence Interval	
		Lower Bound	Upper Bound
O vs A	1e-07	-1.032863	-0.5226923

The post-hoc comparison revealed that statistically significant differences occurred between the Occipital Structure Sensor and the Artec Leo (O vs A) at the Visibility of Landmarks ($p = 1e-07$) location.

Results for the Three-Dimensional Visual Reliability Analysis

Based on this analysis, the repeatability of the quality of the scans is comparable between the two (2) scanners (the Occipital Structure Sensor and Artec Leo) for all locations from the Post-Processing Visual Analysis Likert Scale (Juhnke, Pokorny, and Griffin, 2021), except for the Visibility of Landmark location (see Table 32).

The hypothesis was confirmed. The hypothesis was accepted based on statistical significance occurring within the One-Way ANOVA (see Table 31) and the null hypothesis was rejected (see Table 33).

Table 33. Three-Dimensional Visual Reliability Results Summary.

Three-Dimensional Visual Reliability	
<i>Research Question Three (RQ3):</i> How reliable is the quality of the scans from the three-dimensional scanners (the Occipital Structure Sensor and the Artec Leo) for use in collecting hand anthropometric data?	The Occipital Structure Sensor and Artec Leo are comparable for all locations, except for the Visibility of Landmark location.
<i>Hypothesis Three (H3):</i> The final scans from each three-dimensional scanner across twelve (12) participants will not be statistically identical at each location of the Post-Processing Visual Analysis Likert Scale (Juhnke, Pokorny, and Griffin, 2021).	Accepted.
<i>Null Hypothesis Three (H0(3)):</i> The final scans from each three-dimensional scanner across twelve (12) participants will be statistically identical at each location of the Post-Processing Visual Analysis Likert Scale (Juhnke, Pokorny, and Griffin, 2021).	Rejected.

Three-Dimensional Visual Precision Analysis

Images from the original three-dimensional scan used to create the three-dimensional printed model (see Figure 31), the final scans taken with the Occipital Structure Sensor (see Figure 32), and the final scans taken with the Artec Leo (see Figure 33) for each participant are seen below.

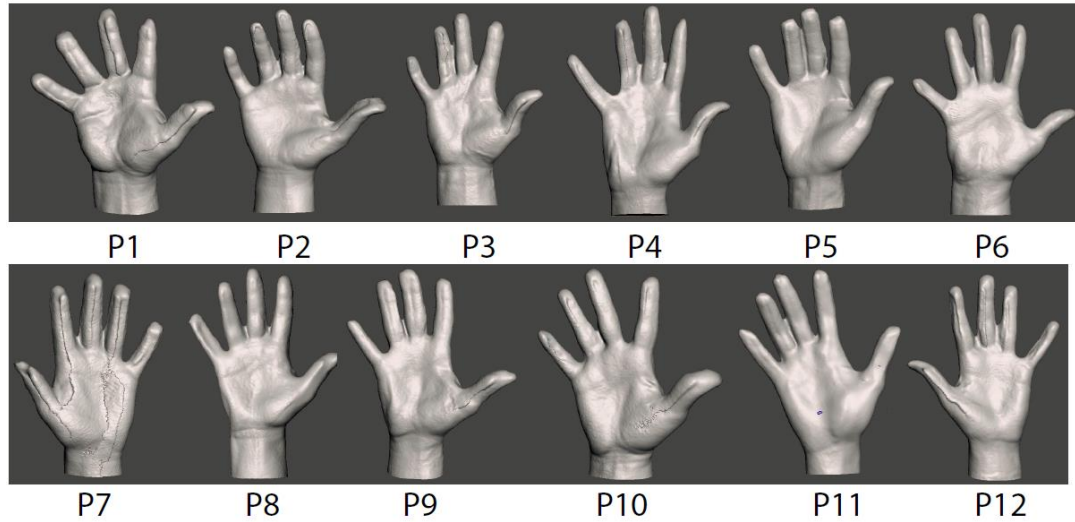


Figure 31. Final scans from original three-dimensional scan used to create the three-dimensional printed model.

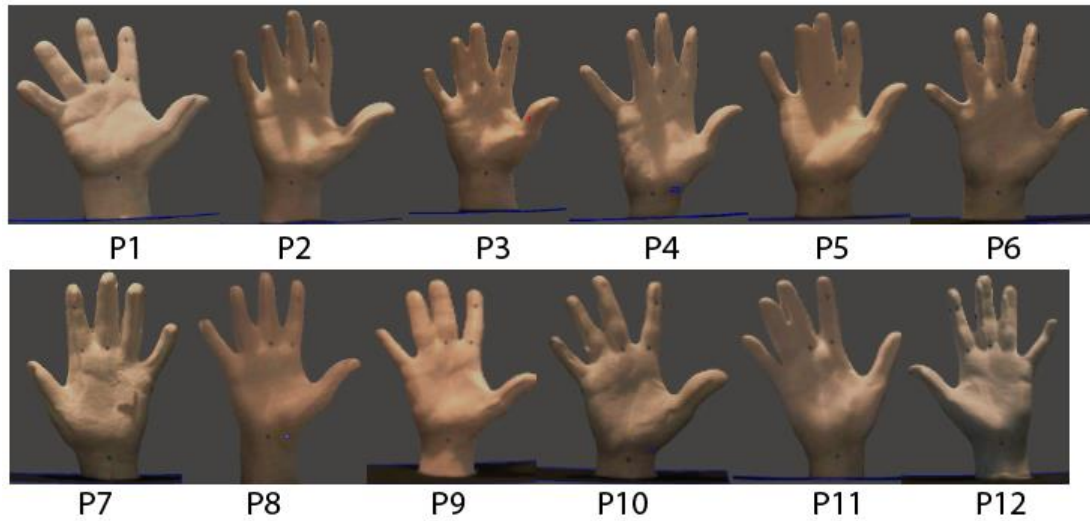


Figure 32. Final scans taken with the Occipital Structure Sensor.

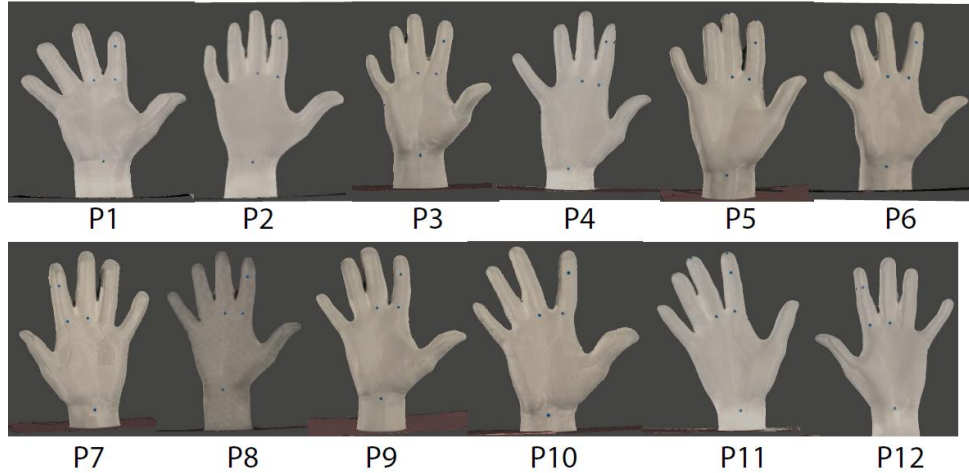


Figure 33. Final scans taken with the Artec Leo.

Descriptive Statistics for the Three-Dimensional Visual Precision Analysis

The information provided by the descriptive statistics for the Three-Dimensional Visual Precision Analysis (see Table 34), was used to assess data prior to running the One-Way ANOVA. The descriptive statistics for the Three-Dimensional Visual Precision Analysis included the mean (M) and standard deviations (SD) from the Occipital Structure Sensor (O), Artec Leo (A), and the original three-dimensional scan used to create the three-dimensional printed model (TPH).

Table 34. Three-Dimensional Visual Precision Analysis Descriptive Statistics.

Visual Analysis	Location	O		A		TPH	
		Mean	SD	Mean	SD	Mean	SD
Hand Visibility	Dorsal Side of Hand	5	0	5	0	5	0
	Palmar Side of Hand	4.21	0.99	3.96	0.96	3.79	0.84
	Clarity of Finger Shape	2.58	0.79	2.58	0.67	2.5	1
Webbing	Quantity of Fingers with Webbing	3.25	0.62	3.17	0.58	3.33	0.65
	Amount of Webbing between Digits 1 and 2	4.92	0.29	4.92	0.29	4.92	0.29
	Amount of Webbing between Digits 2 and 3	4	0.74	3.83	0.94	4.33	0.65

	Amount of Webbing between Digits 3 and 4	2.5	1.17	2.67	1.23	3	1.04
	Amount of Webbing between Digits 4 and 5	5	0	5	0	5	0
Landmarks (^)	Visibility of Landmarks	4.33	0.65	5	0	N/A	N/A
	Clarity of Visible Landmarks	3.83	1.19	4.33	0.78	N/A	N/A

(^) Not a form of measurement for the original three-dimensional scan.

On average, the scores for the original three-dimensional scan used to create the three-dimensional printed model (TPH) were higher at the Hand Visibility and Webbing locations compared to the two (2) three-dimensional scanners (Occipital Structure Sensor (O) and Artec Leo (A)). Between the two (2) three-dimensional scanners (Occipital Structure Sensor (O) and Artec Leo (A)) the averages were similar at the Hand Visibility and Webbing locations.

The greatest differences between the two (2) three-dimensional scanners (Occipital Structure Sensor (O) and Artec Leo (A)) occurred at the Landmark locations. The Artec Leo (A) scored higher on average for both Landmark locations compared to the Occipital Structure Sensor (O).

One-Way ANOVA and Post-Hoc Analysis for the Three-Dimensional Visual Precision Analysis

The One-Way ANOVA for the Three-Dimensional Visual Precision Analysis was used to assess hypothesis four (H4) and null hypothesis four (H0(4)). The significance of the differences among the different means of each hand measurement from the three (3) methods for the Three-Dimensional Visual Precision Analysis was reported via One-Way ANOVA ($p < 0.05$). The information presented in Table 35 includes the degrees of freedom (DF), f-statistic (F), and p-value.

Table 35. Three-Dimensional Visual Precision Analysis One-Way ANOVA.

Visual Analysis	Location	Df	F	Sig.
Hand Visibility	Dorsal Side of Hand	2, 33	1	0.379
	Palmar Side of Hand	2, 33	0.607	0.551
	Clarity of Finger Shape	2, 33	0.04	0.961
Webbing	Quantity of Fingers with Webbing	2, 33	0.219	0.805
	Amount of Webbing between Digits 1 and 2	2, 33	0	1
	Amount of Webbing between Digits 2 and 3	2, 33	1.262	0.296
	Amount of Webbing between Digits 3 and 4	2, 33	0.588	0.561
	Amount of Webbing between Digits 4 and 5	2, 33	1	0.379
Landmarks (^)	Visibility of Landmarks	1, 22	12.57	0.00181**
	Clarity of Visible Landmarks	1, 22	1.478	0.237

(^) Not a form of measurement for the original three-dimensional scan.

*Significant at the .05 level

** Significant at the .01 level

*** Significant at the .00 level

The One-Way ANOVA revealed statistically significant between group differences occurred at the Visibility of Landmarks ($F(1, 22) = 12.57, p = 0.00181$) location. A Post-Hoc Pairwise Analysis took place for the Visibility of Landmarks location from the Three-Dimensional Visual Precision Analysis using Tukey Honestly Significant Difference (HSD) Method (see Table 36).

Table 36. Three-Dimensional Visual Precision Analysis Post-Hoc Pairwise Analysis using Tukey Honestly Significant Difference (HSD) Method.

Visibility of Landmarks	P-adj	95% Confidence Interval	
		Lower Bound	Upper Bound
O vs A	0.001814	-1.056607	-0.276726

The post-hoc comparison revealed that statistically significant differences occurred between the Occipital Structure Sensor and the Artec Leo (O vs A) at the Visibility of Landmarks ($p = 0.001814$) location.

Results for the Three-Dimensional Visual Precision Analysis

Based on this analysis, the Three-Dimensional Visual Precision Analysis is comparable between the original three-dimensional scan used to create the three-dimensional printed model and the three-dimensional scanners (the Occipital Structure Sensor and the Artec Leo), except for the Visibility of Landmark location.

The hypothesis was confirmed. The hypothesis was accepted based on statistical significance occurring within the One-Way ANOVA (see Table 35) and the null hypothesis was rejected (see Table 37).

Table 37. Three-Dimensional Visual Precision Analysis Results Summary.

Three-Dimensional Visual Precision Analysis	
<i>Research Question Four (RQ4):</i> How precise is the quality of the scans from the three-dimensional scanners (the Occipital Structure Sensor and Artec Leo), compared to each other and the original three-dimensional scan, for use in collecting hand anthropometric data?	The original three-dimensional scan used to create the three-dimensional printed model, the Occipital Structure Sensor, and the Artec Leo are comparable for all locations, except for the Visibility of Landmark location.
<i>Hypothesis Four (H4):</i> The final scans from each three-dimensional scanner and the original three-dimensional scan (used to create the three-dimensional printed model) across twelve (12) participants will not be statistically identical at each location of the Post-Processing Visual Analysis Likert Scale (Juhnke, Pokorny, and Griffin, 2021).	Accepted.
<i>Null Hypothesis Four (HO(4)):</i> The final scans from each three-dimensional scanner and the original three-dimensional scan (used to create the three-dimensional printed model) across twelve (12) participants will be statistically identical at	Rejected.

each location of the Post-Processing Visual Analysis Likert Scale (Juhnke, Pokorny, and Griffin, 2021).	
---	--

Connection between Three-Dimensional Visual Precision Analysis and Anthropometric Tool Precision Analysis

A review of the Three-Dimensional Visual Precision Analysis notes took place to quantify where landmark visibility issues occurred for the final scans from the Occipital Structure Sensor (O). Six (6) out of twelve (12) scans had incomplete landmarking at the Fingertips of Digits 2 and 3 location. The Three-Dimensional Visual Precision Analysis of the Fingertips of Digits 2 and 3 is shown in Figure 34. Visible landmarks at this location occurred at P1, P2, P7, P10, P11, and P12.

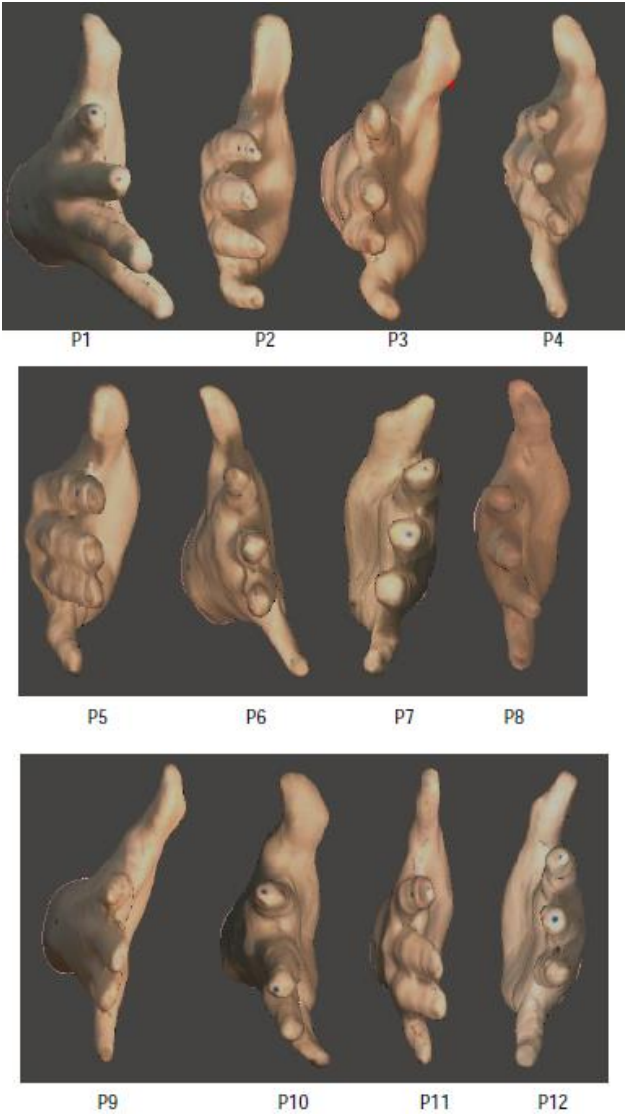


Figure 34. The Three-Dimensional Visual Analysis of the Fingertips of Digits 2 and 3 (visible landmarks at this location occurred at P1, P2, P7, P10, P11, and P12).

Summary

The results from the Three-Dimensional Visual Reliability and the Three-Dimensional Visual Precision Analysis found that the Occipital Structure Sensor and Artec Leo are comparable for all locations, except for the Visibility of Landmark location.

Chapter 6. Discussion and Conclusion

Broader and more diverse databases of hand anthropometric data are essential to improve the fit and sizing of various products that interact with the hand. Full-color, hand-held three-dimensional scanners allow research to occur outside of a lab setting, providing further opportunities for collecting hand anthropometric data. The use of full-color, hand-held three-dimensional scanners could also allow for a wide variety of hand anthropometric data to be gathered from functional hand positions. Functional hand positions provide critical measurements that could significantly impact the future design of products that interact with the hand. However, as of this writing, the two (2) full-color, hand-held three-dimensional scanner examined in this study (the Occipital Structure Sensor and the Artec Leo) have not been validated for the collection of anthropometric hand data. Validation studies have previously taken place using three-dimensional scanners to collect anthropometric data from the hand. The three-dimensional scanners used in previous validation studies have either lacked color-capture capabilities (Li, Chang, Dempsey, Ouyang, & Duan, 2008 and Yu, Yick, Ng, & Yip, 2013), are not hand-held (Yu, Yick, Ng, & Yip, 2013 and Dunbar & Chapates, 2019), or needed further analysis to confirm viability (Pokorny, Seifert, Griffin, et al., 2019).

The purpose of this study was to examine the reliability and precision of three (3) different tools for collecting anthropometric data of the hand. The tools compared in this study include traditional anthropometric tools (caliper and tape measure) and two (2) full-color, hand-held three-dimensional scanners (Occipital Structure Sensor and Artec Leo). Additionally, a visual analysis of the three-dimensional models provided from the two (2) full-color hand-held three-dimensional scanners occurred in the post-processing stage to determine the three-dimensional visual reliability and three-dimensional visual precision.

Discussion

This research validates the Artec Leo for use in the collection of three-dimensional anthropometric hand data. The Occipital Structure Sensor also had promising results for collecting three-dimensional anthropometric hand data when full landmarking is present. Both the Artec Leo and Occipital Structure Sensor are full-color, hand-held three-dimensional scanners. The validation of full-color, hand-held three-dimensional scanners expands many future anthropometric research opportunities for the hand (see Figure 35). First, these scanners allow for research to occur outside of a lab setting, which could provide further opportunities for collecting targeted hand anthropometric data and the availability to collect broader and more diverse

databases. Second, the use of full-color, hand-held three-dimensional scanners could also allow for the capability to collect functional hand positions. Functional hand positions may assist in further understanding the hand's dynamic movements and any impact that they may have on measurement change in critical locations. Third, three-dimensional scanners provide an opportunity to collect a wider variety of measurements than traditional methods or two-dimensional capture, such as specific surface measurements, that could improve the fit of products. Finally, the ability to capture full-color three-dimensional scans from human participants allows access to models which could be reassessed, referenced, or used at any time during the design process.

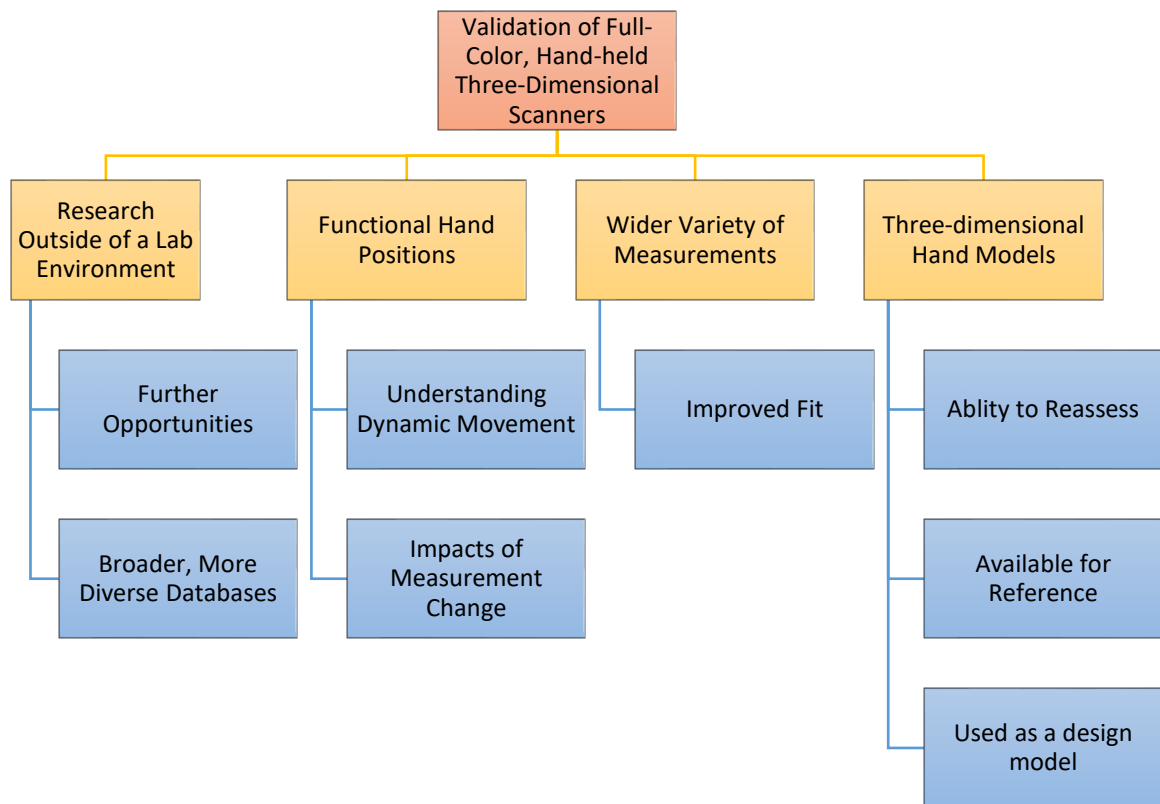


Figure 35. Opportunities from the validation of full-color, hand-held three-dimensional scanners.

This study introduces quantifying visual analysis within comparison studies that use three-dimensional scanning to collect hand anthropometric data. Visual analysis occurs within three-dimensional hand scanning, whether quantified or not, as three-dimensional collection relies on assessing the scans' quality (see Figure 36). The visual assessment of three-dimensional hand scans was mentioned within most of the previous comparison studies reviewed for this study. Dunbar & Chapates (2019) noted that although best is not a quantitative measurement, they could

still define the best surface mesh. Within this study, a Post-Processing Visual Analysis Likert Scale (Juhnke, Pokorny, and Griffin, 2021), previously used to visually analyze scans within data collection, provided clear definitions for three locations (hand visibility, webbing, and landmarking) to quantify the overall quality of the scans within the visual assessment. The visual analysis effects were essential to understanding where the quality of the scans taken by both scanners might have affected the outcomes from the data collection.

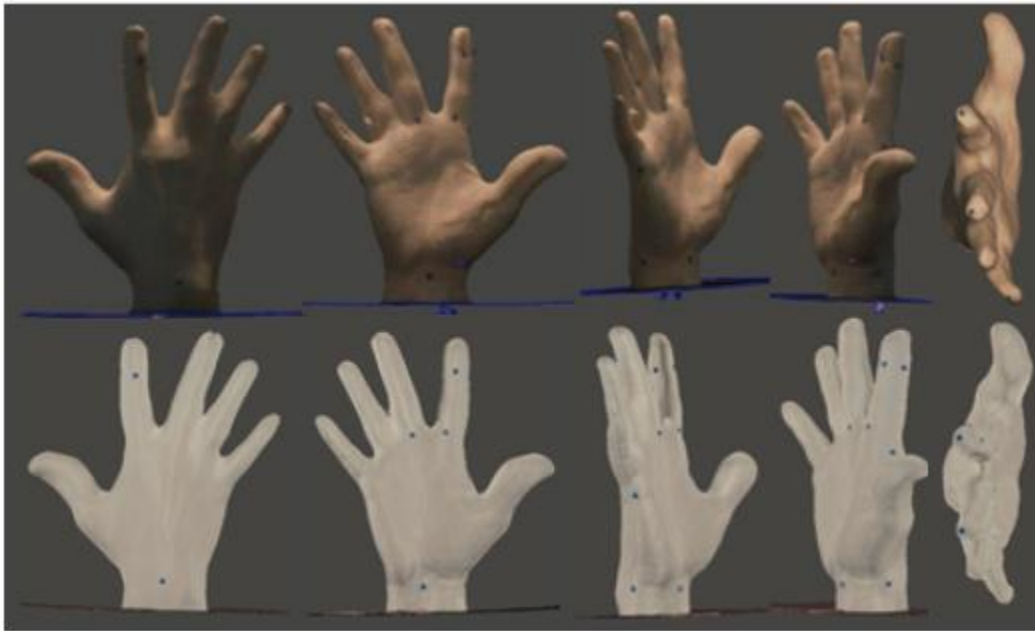


Figure 36. Visual Analysis from Occipital Structure Sensor (Top Row) and Artec Leo (Bottom Row).

Limitations

The twelve (12) three-dimensional hand scans were printed using white PLA materials. The ability for both three-dimensional scanners (the Occipital Structure Sensor and the Artec Leo) to capture a wide variety of skin colors is essential to developing products that interact with the hand. Since statistically significant differences occurred at the Visibility of Landmarks location for the two (2) visual analysis sections with the white PLA material, both the Visibility and Clarity of Landmarks needs to be assessed with a range of various skin colors.

The cost of three-dimensional printing the hand scans was prohibitive to the inclusion of many participants. This study's sample size was not large enough to detect statistical significance per ISO 20685:2018 standards, which recommends 40 test subjects. Future studies should include more participants.

The participants' demographics from the original three-dimensional scans chosen for this study did not reflect a racially diverse database. The six (6) male and six (6) female participants were of Caucasian and Asian descent. In the future, comparing racially diverse participants will be included.

The original three-dimensional scans chosen for this study had minor deformities, yet even minor deformities on the hand may have influenced surface measurements. Ideally, the hand scans taken with three-dimensional scanners will be free of deformities. An evaluation should classify the number of deformities and at what location they can occur with minimal impact on anthropometric hand measurement.

The three-dimensional hand models were examined in one (1) hand position (the splayed hand position). Three-dimensional hand scanning allows for functional hand positions to be collected. The Occipital Structure Sensor has been used for studies where three-dimensional scanning took place with functional hand positions (Griffin, Kim, Carufel, Sokolowski, Lee, & Seifert, 2019 and Seifert, Curry, & Griffin, 2019). The Artec Leo has not been tested for this purpose.

The three-dimensional hand models were also only examined from one (1) angle (approximately 90 degrees). Capturing the hand from different angles could provide clearer visibility at the Fingertips of Digits 2 and 3 landmark locations.

Not having clear visibility of landmarking at Fingertips of Digit 2 and 3 for half (six (6) out of twelve (12)) of the final scans taken with Occipital Structure Sensor led to independent identification of landmarks at the impacted two (2) measurements, Hand Length, and Index Finger Length.

Recommendation for Future Research

Based on the results of this study, the following recommendations should be considered for future research. The methodology for this study needs to be validated on a larger sample size of human hands. The two (2) three-dimensional scanners need to be examined to assess their ability to capture various skin tones and colors from a diverse population of participants. The hand should be tested in functional hand positions using the Artec Leo. An evaluation should take place to classify the number of deformities and at what location they can occur on three-dimensional hand scans with minimal impact on anthropometric hand measurement. Further testing needs to occur

at various angles (beyond 90 degrees). Finally, clear visible landmarks are needed to make reliable landmarking decisions that do not rely on independent landmarking identification.

Conclusions

Three major conclusions can be made from this study. The first conclusion is that the results provided by the Artec Leo are comparable to those collected using traditional methods (caliper and tape measure) and validate the Artec Leo for use in further anthropometric data collection for the hand. The second conclusion is that the results provided by the Occipital Structure Sensor are promising compared to those collected using traditional methods (caliper and tape measure). However, it is important to note that only measurements with visible landmarks should be used. The third conclusion is that the use of visual analysis as a form of evaluation for the validation of three-dimensional scanners is crucial to understanding where the scan's quality might affect the outcomes from the data collection.

Chapter 7. Bibliography

Apeageyi, P. R. (2010). Application of 3D body scanning technology to human measurement for clothing fit. *International Journal of Digital Content Technology and its Applications*, 4(7), 58-68.

Ashdown, S. P., Loker, S., Schoenfelder, K., & Lyman-Clarke, L. (2004). Using 3D scans for fit analysis. *Journal of Textile and Apparel, Technology and Management*, 4(1), 1-12.

Baugh, L. (2020, February 1). A New Year of Hand Safety. Retrieved from <https://ohsonline.com/articles/2020/02/01/a-new-year-of-hand-safety.aspx>

Bureau of Labor Statistics. Survey of Occupational Injuries and Illnesses Data. Retrieved from <https://www.bls.gov/iif/soii-data.htm>

Bragança, S., Arezes, P., Carvalho, M., & Ashdown, S. P. (2016). Current state of the art and enduring issues in anthropometric data collection. *Dyna*, 83(197), 22-30.

Chen, L., Chang, C., Wang, M., & Tsao, L. (2018). Comparison of foot shape between recreational sprinters and non-habitual exercisers using 3D scanning data. *International Journal of Industrial Ergonomics*, 68, 337-343.

Dunbar, B. J., & Chapates, P. J. (2019, March). Comparison of 3D Photogrammetric and Laser Hand Scans to Manual Measurement Methods for EVA Glove Fabrication. In *2019 IEEE Aerospace Conference* (pp. 1-11). IEEE.

Gordon, C. C., Churchill, T., Clauser, C. E., Bradtmiller, B., McConville, J. T., Tebbets, I., & Walker, R. A. (1989). *Anthropometric survey of US Army personnel: Summary statistics, interim report for 1988. ANTHROPOLOGY RESEARCH PROJECT INC YELLOW SPRINGS OH.*

Gordon, C. C., Blackwell, C. L., Bradtmiller, B., Parham, J. L., Barrientos, P., Paquette, S. P., ... & Mucher, M. (2012). *2012 anthropometric survey of US army personnel: methods and summary statistics (No. NATICK/TR-15/007). ARMY NATICK SOLDIER RESEARCH DEVELOPMENT AND ENGINEERING CENTER MA.*

Greiner, T. M. (1991). *Hand anthropometry of US army personnel (No. TR-92/011). ARMY NATICK RESEARCH DEVELOPMENT AND ENGINEERING CENTER MA.*

Griffin, L., Kim, N., Carufel, R., Sokolowski, S., Lee, H., & Seifert, E. (2018, July). Dimensions of the Dynamic Hand: Implications for Glove Design, Fit, and Sizing. In *International Conference on Applied Human Factors and Ergonomics* (pp. 38-48). Springer, Cham.

Griffin, L., Sokolowski, S., Lee, H., Seifert, E., Kim, N., & Carufel, R. "Methods and tools for 3D measurement of hands and feet." *International Conference on Applied Human Factors and Ergonomics*. Springer, Cham, 2018.

Gupta, D. (2014). 2 - Anthropometry and the design and production of apparel: An overview. In *Anthropometry, apparel sizing and design* (pp. 34-66). Elsevier.

Gupta, D. (2020). New directions in the field of anthropometry, sizing and clothing fit. In *Anthropometry, Apparel Sizing and Design* (pp. 3-27). Woodhead Publishing.

Habibi, E., Soury, S., & Zadeh, A. (2013). Precise evaluation of anthropometric 2D software processing of hand in comparison with direct method. *Journal of Medical Signals and Sensors*, 3(4), 256–261.

Hirt, B., Seyhan, H., Wagner, M., & Zumhasch, R. (2017). *Hand and Wrist Anatomy and Biomechanics: A Comprehensive Guide*. Stuttgart: Georg Thieme Verlag.

Hoevenaren, I. A., Maal, T. J., Krikken, E., De Haan, A. F. J., Bergé, S. J., & Ulrich, D. J. O. (2015). Development of a three-dimensional hand model using 3D stereophotogrammetry: evaluation of landmark reproducibility. *Journal of plastic, reconstructive & aesthetic surgery*, 68(5), 709-716.

Hsiao, H., & Cooke, N. (2013). Anthropometric Procedures for Protective Equipment Sizing and Design. *Human Factors: The Journal of Human Factors and Ergonomics Society*, 55(1), 6-35.

Hsiao, H., Whitestone, J., Kau, T. Y., & Hildreth, B. (2015). Firefighter hand anthropometry and structural glove sizing: a new perspective. *Human factors*, 57(8), 1359-1377.

International Organization for Standardization. (2017). ISO 7250-1: 2017 Basic human body measurements for technological design—Part 1: Body measurement definitions and landmarks.

International Organization for Standardization. (2018). ISO 20685-1: 2018 3-D scanning methodologies for internationally compatible anthropometric databases—Part 1: Evaluation protocol for body dimensions extracted from 3-D body scans.

- Irzmańska, E., & Okrasa, M. (2018). Evaluation of protective footwear fit for older workers (60): A case study using 3D scanning technique. *International Journal of Industrial Ergonomics*, 67, 27-31.
- Istook, C. L., & Hwang, S. J. (2001). 3D body scanning systems with application to the apparel industry. *Journal of Fashion Marketing and Management*, 5(2), 120-132.
- Jones, L. A., & Lederman, S. J. (2006). *Human hand function*. Oxford University Press.
- Juhnke, B., Pokorny, C., and Griffin, L. (2021). Standardized Functional Hand Grasp Method Development for 3D Scanning. *Journal Article for International Journal of Industrial Ergonomics* (under review).
- Klepser, A., Babin, M., Loercher, C., Kirchdoerfer, F., Beringer, J., & Schmidt, A. (2012). 3D Hand Measuring with a Mobile Scanning System. In *Proc. of 3rd Int. Conf. on 3D Body Scanning Technologies* (pp. 288-294).
- Kouchi, M. (2020). Anthropometric methods for apparel design: Body measurement devices and techniques. In *Anthropometry, Apparel Sizing and Design* (pp. 29-56). Woodhead Publishing.
- Kouchi, M., Mochimaru, M., Bradtmiller, B., Daanen, H., Li, P., Nacher, B., & Nam, Y. Research Institute MOVE. (2012). A protocol for evaluating the accuracy of 3D body scanners. *Work: A Journal of Prevention, Assessment and Rehabilitation*, 41(Supplement 1), 4010-4017.
- Kwon, O., Jung, K., You, H., & Kim, H. E. (2009). Determination of key dimensions for a glove sizing system by analyzing the relationships between hand dimensions. *Applied Ergonomics*, 40(4), 762-766.
- Lane, D. (2003). *Introduction to Statistics*. Houston, Texas: David Lane.
- Li, Z., Chang, C. C., Dempsey, P. G., Ouyang, L., & Duan, J. (2008). Validation of a three-dimensional hand scanning and dimension extraction method with dimension data. *Ergonomics*, 51(11), 1672-1692.
- Lumley, J. S. P., Craven, J. L., & Tunstall, R. (2019). *Bailey & Love's essential clinical anatomy*. Boca Raton, FL: CRC Press.

Nasir, S. H., Troynikov, O., & Watson, C. (2015). Skin deformation behavior during hand movements and their impact on functional sports glove design. *Procedia Engineering*, 112, 92-97.

Padron, M. (2018). Safety Professionals, 'We've Got a Problem'. Retrieved from <https://ohsonline.com/Articles/2018/06/01/Safety-Professionals-Weve-Got-a-Problem.aspx?Page=1>.

Panchal-Kildare, Surbhi, MD, & Malone, Kevin, MD. (2013). Skeletal Anatomy of the Hand. *Hand Clinics*, 29(4), 459-471.

Park, J. (2013). Gauging the emerging plus-size footwear market an anthropometric approach. *Clothing and Textiles Research Journal*, 31(1), 3-16.

Pokorny, Seifert, Griffin, Holschuh, Juhnke, & Savvateev. (2019). Validation of the Artec Eva for Hand Anthropometric Data Collection, *International Textile and Apparel Association Annual Conference Proceedings*. doi: <https://doi.org/10.31274/itaa.8376>.

Robinette, K. M., Blackwell, S., Daanen, H., Boehmer, M., & Fleming, S. (2002). Civilian American and European Surface Anthropometry Resource (CAESAR), Final Report. Volume 1. Summary. *SYTRONICS INC DAYTON OH*.

Skals, S., Ellena, T., Subic, A., Mustafa, H., & Pang, T. (2016). Improving fit of bicycle helmet liners using 3D anthropometric data. *International Journal of Industrial Ergonomics*, 55, 86-95.

Sokolowski, S. L., Griffin, L., & Chandrasekhar, S. Current Technology Landscape for Collecting Hand Anthropometric Data. (2018). *In 9th International Conference and Exhibition on 3D Body Scanning and Processing Technologies*, 142-153.

Standring, S. (2016). *Gray's anatomy: The anatomical basis of clinical practice* (Forty-first ed., Gray's Anatomy). New York]: Elsevier Limited.

Vergara, M., Agost, M. J., & Bayarri, V. (2019). Anthropometric characterization of palm and finger shapes to complement current glove-sizing systems. *International Journal of Industrial Ergonomics*, 74, 102836.

Vergara, M., Agost, M. J., & Gracia-Ibáñez, V. (2018). Dorsal and palmar aspect dimensions of hand anthropometry for designing hand tools and protections. *Human Factors and Ergonomics in Manufacturing & Service Industries*, 28(1), 17-28.

White, R. M. (1980). Comparative anthropometry of the hand (No. NATICK/CEMEL-229). Army Natick Research and Development Labs Ma Clothing Equipment and Materials Engineering Lab.

Yu, A., Yick, K. L., Ng, S. P., & Yip, J. (2013). 2D and 3D anatomical analyses of hand dimensions for custom-made gloves. *Applied ergonomics*, 44(3), 381-392.

Zhuang, Z., Slice, D., Benson, S., Lynch, S., & Viscusi, D. (2010). Shape Analysis of 3D Head Scan Data for U.S. Respirator Users. *EURASIP Journal on Advances in Signal Processing*, 2010(1), 1-10.